Biomaterial-Stem Cell Approaches to Augment Regeneration

Drew Kuraitis

Thesis submitted to the

Faculty of Graduate and Postdoctoral Studies

in partial fulfillment of the requirements

for the Doctorate in Philosophy degree in Cellular & Molecular Medicine

Faculty of Medicine

Ottawa, Canada, 2013

Abstract

Diseases affecting striated muscle are prevalent and deadly in both the Western and developing worlds. Such diseases include peripheral arterial disease and coronary artery disease, characterized by reduced blood flow to extremities and heart muscle, respectively, all of which manifest as reduced function and quality-of-life. Although promising in animal models, many clinical trials of stem cell therapy have yielded modest results at best. Growing evidence suggests that in a disease state, improvements in local environments using natural methods that already exist in the body hold great promise for supporting recovery and regeneration. This may be accomplished by exploiting natural progenitor cell functions and interactions with endogenous extracellular matrix (ECM) components, pro-regenerative cytokines and ligands.

This thesis uses ECM-mimicking, collagen-based matrices to improve the regenerative response. Specifically, such a matrix is demonstrated to improve the potency of *ex vivo* expanded circulating angiogenic cells for treatment of ischemic muscle (Chapter 2). Matrices were also functionalized to release chemoattractant molecules to improve the recruitment of progenitor cells (Chapter 3) and to present progenitor cell-binding ligands for improved cell retention in ischemic muscle (Chapter 4), with the ultimate goal of restoring perfusion. Matrices were also observed to improve muscle function and augment muscle regeneration in models of ischemic and dystrophic muscle (Chapters 4 & 5).

The results of this thesis provide insights into the ability to modulate regeneration *in vivo* with treatment of biomaterials that have been designed to exploit and amplify progenitor cell responses. Specifically, this thesis contains some of the first reports for the use of ECM-

based biomaterials to stimulate passive enrichment of CACs, functional regeneration of muscle, and a potential method of benefitting from necrosis. These data provide an interesting pilot perspective on improvements or alternatives to cell therapy, and that future studies will seek to better tune these prospective therapies so that one day they may be clinically available.

Table of Contents

List of Abbreviations

7-AAD, 7-aminoactinomycin D

ALS, amyotrophic lateral sclerosis

b-FGF, basic fibroblast growth factor

BM, basement membrane *or* bone marrow

BMTx, bone marrow transplantation

CAC, circulating angiogenic cell

CAD, coronary artery disease

CD, cluster of differentiation

CMF, calcium and magnesium-free

CMTMR, 5-(6)-(((4-chloromethyl)benzoyl)amino)tetramethylrhodamine

CPC, circulating progenitor cell

CS-C, chondroitin sulfate-C

CS, chondroitin sulfate

CSA, cross-secitonal area

DAPI, 4'6-diamidino-2-phenylindole

DM, differentiation medium

DMD, Duchenne's muscular dystrophy

DMEM, Dubecco's modified eagle medium

dPBS, Dubecco's phosphate buffered saline

EBM, endothelial basal medium

EC, endothelial cell

ECM, extracellular matrix

EDC, 1-ethyl-3-(3-dimethylaminopropyl)carbodiimide

EDL, extensor digitorum longus

EdU, 5-fluoro-2'-deoxyuridine

EGM-2, endothelial growth medium-2

ELISA, enzyme-linked immunosorbent assay

EPC, endothelial progenitor cell

ERK, extracellular regulated kinase

ESC, embryonic stem cell

FBS, fetal bovine serum

FGF-2, fibroblast growth factor-2

FITC, fluorescein isothiocyanate

FOV, field-of-view

GAG, glycosaminoglycan

GAPDH, glyceraldehyde 3-phosphate dehydrogenase

GCSF, granulocyte colony stimulating factor

GFP, green fluorescent protein

GM, growth medium

HA, hyaluronic acid

HBSS, Hank's balanced salt solution

HGF, hepatocyte growth factor

HS, heparan sulfate

HSPG, heparan sulfate proteoglycan

HUVEC, human umbilical vein endothelial cell

ICAM-1, intercellular adhesion molecule-1

IGF-I, insulin-like growth factor-I

IGF-II, insulin-like growth factor-II

IGFBP-2, insulin-like growth factor binding protein-2

IGFBP-5, insulin-like growth factor binding protein-5

IGFBP-6, insulin-like growth factor binding protein-6

IL-1α, interleukin-1α

IL-1β, interleukin-1β

IL-6, interleukin-6

iPSC, induced pluripotent stem cell

MB, myoblast

MCK, muscle creatine kinase

MCP-1, monocyte chemoattractant protein-1

MES, 2-(N-morpholino)ethanesulfonic acid

MHC, myosin heavy chain

MI, myocardial infarction

MIP-3α, macrophage inflammatory protein-3α

MS, microsphere

MSC, mesenchymal stem cell

NHS, n-hydroxysuccinimide

NMD, necrotic myocyte debris

PAD, peripheral artery disease

PBMC, peripheral blood mononuclear cell

PBS, phosphate buffered saline

PE-Cy7, phycoerythrin-Cy7

PFA, paraformaldehyde

PG, proteoglycan

qPCR, quantitative polymerase chain reaction

SC, satellite cell

SCF, stem cell factor

SDF-1, stromal cell-derived factor-1

SEM, scanning electron microscopy

sLe^X, sialyl lewisX

SM, stromal matrix

SMA, smooth muscle actin

SOD1, superoxide dismutase

TBS, tris buffered saline

TCPS, tissue culture polystyrene

TIMP-1, tissue inhibitor of metalloproteinase-1

TIMP-2, tissue inhibitor of metalloproteinase-2

TNFα, tumor necrosis factor α

VCAM-1, vascular cell adhesion molecule-1

VECAM, vascular endothelial cell adhesion molecule

VEGF, vascular endothelial growth factor

List of Figures

List of Tables

CHAPTER 1. General Introduction

Striated Muscle Diseases

Three types of muscle exist in the body: smooth muscle, cardiac muscle and skeletal muscle. Of these, the latter two are considered to be 'striated muscle', given their highly organized, repeating sarcomeric ultrastructure and similar metabolic activities. Despite having countless biochemical, structural and physiological differences, both cardiac and skeletal muscle can experience similar disease states and both have also demonstrated similar responses to the same therapies.

Coronary artery disease

Coronary artery disease (CAD) persists as the leading cause of death in the Western world. For various reasons, the arteries supplying the heart with blood become constricted, ultimately reducing perfusion in the heart and manifesting as a potentially fatal myocardial infarction (MI) (Jaffe and Strauss, 2007). Post-MI, tissue loss is rapid; within minutes, cells that comprise cardiac muscle and also coronary vessels have died, posing serious risk. This damage leaves behind a barren zone that is ultimately repopulated with dense scar tissue, which impedes normal heart function and recovery (Skyschally et al., 2008; Sutton and Sharpe, 2000).

The downstream events that occur after infarction are mostly attributable to the lack of blood flow. The post-MI "dead zone" remains relatively unpopulated, and there are few cells to aid in the re-growth of blood vessels and restoration of cardiac tone. As scar tissue is deposited, it modifies the post-MI environment and creates a tough, granulomatous microenvironment. Such an environment is not permissive of blood vessel in-growth and prevents adequate reperfusion (Tonnesen et al., 2000). Scar tissue is persistent and

predisposes patients to future episodes and disease. In theory, a well-perfused heart would support vessel and muscle growth, hinder scar deposition and maintain normal structure and physiology. Therefore, strategies are geared towards improving and maintaining blood vessels in the heart, a term called *therapeutic angiogenesis*, as an alternative to surgical intervention (Ruel et al., 2004). The premise of therapeutic angiogenesis is that if perfusion can be restored to the ischemic myocardium, blood vessels may re-grow, the aforementioned consequences of infarction would be reduced, heart function would be restored and patient quality-of-life will then improve.

Peripheral artery disease

Similar to CAD, peripheral artery disease occurs through irreversible loss of vascular tone and blood vessels, resulting in reduced perfusion to the extremities (Belch et al., 2003). This disease affects at least 27 million individuals in the Western world and its prevalence increases with age and other increasingly common co-morbidities, such as diabetes and obesity. This disease is painful and chronic ischemia may result in necrotic arms or legs that require amputation. Like CAD patients, individuals suffering from PAD could benefit from therapeutic angiogenesis; improvements in perfusion would allow for tissue survival, restoration of muscle function and ultimately enhancement of patient qualify-of-life.

Muscular dystrophy

"Muscular dystrophy" is a broad term applied to a large family of diseases that gradually weaken the musculoskeletal system. Of all dystrophies, Duchenne's muscular dystrophy (DMD) is perhaps the best characterized. DMD is a recessive, x-linked disorder affecting approximately 1 in 3500 boys. Due to a mutation in the dystrophin gene, muscle

cells become weak and fragile, and eventually cannot maintain the abilities of normal intercellular communication and contraction (Blake et al., 2002). Afflicted individuals experience degeneration and hyperfibrosis of all skeletal and cardiac muscle, lose the ability to walk during pre-pubescence and carry an average life span of 25 years.

Muscular atrophy

Cachexia, or muscle loss, is a common symptom of various diseases, such as cancer, heart failure and autoimmune diseases. In the aforementioned disease states, the patients' abnormal physiology does not allow for restoration of muscle to pre-disease size or state, yielding a net loss of muscle (Bonaldo and Sandri, 2013). Atrophy occurs when decreases in muscle cell measurements (via protein and cytoplasm loss) leads to a reduction in muscle size. In constrast to muscular dystrophies, the pathways that lead to muscle atrophy are passive and atrophies are not generally hallmarked by aggressive cell death or remodeling. In amyotrophic lateral sclerosis (ALS), motor neurons slowly degenerate and this loss of innervation leads to disuse atrophy (Pasinelli and Brown, 2006). ALS is the most common motor neuron disease that manifests as gradual muscle weakening and loss of function, and within 5 years of diagnosis, most patients die from respiratory failure.

This thesis will address and discuss various types of diseases that affect striated muscle. Although the term *myopathy* correctly refers to diseases that originate and affect the muscle specifically, this thesis uses *myopathy* in a broad sense to refer to pathologies of muscle, which includes ischemia and ALS.

Regeneration of Diseased Muscle

The vasculoregenerative response

Endogenous mechanisms for self-guided regeneration exist and have been observed in ischemic muscle. In both ischemic cardiac and skeletal muscle, an ischemic event triggers the production of small signaling molecules, or cytokines, to initiate the regenerative response. Cytokines, such as stromal cell-derived factor-1 (SDF-1) and vascular endothelial growth factor (VEGF) are released in a gradient fashion in order to guide the body's own progenitor cells towards the site of injury (Gnecchi et al., 2008). These signaling molecules are able to affect progenitor cell populations in various fashions: cell proliferation increases; cell emigration and homing from bone marrow, blood and muscle tissue occurs; cells migrate and engraft at the site of injury; engrafted cells coordinate regeneration via differentiation into new blood vessel or muscle cells, secondary recruitment of other progenitor cells, and also modulation of local inflammation and remodeling. Regardless of the mechanisms involved, the ultimate goal is to first restore perfusion to ischemic muscle, as without an adequate blood supply, nervous and muscular tissues will not be able to regenerate themselves in any significant capacity (Grounds, 2008a; Ko et al., 2007). New blood vessel growth can be of three types: vasculogenesis, or the *de novo* generation of new blood vessels from progenitor cells; arteriogenesis, or the growth of pre-existing vessels to functional arteries; and, angiogenesis, or the growth of new capillaries from pre-existing capillaries.

After ischemic injury, reduced oxygen and nutrient availability in combination with increased reactive oxygen species induce severe cell death. These changes also cause rapid alterations of the native extracellular matrix (ECM) by inducing production of proteases and also recruitment of immune cells that remove damaged ECM (Barallobre-Barreiro et al.,

2012; Muller et al., 2013; Wang et al., 2013). Perhaps the greatest change in ECM ultrastructure that persists is the deposition of collagen fibres. The process of fibrosis generates scar tissue that is less labile and ultimately less permissive for cell invasion and the in-growth of vasculature. This long-lasting pathophysiological change is considered irreversible and once fibrotic tissue has been deposited, the tissue's capacity for regeneration is significantly hampered. Ideally, the regenerative response would be able to overcome these inhibitory changes in the ECM. In an otherwise healthy state, the ECM would recover from an ischemic insult and guide regeneration by guiding progenitor cells and blood vessel growth (Bayomy et al., 2012); however, these endogenous abilities for regeneration are further hindered by co-morbities common in the Western world today: the growth of new blood vessels, involvement of progenitor cells and healthy remodeling of the extracellular matrix are all severely impaired in aged individuals, as well as in obese patients, diabetic patients and patients with heart disease (Devaraj and Jialal, 2012; Tobler et al., 2010).

The myoregenerative response

Post-natal skeletal muscle has a remarkable ability to repair itself. This is largely due to the presence of muscle precursor cells, or satellite cells (SCs). SCs reside under the basal lamina of mature muscle fibres. In response to various stimuli, such as exercise, damage or injury, quiescent SCs are activated, proliferate and migrate towards damaged myofibres (Le Grand and Rudnicki, 2007). Here, they begin differentiation and develop into an elongated myotube. Multiple myotubes fuse to form multinucleated myocytes. As these cells mature into myocytes, the expression of markers such as myf5, desmin, MyoD, myogenin, Mef2C and MCK rise and fall, allowing for cell maturation to be monitored using molecular techniques.

In addition to its importance in blood vessel growth, it is believed that the ECM plays a key role in directing SC maintenance and muscle regeneration (Yin et al., 2013), although this function is poorly understood. The role of the ECM in myogenesis is also believed to be abnormal in diseased or dystrophic muscle (Zanotti et al., 2007). Also similar to the vasculogenic response, the myogenic response tends to be impaired in individuals who require it most. SC number and integrity decreases with age, and the regenerative capacity of SCs is greatly reduced in individuals suffering from myopathies such as DMD or ALS (Pradat et al., 2011).

Cell Therapy to Augment Regeneration

Cell therapy is no longer in its infancy nor is it a new concept. To date, there have been dozens of clinical trials to assess the ability of transplanted cells to aid in the regeneration of diseased tissue. Due to the socioeconomic burden and great prevalence of CAD, many of these trials have focused on cells to restore perfusion to the ischemic heart.

After an ischemic event, the local environment experiences many changes related to death, inflammation and ECM remodeling and these changes present challenges to successful cell therapy. Furthermore, there are many variables of cell therapy that still need to be optimized in order for clinical practice. Such hurdles include: optimization of autologous cell harvest, *ex vivo* amplification of cells, preparation of cells for transplantation, and the ideal methods of transplantation to the ischemic heart.

Circulating angiogenic cells

The circulating angiogenic cell (CAC) has perhaps received the most clinical attention for regenerating ischemic tissue (Abdel-Latif et al., 2007; Dimmeler et al., 2008). Working under the hypothesis of *therapeutic angiogenesis*, CACs are delivered to ischemic skeletal or cardiac muscle with the hope of augmenting perfusion and therefore allowing for regeneration and normal function.

First described in 1997, the CAC was termed the endothelial progenitor cell (EPC) and was shown to differentiate into new blood vessels, highlighting its therapeutic potential. Since its inaugural description, the identity of the EPC has become convoluted and controversial; depending on the source, isolation technique, phenotype and cell function, EPCs may be referred to as CACs or circulating progenitor cells (CPCs) (Prater et al., 2007; Yoder and Ingram, 2009). Regardless of the terminology used, CACs, EPCs and CPCs share many broad commonalities: they are of bone marrow origin, they are mononuclear, they express at least a subset of progenitor cell surface markers, and via transdifferentiation or paracrine effects, they are able to augment blood vessel growth. The chapters in this thesis will use the acronyms CAC, EPC and CPC interchangeably; however, the focus will reflect the current state of cell biology in the literature and use CAC and CPC since the cells used in these studies did not fulfill all criteria to use the name 'EPC' set forth by the American Heart Association at the time of experimentation.

CACs remain an attractive cell source because of the feasibility associated with their usage. CACs may be harvested and delivered in an autologous fashion. They are also present in significant numbers (the potent $CD34^{+}VEGFR2^{+}$ phenotype comprises up to 2% of circulating peripheral blood mononuclear cells (Sofrenovic et al., 2012)) and the risk of

unwanted cell growth is far less than that of embryonic or mesenchymal stem cells. Recent meta-analyses of CAC and CAC variant populations have summarized their efficacy based on clinical trial data; however, the positive results in these studies are only considered modest and the degree of improvement seen in animal studies was not present in human studies (Cleland et al., 2006; Delewi et al., 2013; Martin-Rendon et al., 2008). It is believed that the success of CAC therapy is limited for many reasons, including poor cell engraftment, persistence and survival, and also the delivery of sub-optimal cells from diseased patients (Aicher et al., 2003; Li et al., 2009).

Satellite cells

Like CACs, SC clinical trials have failed to produce results that would see their clinical usage a common technique (Tedesco et al., 2010). Similarly, the overall lackluster performance of transplanted SCs is attributed to poor engraftment and viability, and the depletion of the SC niche (Fan et al., 1996; Huard et al., 1992). During myodegenerative diseases or injury, SCs naturally respond to injured tissue and mount their own regenerative responses. Thus, both CACs and SCs have potential clinical benefits, but their usage is hampered by their inherent potential and also unconvincing clinical trials.

Acellular Therapy to Augment Regeneration

Given that the regenerative abilities of transplanted cells have now been shown to be underwhelming, investigation into cell-free interventional methods to guide tissue regeneration has become a current and competitive field. The initiation and maintenance of regeneration by delivered acellular molecules still relies on the ability of endogenous cells to

participate in the regenerative response; however, the therapeutic application of these materials also considers strategies by which the efficacy of the endogenous cell response may be improved or enhanced.

Growth factor therapy

During vasculo- and myoregenerative efforts, small growth factor molecules are released in an attempt to coordinate cell activation, migration, recruitment and differentiation. Given the known regenerative effects of many growth factors, it can be hypothesized that the delivery of specific, regenerative growth factors alone will aid in regeneration (Gnecchi et al., 2008). Much support for this hypothesis comes from conditioned medium studies whereby transplantation of cells or the medium that these cells were maintained in (which contain their secreted growth factors) yielded comparable results (Gnecchi et al., 2006; Urbich et al., 2005).

Of note is SDF-1, which is released in response to ischemia and mediates progenitor cell recruitment (Askari and Penn, 2003; Askari et al., 2003). After an ischemic event, SDF-1 production is increased transiently and returns to basal levels after 4 to 5 days. Given its potent chemoattractant ability, a prolonged presence of SDF-1 was hypothesized to improve cell recruitment and ultimately improve the regenerative response. Experiments have shown this to be true (Jin et al., 2006; Kucia et al., 2004; Segers et al., 2007), highlighting the potential of maintaining growth factor signals *in vivo* as a therapeutic option. Currently, studies are investigating other factors for mobilization and attraction, such as granulocyte colony stimulating factor, hepatocyte growth factor, stem cell factor and vascular endothelial growth factor.

Therapeutic application of biomaterials

As discussed, the integrity and composition of the ECM during disease is often compromised and these changes negatively impact the ability of tissues to regenerate. During embryonic development and also post-natal regeneration, the ECM plays important and integral roles in directing normal cell growth and behavior (Bayomy et al., 2012; Daley et al., 2008). Thus, recapitulation of normal or healthy ECM may prove to be a new and effective method for augmenting and guiding tissue regeneration.

A 'biomaterial' is currently defined as *a material intended to interface with biological systems to evaluate, treat, augment or replace any tissue, organ or function of the body* (Williams, 1999). This definition is broad and encompasses many materials, such as dental ceramics, metal bone plates and cardiac stents (Huebsch and Mooney, 2009). The chapters presented in this thesis will focus on the use of natural biomaterials (i.e., materials made from naturally-occurring molecules produced in the body in some capacity), which allows us to by-pass limitations associated with other therapies. Since the components of these materials are already produced endogenously, the risk of a harmful inflammatory response is minimized (materials are not recognized as foreign or dangerous), the potential for cell interaction is greater (cells already possess receptors for these materials), and the ability for material degradation and incorporation can be anticipated (natural degradation pathways already exist for these materials). Various strategies exist to enhance biomaterials using ECM components. Improved regenerative responses may be elicited by changing the material composition, such as by adding laminin or glycosaminoglycans (Kuraitis et al., 2012c). Furthermore, if biomaterials can be used in a manner that produces results comparable to cell therapies, then biomaterial therapy will confer even more advantages, such as not requiring

autologous cell sources, the ability to be available off-the-shelf and ready for rapid delivery, and also reduced cost via inexpensive, non-cellular scale-up operations.

Thesis objectives

Aims

The primary aim of this research was to improve the understanding of biomaterial therapy for various muscle diseases and also to test clinically relevant materials in appropriate models to assess and describe their effects.

Specifically, Aim #1 was to use biomaterials to improve CAC cell therapy. Given the variability in both the production and harvest of CAC populations, and the subsequent modest results from clinical trials of CAC therapy, this Aim sought to generate therapeutically superior CACs by improving their culture methods (Chapter 2). CACs were isolated using traditional techniques, but then exposed to a soft biomaterial matrix. Cells were then harvested and evaluated *in vitro* and *in vivo* to determine if matrix culture confers any relevant changes in CAC function.

The study in Aim #2 sought to combine biomaterial and growth factor therapies in order to restore perfusion to ischemic skeletal muscle (Chapter 3). SDF-1 was incorporated into a biomaterial matrix system whereby the growth factor was slowly released. This system was delivered intramuscularly and the ability of the SDF-1 releasing biomaterials was assessed with regards to its ability to attract CACs and also aid in the restoration of perfusion.

Both Aims #3 (Chapter 4) and #4 (Chapter 5) attempted to augment regeneration of ischemic, atrophic and dystrophic muscle. Biomaterials, similar to those of the previous aims, were applied to ischemic or diseased muscle. The capacity of these materials to accelerate vascular and muscular regeneration, and the ideal context in which they may be most efficacious, was assessed.

Hypotheses

It was hypothesized that:

1. Pre-exposure of CACs to an ECM-like biomaterial matrix will prime them for transplantation and enhance their efficacy at restoring perfusion;
2. The use of an SDF-1-releasing system for treating ischemic muscle will rapidly restore perfusion, mediated by improved recruitment of endogenous CACs;
3. Application of a biomaterial mimic of skeletal muscle ECM that also has vasculoregenerative effects will be able to restore both perfusion and muscle tone to muscle damaged by ischemia; and,
4. The disease state is integral to a tissue's ability to respond to biomaterial therapy, and necrosis plays an important an interactive role in myogenesis when an ECM mimic is applied.

Role in research

At the beginning of each chapter, the role of co-authors is described for the respective studies. Other than the stated co-author contributions, the experiments were designed, performed and analyzed by myself.

CHAPTER 2. *Ex vivo* generation of a highly potent population of circulating angiogenic cells using a collagen matrix

This chapter has been published in the *Journal of Molecular and Cellular Cardiology*, as per the following citation:

D. Kuraitis, C. Hou, Y. Zhang, B. Vulesevic, T. Sofrenovic, D. McKee, Z. Sharif, M. Ruel and E.J. Suuronen (2011) Collagen biomatrices for endothelial progenitor cell enrichment and functional enhancement. J Mol Cell Cardiol 51(2):187-97.

Notes on Chapter

Our lab had previously used the matrix described within this chapter for CAC delivery in a model of hindlimb ischemia (Suuronen et al., 2006). Matrix-deployment of CACs appeared to be more efficacious than matrix or CAC treatment alone when delivered to ischemic skeletal muscle. The study in this chapter was first designed to examine the effects that the matrix may have on CACs, but later revelations indicated that the matrix itself induced a potent phenotypic shift towards a more regenerative state and that exposure to the matrix could "prime" CACs, ultimately improving the reperfusion phenomenon after cell transplantation into ischemic muscle.

Contributions of co-authors to results and/or manuscript:

C. Hou performed Western blotting [Fig. 2-2E-F] and ERK inhibition [Fig. 2-5C,D] and wrote the respective parts of the Materials & Methods section.

Y. Zhang assisted with adhesion, angiogenesis and invasion assays [Figs. 2-4,5].

B. Vulesevic performed Western blotting [Fig. 2-5A,B] and assisted with reading cytokine arrays [Fig. 2-7].

Z. Sharif assisted with the invasion assay [Fig. 2-5C]

E.J. Suuronen and M. Ruel were involved in experimental planning, analysis and manuscript editing.

Abstract

Biomaterials that have the ability to augment angiogenesis are highly sought-after for applications in regenerative medicine, particularly for revascularization of ischemic and infarcted tissue. We evaluated the culture of human circulating angiogenic cells (CAC) on collagen type I-based matrices, and compared this to traditional selective-adhesion cultures on fibronectin. Culture on a collagen matrix supported the proliferation of $CD133^+$ and $CD34^+CD133^+$ CACs. When subjected to serum starvation, the matrix conferred a resistance to cell death for $CD34^+$ and $CD133^+$ progenitors and increased phosphorylation of Akt. After 4 days of culture, phenotypically enriched populations of endothelial cells ($CD31^+CD144^+$) and progenitor cells ($CD34^+CD133^+$) emerged. Culture on matrix upregulated the phosphorylation and activation of ERK1/2 pathway members, and matrix-cultured cells also had an enhanced functional capacity for adhesion and invasion. These functional improvements were abrogated when cultured in the presence of ERK inhibitors. The formation of vessel-like structures in an angiogenesis assay was augmented with matrix-cultured cells, which were also more likely to physically associate with such structures compared to CACs taken from culture on fibronectin. *In vivo*, treatment with matrix-cultured cells increased the size and density of arterioles, and was superior at restoring perfusion in a mouse model of hindlimb ischemia, compared to fibronectin-cultured cell treatment. This work suggests that a collagen-based matrix, as a novel substrate for CAC culture, possesses the ability to enrich endothelial and angiogenic populations and lead to clinically-relevant functional enhancements.

Introduction

Coronary artery disease (CAD) persists as the leading cause of death in both men and women in the Western world. Invasive treatments exist for those suffering from severe CAD; although, the current options are short-term, and do not offer long-term solutions for afflicted patients. To address this, new therapeutic approaches under investigation aim to promote the regeneration of ischemic myocardium, using stem/progenitor cells, cytokines, and biomaterial-based scaffolds. One hope is that if blood flow can be restored, then further cardiomyocyte loss may be prevented and damaged regions may be repopulated by proliferating cardiomyocytes and/or activated resident cardiac stem cells, and heart function can be somewhat improved.

An important cell population in cell-based vascular homeostasis and regeneration is the circulating angiogenic cell (CAC)[1-3]. CACs are a mixed population of mononuclear cells that are derived from the bone marrow, and enter the circulation in response to a variety of factors. CACs can home to hypoxic or ischemic sites, where they may take part in angiogenesis by differentiating into endothelial cells (ECs)(Asahara et al., 1999; Kalka et al., 2000; Murohara et al., 2000; Schatteman et al., 2000). CAC transplantation has shown promising results in revascularization of ischemic tissue (Hur et al., 2004; Kalka et al., 2000; Kawamoto et al., 2001; Murohara et al., 2000; Yoon et al., 2005).

Traditionally, CACs have been obtained from the adhesion-selective culture of peripheral blood mononuclear cells on fibronectin. However, this yields a highly heterogeneous CAC population (Kalka et al., 2000). Therefore, one challenge to achieving successful therapy using CACs is the improvement of culture methods that will yield a better characterized

population of therapeutic cells. Due to the positive effects of chemokines and homing signals produced by adult cell sources (Cho et al., 2007; Gnecchi et al., 2008), the heterogeneity of the differentiated cell population might be advantageous, but control of this heterogeneity is desirable. To address this, the use of 3D extracellular matrix (ECM) microenvironments rather than 2D monolayer cultures may offer better control over cell fate and function (Lutolf et al., 2009; Metallo et al., 2007), and thus provide a more potent population of therapeutic cells.

Collagens are the main components of the heart's and blood vessels' extracellular matrix, and therefore collagen-based materials constitute a candidate choice for creating microenvironments for cardiovascular applications. Collagen-based matrices have been used successfully for the transplantation of CACs to restore perfusion and function to ischemic tissues (Suuronen et al., 2006; Zhang et al., 2008). In these studies, the use of a matrix conferred additional therapeutic effects compared to treatment with cells alone. While improved cell retention is likely to play a role, the mechanisms involved in matrix-assisted cell therapy are yet to be fully elucidated. However, the evidence suggests that collagen matrices may enhance the therapeutic potential of the delivered cells.

Therefore, the aim of the present study was to assess a collagen I-based matrix as a potential substrate for CAC culture and revascularization therapy. Specifically, we investigated the *in vitro* effects of the matrix on CAC proliferation, survival and differentiation, and on clinically relevant functional properties of CACs, such as adhesion, invasion and angiogenesis. Matrix-cultured cells were also tested *in vivo*, for their ability to vascularize and restore perfusion in the ischemic mouse hindlimb.

Materials & Methods

Materials

All reagents were obtained from Sigma-Aldrich (Oakville, Canada), unless indicated otherwise.

CAC Isolation & Culture

Methods were approved by the Human Research Ethics Board of the University of Ottawa Heart Institute. Under informed consent, approximately 100ml of peripheral blood was procured from healthy volunteers, and density-gradient centrifuged on Histopaque 1077. Peripheral blood mononuclear cells (PBMCs) were removed with the buffy coat, washed twice (0.11% EDTA, 1% FBS, in dPBS) and plated on fibronectin-coated tissue culture polystyrene (TCPS) plates in Endothelial Growth Medium-2 (EGM-2; Clonetics, Guelph, Canada; FBS, VEGF, R^3-IGF-1, and hEGF supplements added). After 4 days in culture, supernatant and non-adherent cells were discarded. Adherent cells were trypsinized (0.25%), lifted with dPBS, and considered to be circulating angiogenic cells (CACs).

Biomatrix Preparation

Similar to methods described previously (Suuronen et al., 2004), matrix was prepared from collagen I (BD Bioscience, Mississauga, Canada) and chondroitin sulfate-C (CS-C; 9:1 CS–C:CS-A). Collagen was mixed in a cold glass tube with 500µl of buffer (29ml buffer made from: 9ml FBS, 9ml 10X DMEM, 10ml 200mM HEPES, 3-5 drops gentamycin) on ice. The final concentration of collagen was 2.35mg/ml. CS-C was added to a total concentration of 11.49 mg/ml. Glutaraldehyde (1.5%) in 1X DMEM was used to cross-link the CS-C and collagen and left for 45 minutes on ice; 20% glycine was then added to react

with excess glutaraldehyde and left for 45 minutes on ice. Matrix solution was added to 24-well plates (500µl each) or was evenly spread on a 10cm tissue culture dish, and gels were formed at 37˚C for 30 minutes. After gelation, EGM-2 was added to each gel to prevent dessication, and pH was maintained between 7.2 and 7.5.

CAC Characterization

CACs were lifted from fibronectin-coated plates using 0.25% trypsin for 5 minutes, and vigorous pipetting with dPBS, prior to staining for progenitor markers CD34 and CD133, endothelial markers CD31 and CD144, and common leukocyte antigen CD45 for 30 minutes at 4˚C in HBSS. Cells were washed and resuspended in 0.5% BSA in dPBS and subsequently analyzed by flow cytometry.

Proliferation Assay

CACs were lifted from fibronectin-coated plates, and 5×10^5 cells were plated on matrix-coated plates, and additional fibronectin plates, as controls, with 10µM 5-ethynyl-2'-deoxyuridine (EdU) in 1ml EGM-2. EdU is taken up by cells as a thymidine analog and incorporates into new DNA, and is used to indicate DNA replication and cell proliferation. After 24 hours, cells were lifted as previously described, and stained for CD133 for 30 minutes at 4˚C in HBSS. The incorporation of EdU into DNA was then determined by fixing and permeabilizing the cells, and staining with an AlexaFluor488 azide, as per the kit manufacturer's protocol (Invitrogen, Burlington, Canada). Cells were then stained for CD34 and CD144 for 30 minutes at 4˚C in HBSS, then cells were washed and resuspended in 0.5% BSA in dPBS for analysis by flow cytometry.

Apoptosis Assay

CACs were lifted from fibronectin-coated plates, and 5×10^5 cells were plated on matrix-coated plates, and additional fibronectin plates. Cells were subjected to serum starvation to induce apoptosis, by culture in 1ml EGM-2 without serum and VEGF (26). After 48 hours, cells were lifted as previously described, before being stained for CD34, CD133, and CD144 for 30 minutes at 4˚C in HBSS. Cells were then washed and resuspended in 2.5µg/ml 7-Aminoactinomycin D (7-AAD) in 0.5% BSA in dPBS for subsequent analysis by flow cytometry. 7-AAD does not pass through intact membranes of viable cells. It is used to indicate dead or dying cells, as it can diffuse through damaged membranes and bind to DNA.

AKT protein expression

CACs were seeded on matrix- or fibronectin-coated plates, subjected to serum-starvation and incubated at 37ºC under hypoxic conditions (1% O_2 with 5% CO_2) for 48 hours. Cells were then lysed using 2% SDS, 2% β-mercaptoethanol, 1% sodium orthovanadate, in 50mM Tris-HCl, pH 6.7, supplemented with phosphatase and protease inhibitor cocktail tablets (Roche, Laval, Canada). For Western blotting, equal amounts of lysate were loaded into 10% Precise Protein Gels (Fisher, Ottawa, Canada) and resolved by SDS-PAGE. Gels were run according to manufacturer's protocol and protein transfer was performed at 4ºC onto polyvinylidene fluoride membranes (Immobilon-FL, Millipore). Membranes were then blocked in 5% nonfat dry milk in TBS-Tween 20 buffer for 1 hour before probing with primary antibodies. To detect Akt expression, blots were incubated with Akt (pan) and p-Akt1 (Cell Signaling Technology, Pickering, Canada), at 1:1000 in 5% BSA, 1X TBS, 0.1% Tween-20 at 4ºC overnight. Secondary antibody (Anti-rabbit IgG, HRP-linked antibody from Cell Signaling Technology) was applied at 1:1000 dilution for 1 hour at room temperature and the signal detected using the Pierce SuperSignal West Pico chemiluminescence kit.

Equal loading was confirmed using anti-GAPDH (mouse monoclonal, Millipore). Bands were quantified using densitometry and results are expressed as a ratio of p-Akt1:Akt (pan).

Differentiation Assay

CACs were lifted from fibronectin-coated plates, and 5×10^5 cells were plated on matrix-coated plates, and additional fibronectin plates, in 1ml EGM-2. After 4 days in culture at 37˚C, cells were lifted as previously described. Cells were stained for CD31, CD34, CD133, and CD144 for 30 minutes at 4˚C in HBSS, then washed and resuspended in 0.5% BSA in dPBS for immediate analysis by flow cytometry.

Flow Cytometry

The following antibodies were used: CD31-FITC (Beckman Coulter, Mississauga, Canada); CD34-PE-Cy7 (eBioscience, San Diego, USA); CD133-APC (Miltenyi Biotec, Bergisch-Gladbach, Germany); CD144-PE (Beckman Coulter); and anti-EdU-Alexa488 (Invitrogen). In controls, isotype-matched FITC-, PE-Cy7-, APC-, PE- and Alexa488-conjugated antibodies were used. All flow cytometry was performed on a FACSAria™ (BD Biosciences, Mississauga, Canada) immediately after sample staining was complete. Data was analyzed using FACSDiva software.

Adhesion Assay

After 4 days of culture, cells were lifted as previously described. CACs (2×10^4) were resuspended in 1ml of EGM-2 and seeded in 12-well dishes containing fibronectin-coated coverslips. After 1 hour at 37ºC, with or without the ERK inhibitor PD98059 (20 μmol/L, added directly in the media), the media was aspirated and adherent cells were fixed with 4% paraformaldehyde. Coverslips were washed twice with dPBS, and placed on slides with 4',6-diamidino-2-phenylindol-(DAPI) containing mounting medium (Vector Laboratories). Six

random fields-of-view were imaged using a Zeiss Z1 fluorescent microscope, and $DAPI^+$ cells were counted.

Angiogenesis Assay

ECMatrix (Chemicon, Temecula, USA) was prepared as per the manufacturer's protocol, and 80µl of the mix was added into wells of a 96-well plate and incubated at 37ºC for 1 hour. Immortalized human umbilical vein endothelial cells (HUVECs; (Gagnon et al., 2002)) were maintained in HUVEC media (10% FBS, 1% L-Glutamine, 2µg/ml sodium heparin, 1% penicillin/streptomycin, 30µg/ml endothelial growth supplement (BD Biosciences), in M199 media, pH 7.2). When confluent, HUVECs were lifted similarly to CACs, and stained with CellTracker™ Orange (5-(and-6)-(((4-chloromethyl)benzoyl)amino) tetramethylrhodamine (CMTMR; Invitrogen), as per the manufacturer's protocol. After 4 days of culture, CACs were lifted as previously described, and incubated at 37ºC in 50µg/mL DAPI. Both cell populations were washed twice to remove excess dye, and then 1×10^4 of each cell type were co-cultured in one well containing the ECMatrix for 18 hours. Afterwards, supernatant was removed and cells were imaged using a Zeiss Z1 fluorescent microscope. Total endothelial network length was quantified using Image-Pro Express software, and $DAPI^+$ cells were counted as either contributing to structure formation (co-localization of DAPI and CMTMR), or not contributing (no co-localization). Experiments were performed in triplicate, and 3 random fields-of-view were imaged per well.

Invasion Assay

Cell populations generated from fibronectin and matrix culture methods were added to the upper chamber of a Cytoselect Basement Membrane Cell Invasion Assay (Cell Biolabs Inc., San Diego, CA) in serum-free media with or without PD98059 (20umol/L). The lower

chamber contained EGM-2 with serum and VEGF. After 48 hours, cells that had penetrated the basement membrane and adhered to the lower insert membrane were stained, lysed, and quantified at 560nm, as per the manufacturer's protocol.

ERK Protein Expression

After 4 days of culture, cells were lifted and stained with 7-AAD. Viable cells (7-AAD$^-$; 5×10^5) from each substrate were sorted using FACS. Cells were lysed and sample protein lysates were assayed by Western blotting as described above. Briefly, ERK1/2 and p-ERK1/2 primary antibodies (New England Biolabs, Pickering, Canada) were applied, both at 1:1000 dilution, and protein signal detection was conducted. Equal protein loading was confirmed using anti-GAPDH and bands were quantified by densitometry. ERK protein expression results are given as a ratio of p-ERK1/2:total ERK1/2.

Animal Model

All procedures were performed with the approval of the University of Ottawa Animal Care Committee, in accordance with the National Institute of Health's Guide for the Care and Use of Laboratory Animals. A unilateral hindlimb ischemia mouse model was used to compare collagen matrix- versus fibronectin-cultured CACs *in vivo*. The left proximal femoral artery of 8-9 wk old athymic nude CD1 mice (Jackson Laboratories, Bar Harbor, USA) was ligated to induce ischemia, as described (Limbourg et al., 2009). Survival for all treatment groups was 100%. Immediately following ligation, mice randomly received one of the following treatments in a volume of 50uL dPBS, administered by multiple injections into the ischemic main adductor muscle using a 27-gauge needle: (1) 5×10^6 4-day matrix cultured CACs; (2) 5×10^5 4-day fibronectin cultured CACs; or (3) dPBS only (n=6 for all treatment groups).

Laser Doppler Perfusion Analysis

Hindlimb blood perfusion was measured using a multifiber needle probe and a laser Doppler blood flow monitor from Moor Instruments (Axminster, UK) in both ischemic and non-ischemic hindlimbs before and after femoral artery ligation, as well as on days 4, 7, 10 and 14 postoperatively. The results are expressed as a ratio of ischemic/non-ischemic hindlimb blood flow.

Histology and Immunohistochemistry

Mice were sacrificed after 14 days and blood samples were procured from all animals via cardiac puncture and the sera collected for cytokine array analysis. Gastrocnemius muscle was dissected and split two ways: the upper half was snap frozen for cytokine analysis, and the lower half was embedded in OCT and cooled in liquid nitrogen.

Muscle sections of 5μm were prepared and arterioles were identified by direct staining with α-smooth muscle actin antibody (prediluted rabbit polyclonal; Abcam) followed by secondary antibody at 1:600 dilution (Alexa Fluor 488, anti-rabbit IgG; Invitrogen). Imaging was performed with a Zeiss Z1 fluorescent microscope. To quantify arteriole density, 6 random microscopic fields were counted per sample in a blinded fashion. Cross-sectional arteriole area was determined using ImagePro Plus. Additional hindlimb sections were incubated with monoclonal anti-human mitochondria (1:40; Chemicon) or monoclonal anti-human nuclei MAB1281 (1:50; Millipore), following the manufacturer's instructions.

Cytokine Arrays

Frozen sections of muscle explants and terminally-collected serum were lysed and prepared for anti-mouse cytokine arrays (Raybiotech, Norcross, USA). Protocols were

carried out as per the manufacturer's recommendations. Results are expressed as relative levels of cytokine-to-total protein.

Statistical Analysis

Due to donor variability, data was reported as the mean fold-change of treatment-to-control ± standard error, and analyzed using paired *t*-tests. For flow cytometry, values for calculating the fold-change were expressed as delta mean fluorescence intensity (MFI) values (i.e. specific MFI minus isotype control MFI). Probability values of $P<0.05$ were considered statistically significant. All flow cytometry experiments were performed with $n=5$, functional assays were performed with $n=4$, and animal work was performed with $n=6$.

Results

Cell Proliferation

After 24 hours of culture, CAC proliferation on matrices was increased 1.7-fold compared to culture on fibronectin (Fig. 2-1; $P<0.05$). Further analysis showed that there was no significant change in the number of proliferating cells positive for CD144 ($P=0.4$); however, a trend for increased proliferation was observed for $CD133^+$ cells (by 2.9-fold) and significantly more proliferating $CD133^+CD34^+$ cells (by 1.6-fold) were seen on matrix compared to fibronectin (Fig. 2-1; $P=0.1$ and 0.02, respectively). CACs that were single-positive for CD34 showed reduced proliferation on matrices, corresponding to 0.7-fold of their proliferation on fibronectin (Fig 2-1; $P<0.001$).

Cell Survival and Akt Phosphorylation

Cell death from serum starvation averaged 45±36% across all groups and varied greatly among donors. For seeded CACs, there was no difference in viable cells from either fibronectin or matrix (Fig. 2-2A, B; $P=0.2$). However, there were 3.8-fold more viable $CD34^+$ cells and 7.8-fold more viable $CD133^+$ cells on the collagen matrices compared to fibronectin (Fig. 2-2A, C, D; $P=0.07$ and 0.02, respectively). Serum-starved hypoxic CACs cultured on matrix had a 1.6-fold increase in p-Akt (Fig. 2-2E, F; $P=0.05$).

Figure 2-1. Fold-change in the total number of proliferating cells, as indicated by positive staining for EdU, and the fold-change in proliferating $CD144^+$, $CD34^+$, $CD133^+$, and $CD34^+CD133^+$ after 24 hours of culture. (n=5)

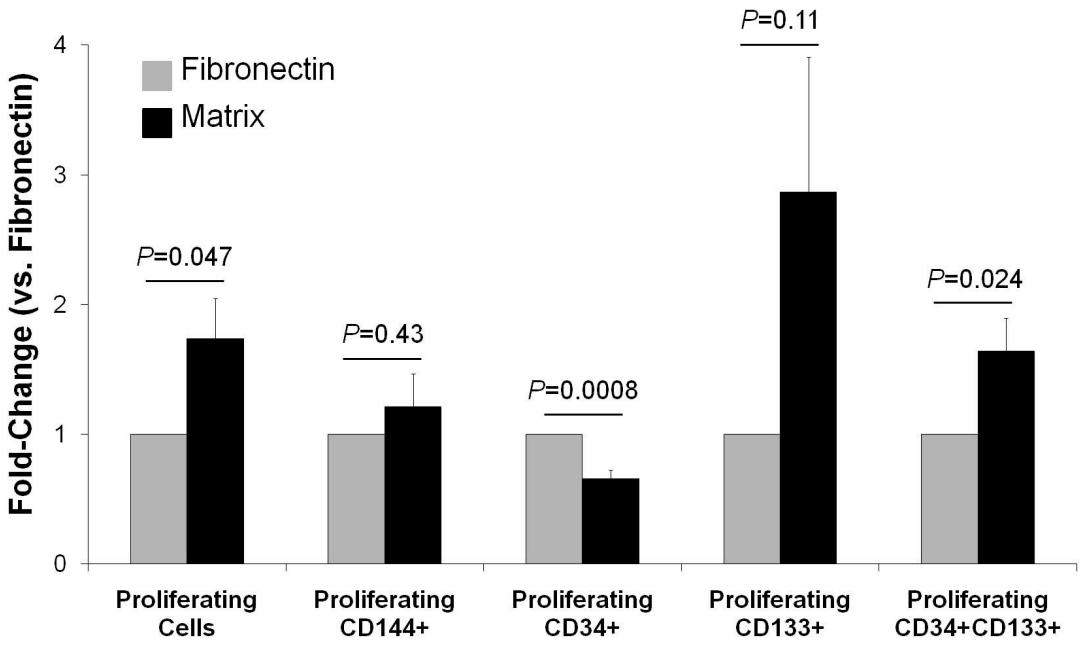
Fold-Change (vs. Fibronectin)
4
3
2
1
0
Fibronectin
Matrix
P=0.047
P=0.43
P=0.0008
P=0.11
P=0.024
Proliferating Cells
Proliferating CD144+
Proliferating CD34+
Proliferating CD133+
Proliferating CD34+CD133+

Figure 2-2. Cell Viability after 48 hours of serum deprivation to induce apoptosis. Fold-changes in the number of viable cells, and fold-changes in viable $CD144^+$, $CD34^+$, and $CD133^+$ cells after 48 hours of culture in serum-starved conditions (A). Representative histograms of total viable cells (B), $CD34^+$ cells (C) and $CD133^+$ cells (D) depict fibronectin-cultured populations in grey, and matrix-cultured populations in black. (n=5) Western blotting for p-Akt and total Akt (E) reveal an increase in relative levels of p-Akt on matrix-cultured cells (F). (n=4)

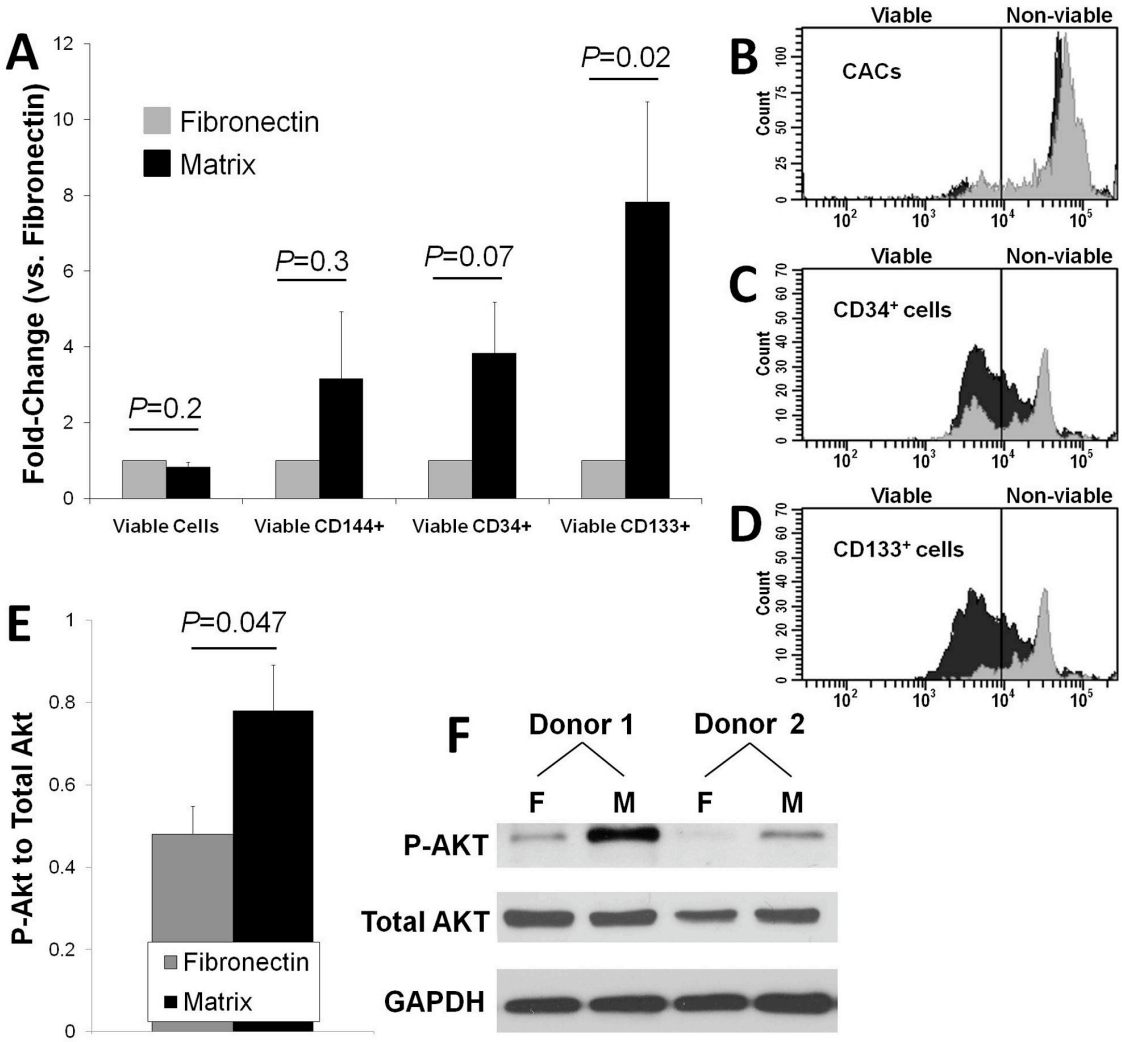
A
Fold-Change (vs. Fibronectin)
Fibronectin
Matrix
P=0.2
P=0.3
P=0.07
P=0.02
Viable Cells
Viable CD144+
Viable CD34+
Viable CD133+
B
Viable
Non-viable
CACs
Count
C
CD34+ cells
D
CD133+ cells
E
P-Akt to Total Akt
P=0.047
Fibronectin
Matrix
F
Donor 1
Donor 2
F
M
F
M
P-AKT
Total AKT
GAPDH

Enrichment of Endothelial and CAC Phenotypes

After 4 days of culture on collagen matrices, 2.3- and 3.2-fold more CACs expressed the endothelial cell markers CD31 and CD144, respectively, compared to CACs at day 0 (Fig. 2-3A, B; P=0.03; P=0.02). Additionally, there were 3.7-fold more $CD31^+CD144^+$ cells (Fig. 2-3A, B; P=0.003). Differences were also noted in progenitor markers for CACs cultured on matrices: there were 2.6-fold more $CD34^+$ cells (P=0.02); 4.2-fold more $CD133^+$ cells (P=0.06); and 3.4-fold more $CD34^+CD133^+$ cells (P=0.03), compared to CACs at day 0 (Fig. 2-3C, D). Although populations expressing endothelial markers also expressed the common leukocyte antigen CD45, the proportions of $CD31^+CD45^-$ and $CD31^+CD144^+CD45^-$ cells were greater in the matrix-cultured populations. Specifically, in $CD45^-$ populations, there were 1.4- and 3.6-fold more $CD31^+$ (P=0.03) and $CD31^+CD144^+$ (P=0.05) cells, respectively, after culture on matrix (Fig. 2-3E).

Augmentation of Angiogenesis

When co-cultured with endothelial cells, matrix-cultured CACs supported a greater formation of capillary-like networks, by 18% (P=0.02; Fig. 2-4A, C, D). These cells also had a greater presence (by 1.9-fold; P=0.02) within or adjacent to the formed capillary-like structures, as indicated by co-localization of CACs (DAPI) and endothelial cells (red, CMTMR; Fig. 2-4B, C, D).

Figure 2-3. The fold-change in the number of cells expressing endothelial markers CD31 and CD144 after 4 days of culture on fibronectin or matrix, relative to baseline measurements (A). Representative histograms of $CD31^+$ and $CD144^+$ cells on fibronectin and matrix (B). The fold-change in the number of cells expressing progenitor markers CD34 and CD133 after 4 days of culture on fibronectin or matrix, relative to baseline measurements (C). Representative histograms of $CD34^+$ and $CD133^+$ cells on fibronectin and matrix (D). IgG controls are indicated as grey and cell counts are black. Gating on non-leukocyte, CD45-negative cells shows an increase in endothelial phenotypes after matrix culture (E). (n=5)

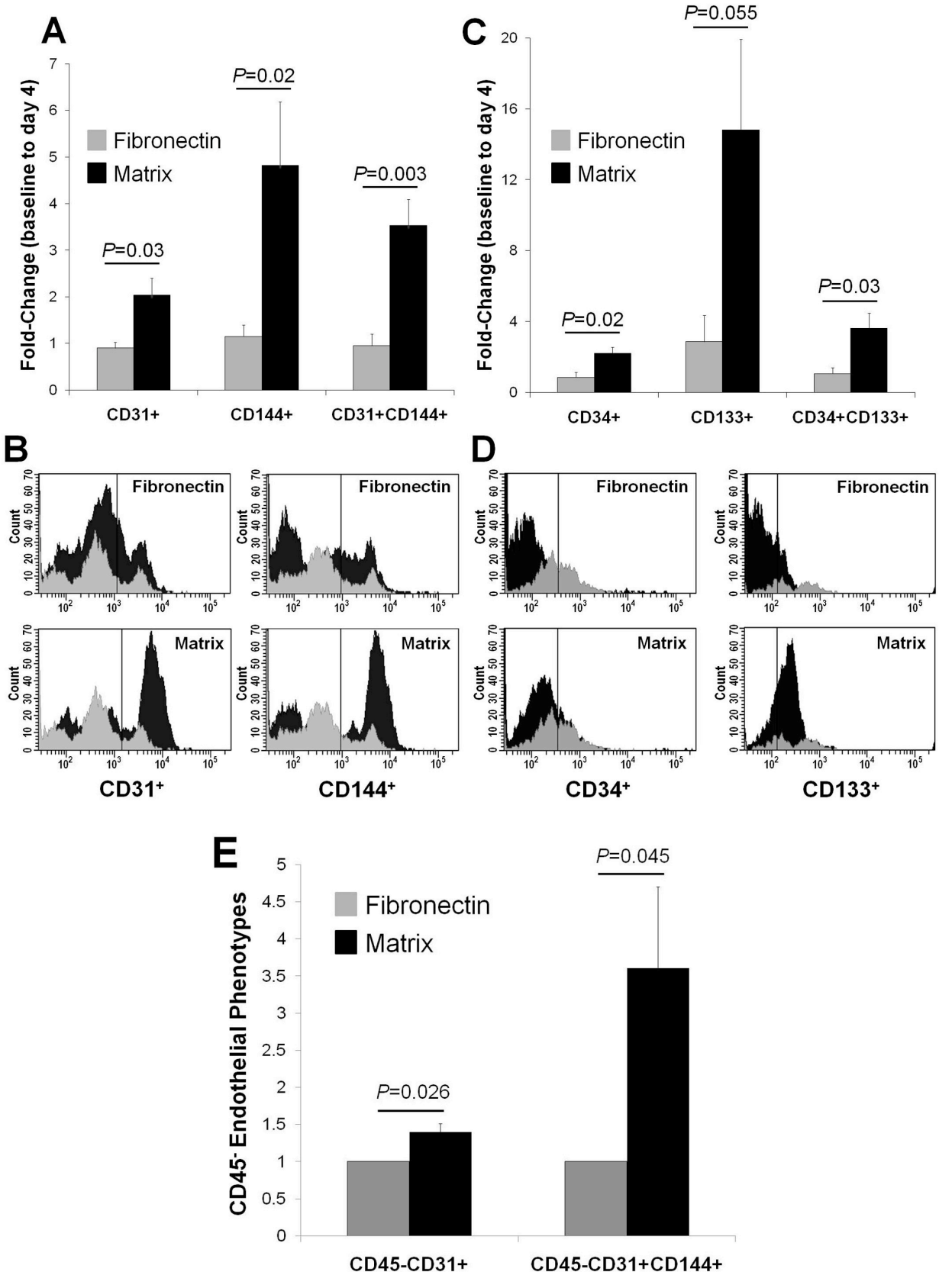
A
Fold-Change (baseline to day 4)
Fibronectin
Matrix
P=0.03
P=0.02
P=0.003
CD31+
CD144+
CD31+CD144+
C
Fold-Change (baseline to day 4)
Fibronectin
Matrix
P=0.02
P=0.055
P=0.03
CD34+
CD133+
CD34+CD133+
B
Fibronectin
Matrix
Count
CD31+
CD144+
D
Fibronectin
Matrix
Count
CD34+
CD133+
E
CD45- Endothelial Phenotypes
Fibronectin
Matrix
P=0.026
P=0.045
CD45-CD31+
CD45-CD31+CD144+

Figure 2-4. Assessment of CAC contribution to angiogenesis. Vessel-like HUVEC structures are stained in red; CACs are stained with DAPI (blue). Co-culture of HUVECs with CACs cultured on matrix increased total network length (A), and significantly more of these CACs were proximally associated with structures (B), as measured by co-localization of DAPI with HUVEC structures (white arrows). Representative images of co-cultures with fibronectin- (C) and matrix- (D) cultured CACs. Scale bar = 100μm. (*n*=4)

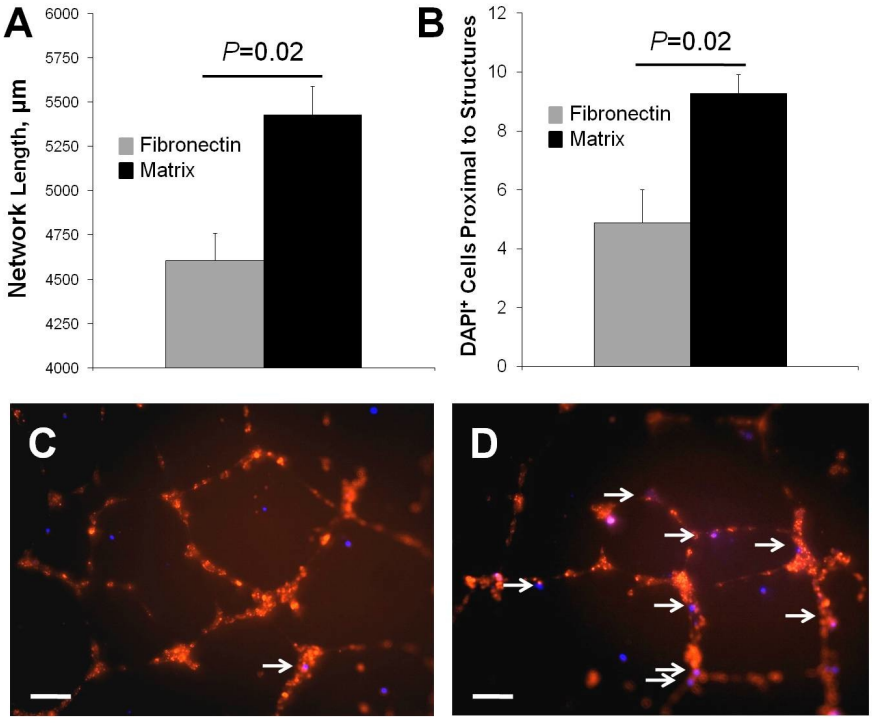
A
Network Length, µm
6000
5750
5500
5250
5000
4750
4500
4250
4000
P=0.02
Fibronectin
Matrix
B
DAPI+ Cells Proximal to Structures
12
10
8
6
4
2
0
P=0.02
Fibronectin
Matrix
C
D

ERK1/2 Phosphorylation and Involvement in CAC Adhesion and Migration

Cells cultured on matrix had 1.4-fold more phosphorylated ERK1 (P=0.05) and 1.1-fold more phosphorylated ERK2 (P=0.04), when expressed as a ratio of p-ERK1/2 to total ERK1/2 (Fig. 2-5A, B), compared to cells cultured on fibronectin. More matrix-cultured cells migrated into a basement matrix hydrogel, by 1.4-fold (Fig. 2-5C; P=0.002). When ERK was inhibited, there was a 23% reduction in migration of matrix-raised CACs, compared to fibronectin-raised CACs (Fig. 2-5C; P=0.003). CACs cultured on matrix displayed greater adhesion potential (by 4.0-fold) when harvested and exposed to fibronectin (Fig. 2-5D; P=0.02). This difference was abrogated when ERK was inhibited (P=0.6).

Figure 2-5. Phosphorylation of ERK1/2 in cells after 24 hours of culture. Ratio of phosphor-ERK1/2 to total ERK1/2 (A). Western blot of fibronectin- (*F*) and matrix- (*M*) cultured cells that were lysed and probed for ERK1/2, p-ERK1/2, and GAPDH (B). (*n*=3) Increased migration (C) and adhesion (D) was observed for matrix-cultured cells. Both of these functional improvements were abrogated for CACs in the presence of ERK inhibitor. (*n*=4)

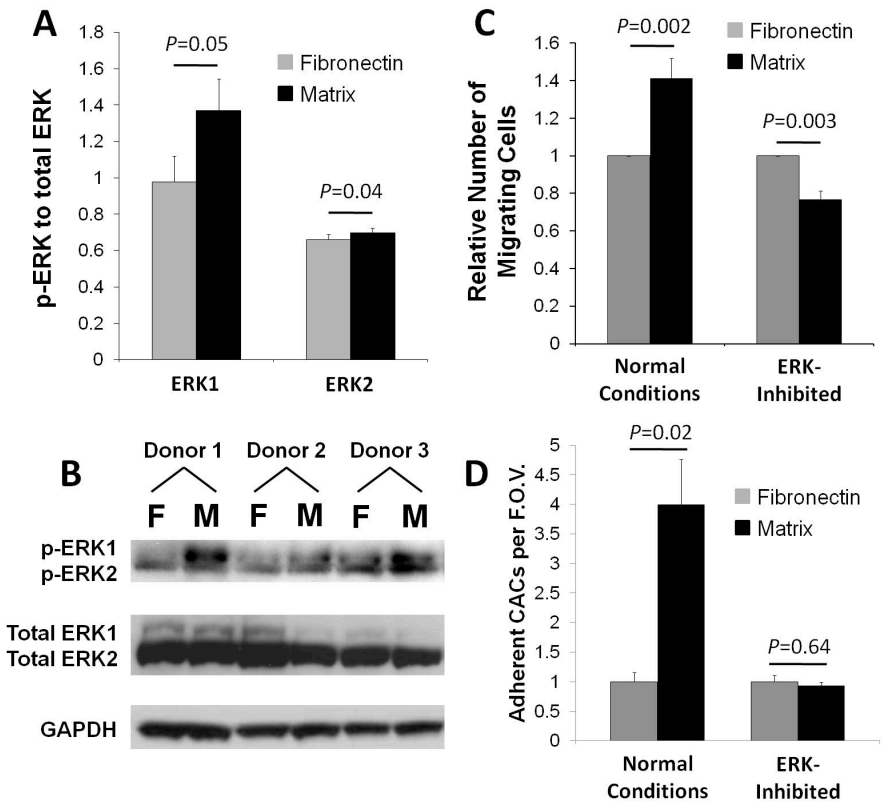
A
p-ERK to total ERK
1.8
1.6
1.4
1.2
1
0.8
0.6
0.4
0.2
0
P=0.05
P=0.04
Fibronectin
Matrix
ERK1
ERK2
B
Donor 1
Donor 2
Donor 3
F
M
F
M
F
M
p-ERK1
p-ERK2
Total ERK1
Total ERK2
GAPDH
C
Relative Number of Migrating Cells
1.6
1.4
1.2
1
0.8
0.6
0.4
0.2
0
P=0.002
P=0.003
Fibronectin
Matrix
Normal Conditions
ERK-Inhibited
D
Adherent CACs per F.O.V.
5
4.5
4
3.5
3
2.5
2
1.5
1
0.5
0
P=0.02
P=0.64
Fibronectin
Matrix
Normal Conditions
ERK-Inhibited

Perfusion and Arteriole Assessment of CAC-Treated Ischemic Hindlimbs

The viability at the time of transplantation was 92.6±2.8% and 94.8±2.6% for fibronectin- and matrix-cultured CACs, respectively (P=0.2). At day 4 post-treatment, mouse hindlimbs receiving PBS experienced a further 20% reduction in perfusion (Fig 2-6A; P=0.05). The perfusion defect created by ligation surgery remained unchanged in animals receiving fibronectin-raised CACs, which was maintained up to 14 days (Fig. 2-6A; P>0.9). At later time points (days 7-14), there was a trend for improved perfusion in these animals over PBS recipients (Fig. 2-6A; P=0.09). Animals receiving matrix-cultured CACs exhibited increased perfusion by day 4, and this was maintained through day 14, compared to other treatments (Fig. 2-6A; P<0.02 from days 4 to 14).

At termination (day 14), a trend for increased arteriole density in hindlimbs receiving matrix-raised CACs was observed (Fig. 2-6B; P=0.09). The average cross-sectional area of arterioles increased with CAC transplantation, compared to PBS, specifically by 1.8- and 3.4-fold for fibronectin- (P=0.01) and matrix-raised CACs (P=0.04), respectively (Fig. 2-6C-F).

Figure 2-6. Transplantation of CACs (matrix- or fibronectin-cultured) for the treatment of hindlimb ischemia in mice. Matrix-cultured cells improved perfusion early after administration (A), whereas perfusion was maintained in animals receiving fibronectin-raised cells, and was further reduced in PBS-treated animals. Matrix-raised CAC treatment tended towards an increase in arteriole density (B), and yielded significantly larger arterioles (C). D, E, F are representative images of arterioles in PBS, fibronectin-CAC and matrix-CAC treatments, respectively. *P<0.05 vs. all other treatments; **0.05<P<0.1 vs. PBS; ***P<0.05 vs. post-op perfusion; $^{\dagger}P$<0.05 vs. PBS.

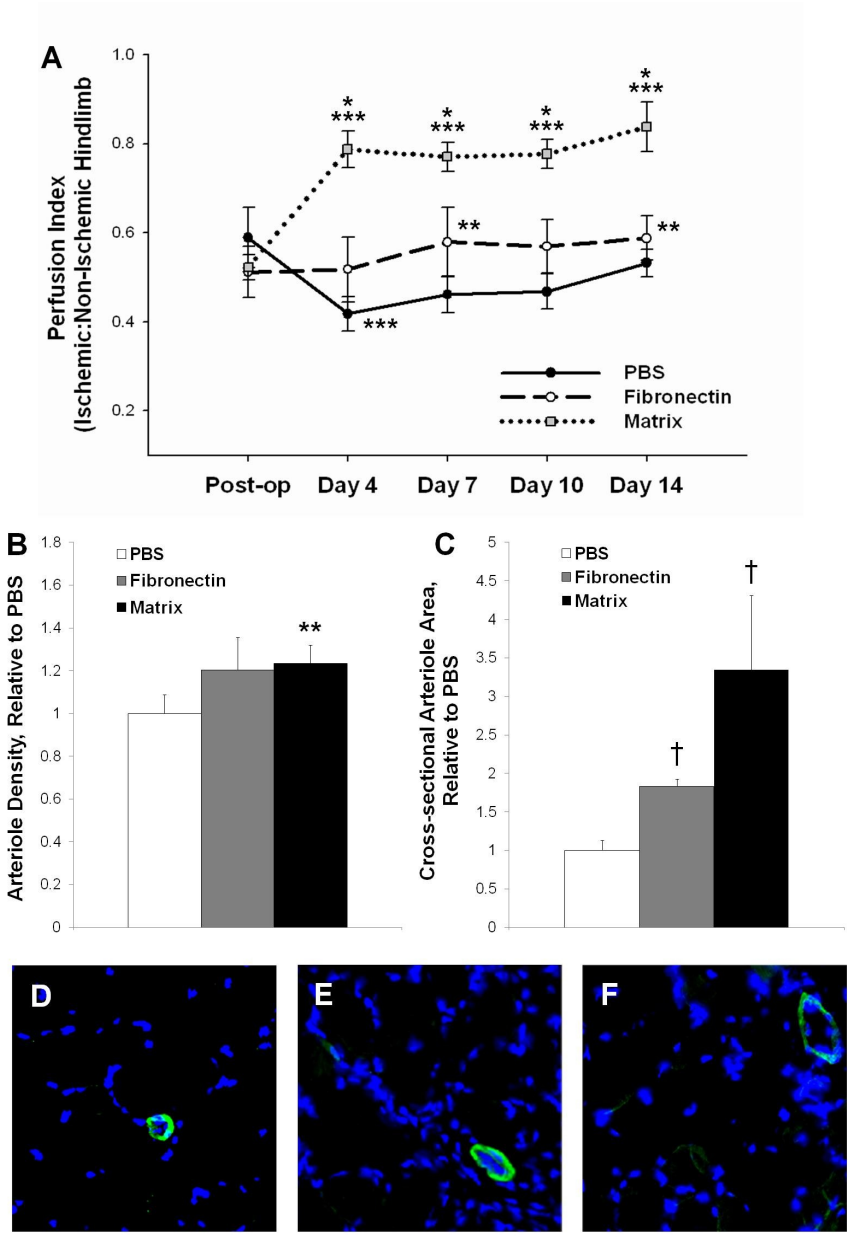
A
Perfusion Index
(Ischemic:Non-Ischemic Hindlimb
1.0
0.8
0.6
0.4
0.2
Post-op
Day 4
Day 7
Day 10
Day 14
PBS
Fibronectin
Matrix
B
Arteriole Density, Relative to PBS
C
Cross-sectional Arteriole Area, Relative to PBS
D
E
F

Human Cell Engraftment

Despite the use of anti-human antibodies, no persistent transplanted human cells could be detected in sections at the time of sacrifice.

In vivo Cytokine Profiles

Many cytokines were significantly increased in the serum of animals receiving CAC transplantation. Treatment with matrix-raised CACs increased levels of granulocyte colony-stimulating factor (G-CSF), interleukin (IL)-1α, IL-1β, IL-6, IL-10, stem cell factor (SCF), stromal cell-derived factor-1α (SDF-1α) and vascular endothelial growth factor (VEGF) (Fig. 7A; all $P<0.05$). Fibronectin-raised CACs trended towards increases in IL-1α, SDF-1α and VEGF (Fig. 2-7A; all $P<0.1$). In the hindlimb muscle, matrix-raised CACs increased local levels of IL-1β (Fig. 2-7B; $P<0.05$), and both CAC populations trended towards increases in IL-1α levels (Fig. 2-7B; $P<0.1$).

Figure 2-7. Cytokine profiles of serum (A) and hindlimb (B) of mice 2 weeks after treatment. Relative levels of granulocyte-colony stimulating factor (G-CSF), interleukin (IL)-1α, IL-1β, IL-6, IL-10, monocyte chemoattractant protein-1 (MCP-1), stem cell factor (SCF), stromal cell-derived factor-1α (SDF-1α), tumor necrosis factor-α (TNF-α), vascular cell adhesion molecule-1 (VCAM-1), and vascular endothelial growth factor (VEGF) were assessed. *P<0.05 vs. PBS; **0.05<P<0.1 vs. PBS.

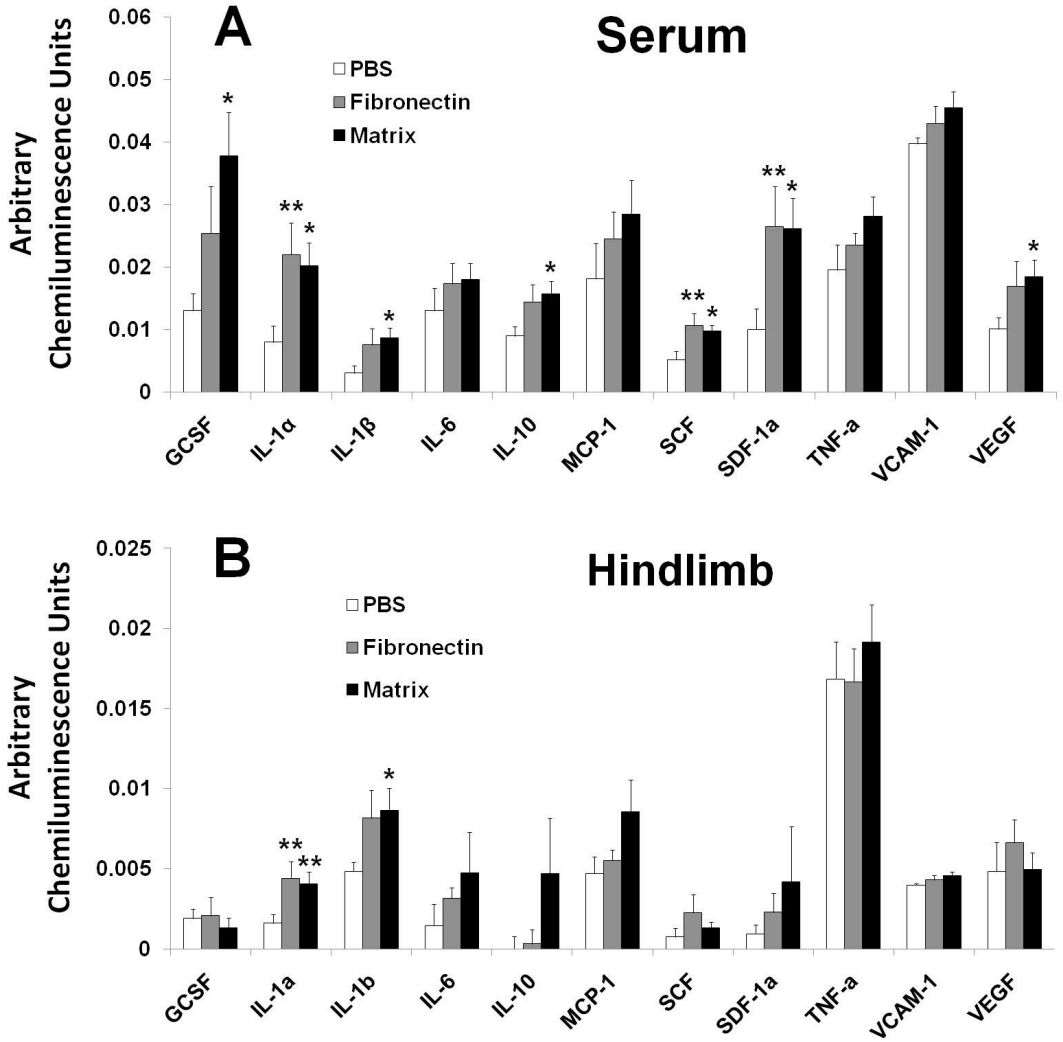
A
Serum
PBS
Fibronectin
Matrix
Arbitrary Chemiluminescence Units
0.06
0.05
0.04
0.03
0.02
0.01
0
GCSF
IL-1α
IL-1β
IL-6
IL-10
MCP-1
SCF
SDF-1a
TNF-a
VCAM-1
VEGF
B
Hindlimb
PBS
Fibronectin
Matrix
Arbitrary Chemiluminescence Units
0.025
0.02
0.015
0.01
0.005
0
GCSF
IL-1a
IL-1b
IL-6
IL-10
MCP-1
SCF
SDF-1a
TNF-a
VCAM-1
VEGF

Discussion

In this study, we found that a collagen matrix may be superior to fibronectin for the culture of circulating angiogenic cells with respect to increased proliferation, resistance to apoptosis, and endothelial cell differentiation, in addition to enriching functionally enhanced populations and improving the regenerative response in ischemia. Fibronectin is used throughout the literature as the primary substrate for obtaining CACs through adhesion-selective culture (Kalka et al., 2000). CACs are grown on fibronectin-coated plates until they reach their desired phenotype, early- or late-outgrowth stages. Although early-stage CACs readily adhere to fibronectin, their proliferation has been reported as being negligible (Hristov and Weber, 2004; Hur et al., 2004). In the present study, CAC proliferation was significantly increased on collagen matrices after 24 hours of culture, compared to fibronectin. Further analysis showed no significant change in proliferating $CD144^+$ cells, and a reduction in proliferating $CD34^+$ cells. Rather, it was the $CD133^+$ cells, whether or not they also expressed CD34, which showed increased proliferation on the collagen matrix. Since the lack of a sufficient number of *ex vivo* cultured CACs is considered to be a limitation for their use in therapy, a collagen matrix is presented as a possible superior alternative method for the culture and expansion of CACs.

During serum starvation, cells are expected to undergo apoptosis via the dsRNA-dependent protein kinase pathway (Srivastava et al., 1998). After serum deprivation, there was a slight reduction in the total number of viable cells (total CACs) cultured on collagen matrices compared to fibronectin; however, significantly more cells expressing progenitor markers ($CD34^+$ and $CD133^+$ cells) were viable on collagen than on fibronectin. This

suggests that cells of progenitor lineage are more resistant to death in a pro-apoptotic environment with culture on collagen matrix.

In hypoxic conditions, CACs have been shown to enhance their resistance to apoptosis via the PI3K/Akt pathway (Dai et al., 2008). Activation of the Akt pathway can also lead to a more "active" CAC phenotype with enhanced transendothlelial migration, and Akt gene transfer to normal muscle showed increased entrapment of endothelial progenitor cells (Hur et al., 2007). With respect to ECs, the Akt pathway can increase survival (Fujio and Walsh, 1999), migration (Morales-Ruiz et al., 2000), and adhesion molecule expression (Radisavljevic et al., 2000), and increases in phosphorylated Akt are indicative of cell survival or cytoprotection (Lu et al.). Mesenchymal stem cells over-expressing the Akt protein were shown to be effective in preventing remodeling and restoring performance of infarcted hearts (Mangi et al., 2003). Taken together with our demonstrated increase in p-Akt during matrix culture in serum starvation and hypoxia, our hypothesis of improved CAC survival mediated by collagen matrix is further supported.

After 4 days of culture on matrix, significantly more cells expressed the endothelial cell markers CD31 and CD144, compared to day 0. By showing that the seeded CACs can acquire endothelial-specific markers, this suggests that the gels are able to promote CAC-to-EC differentiation. As expected, many of the $CD31^{+}CD144^{+}$ cells expressed CD45, indicating leukocyte, and not endothelial, origin; however, the number of $CD31^{+}CD144^{+}CD45^{-}$ endothelial phenotype cells was greater after culture on matrix, providing evidence for the generation of true endothelial cells from matrix-cultured CACs. Interestingly, Akt expression has also been positively correlated with circulating angiogenic cell maturation and differentiation (Mogi et al., 2008), in addition to its previously described

involvement in prevention of apoptosis. In this study, there were more cells expressing the CD34 and CD133 progenitor markers for CACs that were cultured on collagen matrices. It was not expected that the collagen matrix would both differentiate CACs into an endothelial lineage, as well as maintain a population of more primitive, self-renewing progenitor cells. This scenario may be ideal in a therapeutic setting: to be able to support a progenitor cell population, while also encouraging the differentiation of cells to an endothelial phenotype.

Even though cells cultured on fibronectin had the advantage of already being phenotypically fibronectin-adherent, matrix-cultured cells displayed greater adhesion potential to fibronectin after a rapid exposure. Enhanced adhesive potential is a desired trait for therapeutic cell populations, as one of the main limitations of cell therapy is poor engraftment of transplanted cells (Cho et al., 2007; Fukushima et al., 2007). Complementary to this, the enriched progenitor populations also had a greater ability to penetrate a basement membrane towards a chemotactic stimulus in an invasion assay. Cells with a strong ability to transmigrate will have better access to vasculature, and to augment new vessel formation from pre-existing vessels. Although it is debatable whether or not CACs will incorporate into developing vasculature, we have demonstrated that our enriched population preferentially associates itself in close proximity, or even within, developing capillary-like structures in an angiogenesis assay. Matrix-cultured CACs may also have exerted a greater pro-angiogenic effect via cytokine secretion, contributing to the greater total capillary-like network size that was observed. Overall, we have demonstrated the ability to produce potent, pro-angiogenic cells from a heterogeneous CAC culture, which could be a novel source of clinically-relevant transplantable cells.

One important signaling pathway in many active cell types is the extracellular signal-regulated protein kinase (ERK) pathway. ERKs are mitogen-activated protein kinases, which are ubiquitous enzymes involved in the transduction of external signals to regulate intracellular activities, such as cell growth, differentiation, and proliferation (Deng et al., 2006; Robinson and Cobb, 1997; Sharma et al., 2003). Recently, ERK activation in endothelial cells was shown to support neovessel formation (Uraoka et al., 2009) and endothelial proliferation (Srinivasan et al., 2009). It has also been observed that activation of Ras/Raf, upstream pathway regulators, can improve endothelial cell survival via resistance to apoptosis (Alavi et al., 2003). Our results show an increase in ERK pathway activation in CACs after culture on a collagen matrix, which may help to explain the observed increases in progenitor proliferation, differentiation, survival and augmented angiogenesis. The ERK pathway can be activated by integrin binding at the cell's surface; therefore the differences in ERK observed between matrix- and fibronectin-cultured CACs may be attributable to altered integrin-mediated binding, since the two substrates differ in their integrin binding motifs, as previously described [34]. Although the increases in phosphorylated (active) ERK proteins are small, we have shown these low levels to be highly relevant in CAC function. Inhibition of ERK abrogated the improved potential of matrix-cultured CACs, demonstrating the importance of ERK in CAC adhesion to collagen matrix. Also, ERK inhibition not only reduced the ability of matrix-cultured cells to migrate, but reduced this to less than that of the fibronectin-cultured CACs; highlighting the importance of ERK in CAC function, particularly in CACs that have been raised in a 3-D matrix environment.

Transplantation of matrix-raised CACs markedly improved perfusion as early as day 4, suggesting a superior ability to aid in the restoration of blood flow in ischemic tissue. This

observation correlated with a trend for greater arteriole density and an increase in arteriole size. Cross-sectional arteriole area has been shown to increase over 4 weeks after ischemic damage (Ruvinov et al.). Although transplanted CACs were not observed in tissue sections at 2 weeks, their pro-regenerative effects were still present, as evidenced by the increased levels of many vasculogenic and recruiting cytokines in the serum. Our results suggest that maintenance of the CAC-induced response was largely systemic, since there were relatively little cytokine differences in lysed hindlimb. These results are similar to those reported in a recent publication by Cho et al., whereby human cells were transplanted into infarcted mouse myocardium (Cho et al., 2007). In their study, Cho and colleagues observed that the transplanted cells did not persist, that cytokines produced by transplanted cells were not detected after 1 week, and that activated host cells were responsible for maintaining the regenerative response, as indicated by increased systemic cytokines. The use of growth factors/cytokines has been tested as therapy for restoring ischemic tissue, through the application of growth factor-releasing scaffolds (Sun et al.), systemic administration of cytokines (Sato et al., 2001), injection of conditioned medium (Di Santo et al., 2009), or engineering of growth factor-overexpressing stem cells (Tang et al.). With the observed persistence of cytokine effects in the current study, we have demonstrated a new strategy for cytokine-mediated regeneration: *ex vivo* CAC culture on matrices prior to transplantation.

Interactions between collagen type I and several cell types in revascularization and regeneration have been described. Collagen-based biomaterials have been reported to: have a chemotactic effect on endothelial cells (Senger et al., 2002); have the ability to augment differentiation of neonatal cardiomyocytes (Zimmermann et al., 2002); enhance survival of transplanted cardiomyoblasts in infarcted hearts (Kutschka et al., 2006); promote

revascularization of ischemic hindlimbs in a rat model through progenitor cell recruitment (Suuronen et al., 2006; Suuronen et al., 2009); support proliferation of skeletal myoblasts (Lanasa and Bryant, 2009); and improve the retention of transplanted CACs (Zhang et al., 2008). Our study adds to this list of properties by demonstrating that collagen-based matrices are also likely to: 1) stimulate an active CAC phenotype that is capable of EC differentiation; 2) improve the survival and proliferation of $CD34^{+}CD133^{+}$ CACs; 3) produce a population of progenitor cells with enhanced functional capacities, mediated by the ERK pathway; and 4) lead to the generation of a potent population of cells that can restore perfusion in ischemic tissue, making these matrices ideal candidate biomaterials for progenitor culture for cell therapy.

Conclusion

We have shown that CAC culture on a collagen matrix may be superior to traditional fibronectin culture methods for producing a highly potent population of progenitors that have the capacity to proliferate, differentiate, endure harsh environments, and also have improved functional capacities. Functional improvements may be explained by the activation of ERK1/2 pathways, and survival mediated by the increase of p-Akt. *In vivo*, these cells had a superior ability to restore perfusion to ischemic tissue, and induce long-lasting systemic cytokine effects. The culture method presented offers the potential of expanding and producing progenitor populations of high clinical relevance for future cell therapies.

Acknowledgments

This work was supported by grant MOP-77536 from the Canadian Institutes of Health Research (to Drs. Ruel and Suuronen) and by grant NA6121 from the Heart and Stroke Foundation of Ontario (to Dr. Suuronen). DK and TS were supported by Master's studentship awards from the Heart and Stroke Foundation of Ontario, DK was also supported by a Canadian Graduate Scholarship from the Canadian Institutes of Health Research, and YZ was supported by a doctoral research award from the Heart Stroke Foundation of Canada.

CHAPTER 3. A stromal cell-derived factor-1 releasing matrix enhances the progenitor cell response and blood vessel growth in ischemic skeletal muscle

This chapter has been published in *European Cells & Materials*, as per the following citation:

D. Kuraitis, P. Zhang, Y. Zhang, D.T. Padavan, K. McEwan T. Sofrenovic, D. McKee, J. Zhang, M. Griffith, A. Musarò, X. Cao, M. Ruel and E.J. Suuronen (2011) A stromal cell-derived factor-1 releasing matrix enhances the progenitor cell response and blood vessel growth in ischemic skeletal muscle. *Eur Cell Mater* 24:175-95.

Notes on Chapter

Pilot studies performed by a previous honours student (D. McKee) indicated that alginate microspheres were a suitable incorporation system for the controlled release of SDF-1, as observed using ELISA. The studies presented in this chapter sought to maximize the release profile of SDF-1 by incorporating the microsphere system into a collagen matrix, and assess the physical and biological consequences of doing so, using mechanical, *in vitro* and *in vivo* studies, ultimately assessing the therapeutic potential for an SDF-1 releasing system in the context of ischemic skeletal muscle.

Contributions of co-authors to results and/or manuscript:

P. Zhang co-performed animal surgeries and marrow transplantation, and assisted with flow cytometry and histological analysis [Figs. 3-4-6].

Y. Zhang assisted with adhesion and migration assays [Fig. 3-3]

D.T. Padavan contributed to SDF-1 release analyses [Fig. 3-2].

K. McEwan performed rheological assessments [Fig. 3-2A].

T. Sofrenovic helped analyze cytokine array membranes [Fig. 3-8]

D. McKee and J. Zhang contributed to microsphere evaluation [Fig. 3-1B] and analysis of SDF-1 release kinetics [Fig. 3C].

M. Griffith, A. Musarò, X. Cao, M. Ruel and E.J. Suuronen were involved in experimental planning, analysis and manuscript editing.

Abstract

Although many regenerative cell therapies are being developed to replace or regenerate ischemic muscle, the lack of vasculature and poor persistence of the therapeutic cells represent major limiting factors to successful tissue restoration. In response to ischemia, stromal cell-derived factor-1 (SDF-1) is up-regulated by the affected tissue to stimulate stem cell-mediated regenerative responses. Therefore, we encapsulated SDF-1 into alginate microspheres and further incorporated these into an injectable collagen-based matrix in order to improve local delivery. Microsphere-matrix impregnation reduced the time for matrix thermogelation, and also increased the viscosity reached. This double-incorporation prolonged the release of SDF-1, which maintained adhesive and migratory bioactivity, attributed to chemotaxis in response to SDF-1. *In vivo*, treatment of ischemic hindlimb muscle with microsphere-matrix led to increased mobilization of bone marrow-derived progenitor cells, and also improved recruitment of angiogenic cells expressing the SDF-1 receptor (CXCR4) from bone marrow and local tissues. Both matrix and SDF-1-releasing matrix were successful at restoring perfusion, but SDF-1 treatment appeared to play an earlier role, as evidenced by arterioles that are phenotypically older and by increased angiogenic cytokine production, stimulating the generation of a qualitative microenvironment for a rapid and therefore more efficient regeneration. These results support the release of implanted SDF-1 as a promising method for enhancing progenitor cell responses and restoring perfusion to ischemic tissues via neovascularization.

Introduction

Myopathies, such as ischemic heart disease and peripheral arterial disease (PAD) are significant killers in developed nations. In particular, PAD afflicts an estimated 27 million people in Europe and North America (Belch et al., 2003). This disease manifests when the flow of blood to extremities is acutely or chronically reduced (Selvin and Erlinger, 2004; Shamoun et al., 2008). Attributed to the lack of blood flow, symptoms typically include: pain, cramping, weakness and a poor ability to heal. To restore perfusion, current treatments include stent or vascular transplants with surgical intervention, or amputation; however, these options are invasive, carry risks, and amputation significantly reduces quality of life. Therefore, non-invasive options for restoring perfusion would be invaluable for PAD patients. Recent years have seen the generation of many novel approaches for developing tissue substitutes to replace or regenerate ischemic muscle; however, the supply of sufficient and appropriate vasculature represents a major limiting parameter for a successful therapeutic approach (Kaully et al., 2009; Ko et al., 2007).

To augment reparative processes, regenerative therapies using bone marrow-, blood-, or tissue-derived progenitor cells have emerged; however, the results of these treatments are controversial and there is growing evidence to suggest that non-embryonic transplanted cells do not successfully integrate with host tissue (Murry et al., 2006; Suuronen et al., 2007). It is now believed that functional improvement results from neovascularization and the restoration of blood flow to ischemic muscle, and that this phenomenon is initiated, maintained, and enhanced by paracrine factors and secondary recruitment of progenitor cells (Cho et al., 2007; Formigli et al., 2007).

After ischemic injury, an endogenous response to recruit the endogenous progenitor cells is initiated (Hofmann et al., 2005). Regarded as critical to this process is the up-regulation and release of the cytokine stromal cell-derived factor-1 (SDF-1) from ischemic muscle (Askari et al., 2003) and the subsequent recruitment of circulating progenitor cells (CPCs), mobilized from distal tissues, such as bone marrow, into ischemic tissue (De Falco et al., 2004). However, the stem cell recruitment response is short-lived and tissue accumulation is low (Fazel et al., 2006; Wojakowski et al., 2004). Recruited CPCs are observed to be pro-angiogenic (Park et al., 2004; Suuronen et al., 2009) and are thought to augment functional recovery by promoting neovascularization.

This study aims to use the SDF-1 signaling mechanism in an effort to amplify the endogenous response to ischemia and the recruitment of vasculogenic progenitor cells. Herein, we report on the encapsulation of SDF-1 into microspheres, which are added to an injectable collagen-based matrix that thermogels at physiological temperature. We provide evidence that treatment with an SDF-1 releasing collagen matrix improves the vasculogenic response of ischemic muscle, mediated by the recruitment of progenitor cells.

Materials & Methods

All reagents were obtained from Sigma-Aldrich (Oakville, Canada), unless otherwise indicated.

Generation of Microspheres

Through a physical cross-linking reaction, blank (no peptide added) alginate microspheres were created with 1.25% sodium alginate (w/v). The solution was added to a syringe and forced through a J1 Encapsulation Device (Nisco, Zurich, Switzerland) at 1ml/min, using a syringe pump, and 9.8L/min N_2 gas. Microspheres were allowed to fall into a 2% $CaCl_2$ (w/v) cross-linking bath, and kept stirring for 20 minutes before washing with PBS, and snap-freezing in liquid nitrogen. SDF-1 loaded microspheres were created by adding 200ng SDF-1 per g of alginate solution during sodium alginate solubilization. Microspheres with both human (Cedarlane Laboratories, Hornby, Canada) and murine SDF-1 (Biovision, San Francisco, USA) were generated, and stored at -80ºC.

Microsphere Morphology

Microspheres were thawed and suspended in PBS. Images were taken using an inverted phase contrast microscope (Olympus 1x81F), and microsphere size was assessed using Image-Pro Plus. Microsphere ultrastructure was observed using a Phillips XL-30 scanning electron microscope (Hillsboro, USA); WD = 7.0 and keV = 1.2. Microspheres were fixed in 3% glutaraldehyde for 2 h, washed and subsequently dehydrated in various ethanol dilutions (30%, 50%, 70%, 80%, 90%, 95%, 99%) for 5 min each before being critically point-dried. Specimens were mounted on stubs and coated with Pd/Au using a Hummer Sputter Coater (Ladd Research, Williston, USA).

Matrix Preparation

As described previously (Suuronen et al., 2009), a collagen matrix was created on ice, using a cross-linking mixture containing a 1:1 molar ratio of N-(3-dimethylaminopropyl)-N'-ethylcarbodiimide hydrochloride and N-hydroxysuccinimide (EDC/NHS; 13mM) in 2(-N-morpholino) ethanesulfonic acid (MES) buffer, a solution of 1% porcine type I atelocollagen (w/v; Nippon Ham, Tskuba, Japan) and 40% chondroitin sulfate-C (CSC) (w/v; Wako Chemicals, Osaka, Japan). The cross-linked collagen solution was diluted with PBS before adjusting the pH to 7.2±0.2 using 1N NaOH or HCl. The final concentration of collagen and CSC were 0.59% (w/v) and 2.35% (w/v), respectively. The proportion of microspheres in the matrix was 21% (w/v), and when included, the SDF-1 concentration was 40 ng/ml. SDF-1 microsphere-matrix was prepared using the same procedure, except 400mg of microspheres was added in the PBS dilution step. For *in vitro* use, matrices were thermogelled for 20 min at 37°C.

Reagent Sterilization

All liquid reagents (PBS, MES, CSC, alginate) were sterile filtered (0.45 μm). Collagen (1%) was prepared with sterile water and the resulting solution was sterilized by exposure to UV light for a period of 15 min.

Rheology

The rheological properties of the collagen matrix were measured using a Brookfield R/S Plus Rheometer as previously described (Deng et al.). Samples of collagen matrix or microsphere-collagen matrix (1.5ml) were subjected to a constant shear rate of $5s^{-1}$ for 20-30 min using a C50-2 spindle (spindle gap of 4μm, according to the spindle specifications), and the temperature was maintained at 37°C. Rheo3000 v1.2 software was used to monitor

viscosity (Pa·s) and time to gelation (s). The time at which maximum viscosity was reached was considered to be the material's time to gelation. In addition to time viscosity profiles, elastic storage (G') and loss (G") modulus as a function of temperature at a frequency of 1 Hz was also measured.

SDF-1 Release

Microspheres containing human SDF-1 were used to assess release kinetics. Microspheres alone or embedded in a collagen matrix were added to a 20ml flask with 5ml of PBS. At various time points, samples were taken and immediately frozen at -80ºC and fresh PBS was added to replace the removed aliquot volume. SDF-1 content in the supernatant was assessed using an ELISA kit (R&D Systems, Minneapolis, USA), according to the manufacturer's protocol. Data is reported as a ratio of concentration at time *t*, standardized to the maximal release.

Release Kinetics

To analyze SDF-1 release from microspheres (+/- matrix embedding), various release kinetic models were used to describe the observed release kinetics. Correlation coefficients were determined for data fit to zero-order release (Hadjiioannou et al., 1993), first-order release (Bourne, 2002), Higuchi (Higuchi, 1963), Hixson-Crowell (Hixson and Crowell, 1931) and Korsmeyer-Peppas (Korsmeyer et al., 1983) models.

Cell Culture

Procedures for the isolation of human circulating progenitor cells (CPCs) were approved by the Human Research Ethics Board of the University of Ottawa Heart Institute. After obtaining informed consent, total peripheral blood mononuclear cells (PBMCs) were isolated from the blood of healthy human volunteers by Histopaque 1077 density-gradient

centrifugation, as previously described (Ruel et al., 2005). Cells were cultured on fibronectin-coated plates in endothelial basal medium (EBM-2; Clonetics, Guelph, Canada) containing 5% FBS (v/v), VEGF, R^3-IGF-1, and hEGF supplements. After 4 days in culture, supernatant and non-adherent cells were removed, and adherent populations were considered to be circulating progenitor cells (CPCs).

Adhesion Assay

CPCs (2×10^4) were resuspended in 1ml of medium and seeded in 12-well dishes with fibronectin-coated coverslips, containing medium with 50mg of blank microspheres or medium with 50mg of human SDF-1 loaded microspheres. After 1 hour at 37ºC, medium was aspirated and adherent cells were fixed with 4% paraformaldehyde (PFA). Coverslips were washed with PBS and mounted on slides with 4',6-diamidino-2-phenylindol-(DAPI)-containing mounting medium (Vector Laboratories, Burlington, Canada). Six random fields-of-view were imaged using a Zeiss Z1 fluorescent microscope and $DAPI^+$ cells were counted.

Migration Assay

CPCs (2×10^4) in VEGF-free medium were added to the top chamber of a Transwell tissue culture well (Corning, New York, USA). The lower chamber contained VEGF-free medium with 50mg of blank microspheres or VEGF-free medium with 50mg of human SDF-1 loaded microspheres. The bottom of each well contained a fibronectin-coated coverslip. After 24 hours of incubation, cells were fixed, DAPI-stained, visualized, and counted.

Chemokinesis versus Chemotaxis Assay

To investigate the mode of action through which SDF-1 induces CPC migration, assays, based on a previously described protocol for the evaluation of chemokinesis versus chemotaxis (Misiak-Tloczek and Brzezinska-Blaszczyk, 2009), were carried out. Three

treatment conditions (represented as the presence of SDF-1 in the upper well/lower well) were tested: SDF-1/0 (SDF-1 only in the upper well); SDF-1/SDF-1 (SDF-1 in both upper and lower wells); 0/SDF-1 (SDF-1 in the lower well only). SDF-1 was used at a concentration of 9 ng/ml, as this is the approximate amount released from microspheres after 24 h. Quantification was performed in the same manner as described for the migration assay above.

Animal Model

All procedures were performed with the approval of the University of Ottawa Animal Care Committee, in compliance with the National Institute of Health's Guide for the Care and Use of Laboratory Animals. Bone marrow transplantation was performed as previously described (Whitman et al., 2004). Briefly, female C57BL/6J mice (8-9 weeks old, Jackson Laboratories, Bar Harbor, USA) were irradiated with a total of 900 rads from a cesium source, delivered in 2 equal doses, 3 hours apart. Donor bone marrow cells (7×10^6) from green fluorescent protein (GFP) transgenic mice (C57BL/6-Tg(CAG-EGFP)10sb/J, Jackson Laboratories) were injected into the tail vein of irradiated recipient mice. Six weeks after transplantation, proximal femoral arteries in left hindlimbs were ligated as described (Limbourg et al., 2009), using 4.0 silk thread, under 2% isoflurane. Limbs subsequently received 80µl injection of: 1) PBS (n=9); 2) collagen matrix (n=8); or 3) collagen matrix containing murine SDF-1 microspheres (n=8). Treatments were delivered by 3 equivolumetric injections into the adductor muscle downstream of the ligation site, using a 27-gauge needle.

Blood perfusion of both hindlimbs was measured before and after ligation, and at days 4, 7, and 14 post-operatively using a multifiber needle probe (8 separate collecting fibers), and a laser Doppler blood flow monitor (Moor Instruments, Axminster, UK).

Blood samples (~100µl) were procured from the right saphenous veins on days 0 (pre-operative baseline), 1, 4, 7, and 14 post-operatively. PBMCs were isolated using density-gradient centrifugation and immediately characterized using flow cytometry as described below.

Flow Cytometry

Cells were labeled with antibodies against the following antigens: c-kit (Southern Biotech, Birmingham, USA), CXCR4 (BD Biosciences, Mississauga, Canada), and flk-1 (eBioscience, San Diego, USA), and analyzed with a FACSAria flow cytometer (BD Biosciences). Isotype-matched immunoglobulin antibodies were used as controls.

Immunohistochemistry

Animals were sacrificed at day 14. Hindlimb muscle tissue was collected and fixed overnight in PFA before paraffinization. All samples were analyzed in cross-section. Samples were de-paraffinized and hydrated with sequential washes in toluene and decreasing concentrations of ethanol. Antigen retrieval was performed using boiling citrate buffer. All staining was performed in PBS containing 10% normal horse serum (Vector Laboratories). The following antibodies were used: anti-α-smooth muscle actin (SMA; pre-diluted, Abcam, Cambridge, USA), anti-GFP (1:100; Abcam), and anti-CXCR4 (1:50; Abcam). For all tissue sections, mounting medium with DAPI (Vector Laboratories) was used to visualize nuclei. All measurements and cell counts were determined from 6 random microscopic fields-of-view and averaged from 2 blinded observers.

Cytokine Antibody Arrays

Relative cytokine levels in hindlimb lysates and serum from sacrificed animals (n=5 per treatment group) were analyzed using RayBio Mouse Cytokine Antibody Array Kits (Raybiotech, Norcross, USA), according to the manufacturer's protocol.

Statistical Analysis

Unless otherwise stated, values are expressed as means ± standard error. Statistical analyses were performed using SPSS (IBM, Somers, USA). Comparisons of continuous data between groups were performed with a one-way analysis of variance and comparisons between individual groups were performed with a two-tailed Student's t-test. For *in vitro* CPC analysis, results were paired by donor, and subjected to a paired t-test. Probability values of $P<0.05$ were considered statistically significant

Results

Generation of SDF-1 Microspheres

Microspheres had a mean diameter of 38.5μm (± 14.0μm (SD); Fig. 3-1A). When hydrated, microspheres had a smooth, spherical morphology (Fig. 3-1B), and a rougher surface upon dehydration as visualized by SEM (Fig. 3-1C).

Microsphere-Matrix Impregnation

The addition of microspheres to the collagen matrix reduced the time to gelation and caused the matrix to solidify at a greater viscosity, as early as 400s after application (P=0.05; Fig. 3-2A,B), which was maintained over time. Maximum viscosity reached was greater for the matrix containing microspheres (1.42Pa·s), compared to matrix alone (1.18Pa·s;

P=0.003). Microspheres in solution released their SDF-1 content within 1 day, but matrix impregnation prolonged the maximal release up to approximately 10 days (Fig. 3-2C). Analysis of SDF-1 release kinetics shows that release from microspheres best fits a first order model, indicated by the greatest correlation coefficient, but after impregnation in a matrix, release follows the Higuchi model (Table 3-1, Fig. 3-2D).

Figure 3-1 Characterization of SDF-1-containing alginate microspheres. Average size of microspheres was 38.5μm (A). Microspheres displayed a rounded morphology in saline solution (B; 400X), and a lattice structure after drying and imaging using scanning electron microscopy (C; 379X). Scale bars = 50μm.

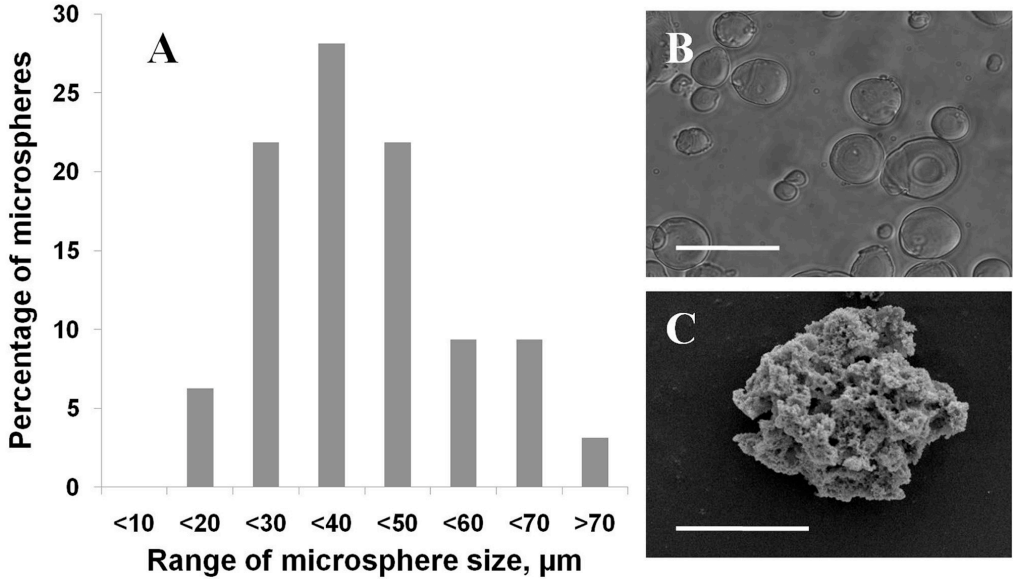
A
B
C
Percentage of microspheres
30
25
20
15
10
5
0
<10
<20
<30
<40
<50
<60
<70
>70
Range of microsphere size, µm

Figure 3-2. Matrix-microsphere effects. After microsphere (MS) impregnation into collagen matrix, rheological properties of the matrix were altered: time to gelation was reduced by 16%, and viscosity increased by 22% (A; *n*=10). Differences in gelation were first noted at 400s. B shows representative modulus versus time curves, which illustrate G' (storage) and G" (loss) values for the different hydrogels. The burst-release effect of SDF-1 was reduced upon incorporation into matrix; the maximal release was delayed from approximately 1 day to 10 days (C; *n*=3). Analysis of release kinetics demonstrates that when microspheres are embedded in a matrix, SDF-1 release fits the Higuchi model (D; R^2=0.94). **P*<0.05 versus matrix without microspheres at the same time point.

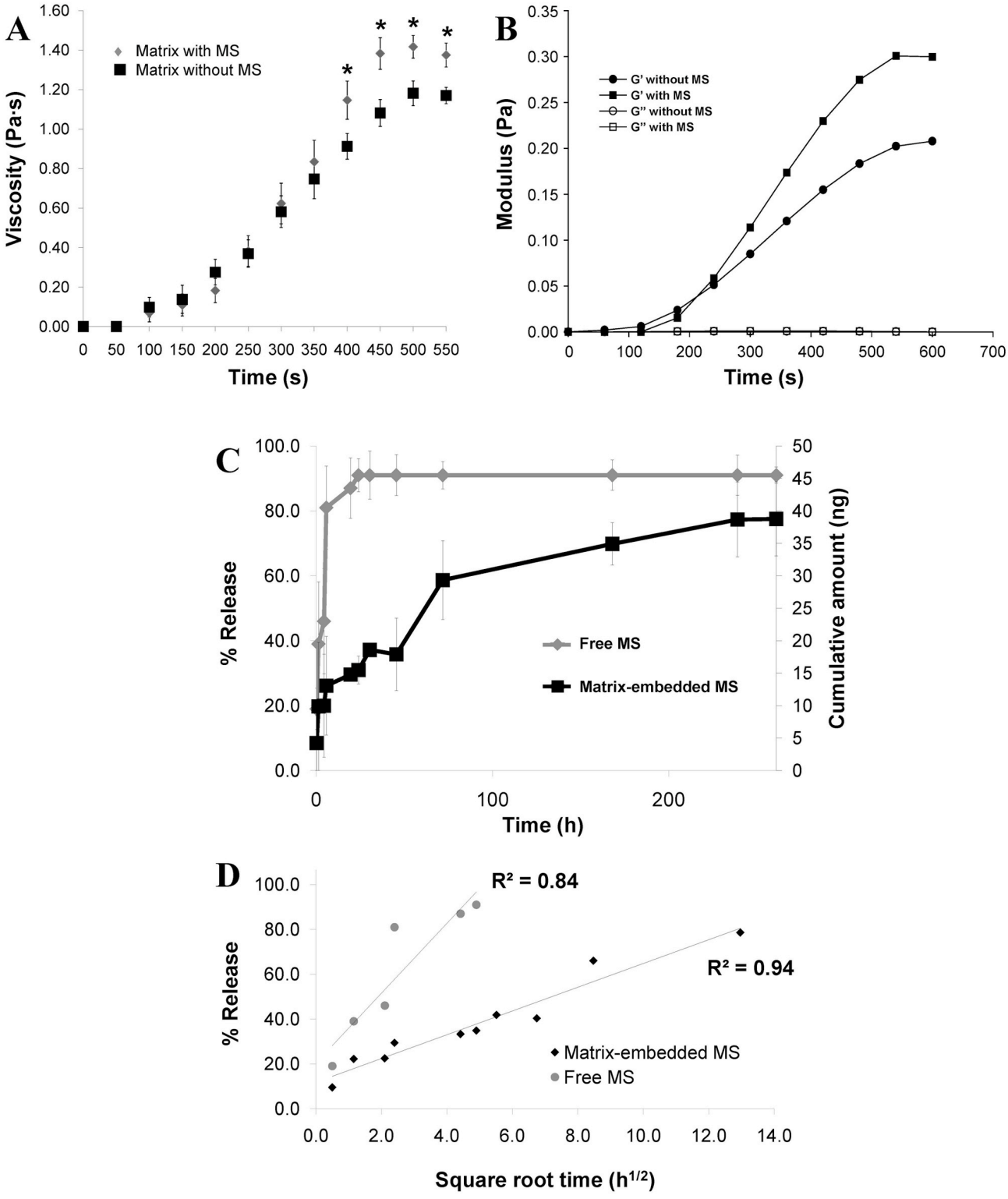
A
Viscosity (Pa·s)
Time (s)
Matrix with MS
Matrix without MS
B
Modulus (Pa)
Time (s)
G' without MS
G' with MS
G" without MS
G" with MS
C
% Release
Cumulative amount (ng)
Time (h)
Free MS
Matrix-embedded MS
D
% Release
Square root time (h1/2)
R² = 0.84
R² = 0.94
Matrix-embedded MS
Free MS

Table 3-1 – Correlation coefficients, r^2, for SDF-1 release from microspheres alone or embedded in a collagen matrix, based on classical drug release models.

	Zero Order	First Order	Hixson-Crowell	Higuchi	Korsmeyer-Peppas
Free MS	.93	.95	.94	.84	.92
Matrix-Embedded MS	.66	.75	.78	.94	.59

Bioactivity of SDF-1 Microspheres

Blank microspheres did not confer any difference in adhesion potential with cultured CPCs, but the addition of SDF-1 loaded microspheres supported an increase in adhesive CPCs by 2.3-fold after 1 hour of exposure (P=0.04; Fig. 3-3A-C). When CPCs were given a chemotactic stimulus of blank or SDF-1 loaded microspheres, 3.2-fold more cells migrated towards the SDF-1-releasing microspheres than the blank ones after 24 hours (P=0.004; Fig. 3-3D-F).

SDF-1 Mediated-Migration of CPCs is Mainly Chemotactic

Compared to the lack of a chemotactic stimulus (absence of SDF-1 in the lower well), chemokinesis, stimulated by equivalent amounts of SDF-1 in the upper and lower chambers, increased CPC movement to the lower chamber by 13% (P=0.04; Fig. 3-3G). The chemotactic stimulus with SDF-1 only in the lower chamber induced the greatest migration of CPCs, by 177% (P=0.006; Fig. 3-3G).

Figure 3-3. Effects of blank (no SDF-1) and SDF-1 loaded microspheres on cultured primary CPCs. In the presence of SDF-1 loaded microspheres (MS), over 2-fold more CPCs were adherent to fibronectin within 1 hour of exposure (A; n=4); B, C are representative images of adherent CPCs in the presence of blank or SDF-1 loaded microspheres, respectively. More CPCs migrated towards SDF-1 microspheres (D; n=4); E, F are representative images of blank and SDF-1 loaded microsphere-induced migration of CPCs, respectively. The effect of SDF-1 on CPC migration was mainly chemotactic, rather than chemokinetic, as evidenced by the greater migratory effect of CPCs towards SDF-1 when it is presented as a gradient (G). Scale bars=100μm. *P<0.05; **P<0.05 vs. all others.

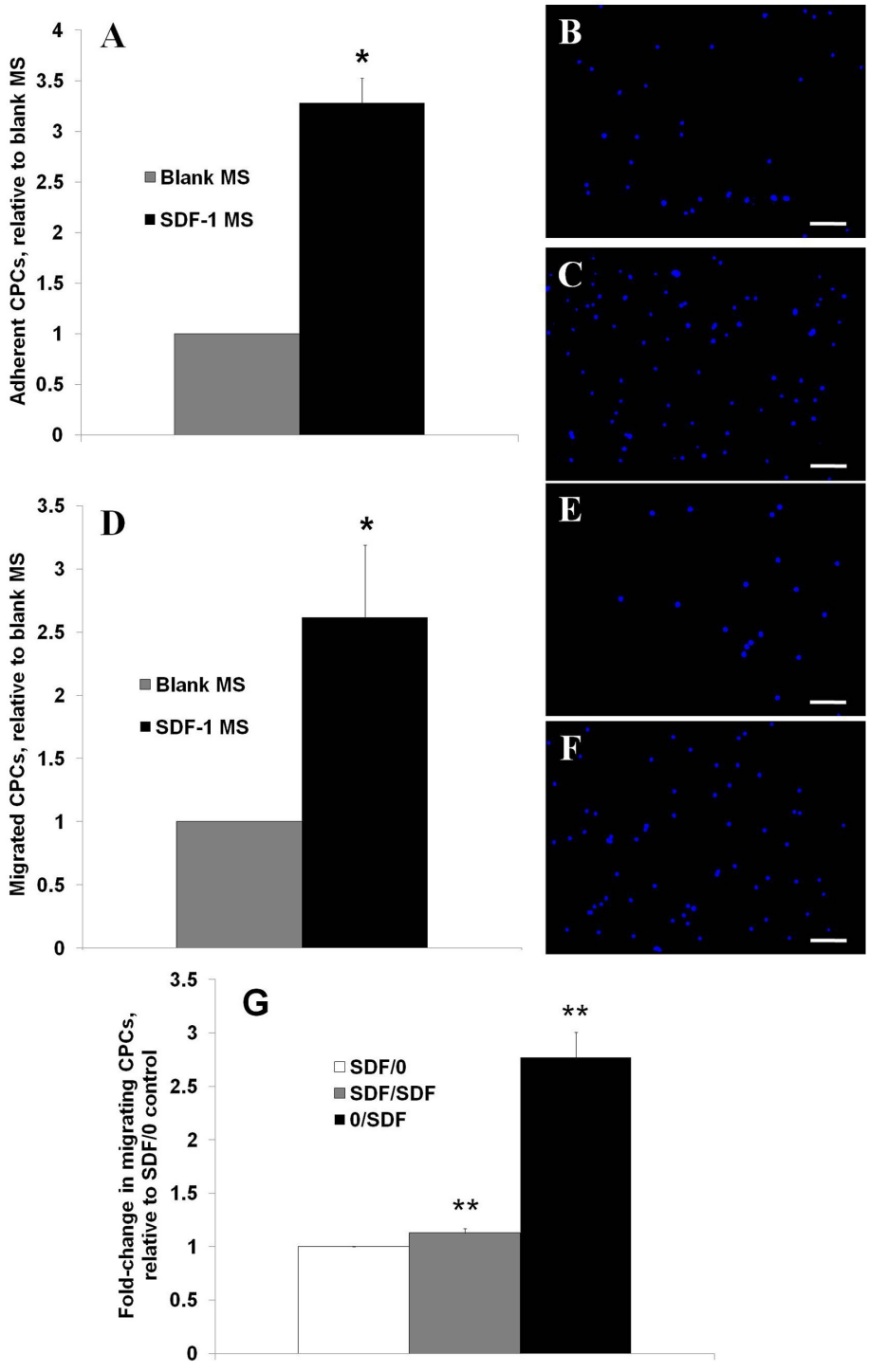
A
Adherent CPCs, relative to blank MS
4
3.5
3
2.5
2
1.5
1
0.5
0
*
Blank MS
SDF-1 MS
B
C
D
Migrated CPCs, relative to blank MS
3.5
3
2.5
2
1.5
1
0.5
0
*
Blank MS
SDF-1 MS
E
F
G
Fold-change in migrating CPCs, relative to SDF/0 control
3.5
3
2.5
2
1.5
1
0.5
0
**
**
SDF/0
SDF/SDF
0/SDF

In Vivo Mobilization of CPCs by SDF-1 Treatment

Based on the *in vitro* chemotactic properties of SDF1 microsphere matrix, we defined whether the construct is able to enhance the recruitment of CPC in an *in vivo* system. GFP^+ (bone marrow-derived) CPCs in the peripheral blood were analyzed over time, and compared to baseline. Interestingly, the SDF-1 microsphere matrix treatment significantly increased circulating $CXCR4^+$ cells (by 45%; P=0.02), $flk\text{-}1^+$ cells (by 105%; P=0.001), and $c\text{-}kit^+$ cells (by 18%; P=0.04) at early time point post injury (Fig. 3-4A) and was able to maintain elevated numbers of circulating $flk\text{-}1^+$ cells (by 149%; P=0.002) and $c\text{-}kit^+$ cells (by 48%; P=0.01) for an extended period (7-14 days) post operation (Fig. 4.4B). Notably, the collagen matrix alone increased circulating flk^+ cells (by 20%; P=0.009) at the earlier evaluation and $c\text{-}kit^+$ cells at both early (by 48%; P=0.01) and late time point (by 29%; P=0.02; Fig. 3-4A,B).

Restoration of Perfusion by Matrix Treatments

Indeed, both matrix treatments (with or without SDF-1 microspheres) were able to restore perfusion to baseline levels by one week post-treatment, compared to PBS controls (Fig. 3-4C; P<0.04), which was maintained at two weeks post-treatment (P<0.05).

Figure 3-4. Functional effects of collagen & SDF-1 microsphere matrix treatments *in vivo*. At early time points after treatment (A; days 1-4), animals receiving SDF-1 microsphere-matrix (SDF-1) had greater numbers of circulating CPCs. This was also observed at later time points (B; days 7-14). By 7 days post-op, hindlimb perfusion was restored to baseline levels with matrix treatments (C; n=6-8 per group). *P<0.05 versus PBS; **P<0.05 versus PBS & collagen.

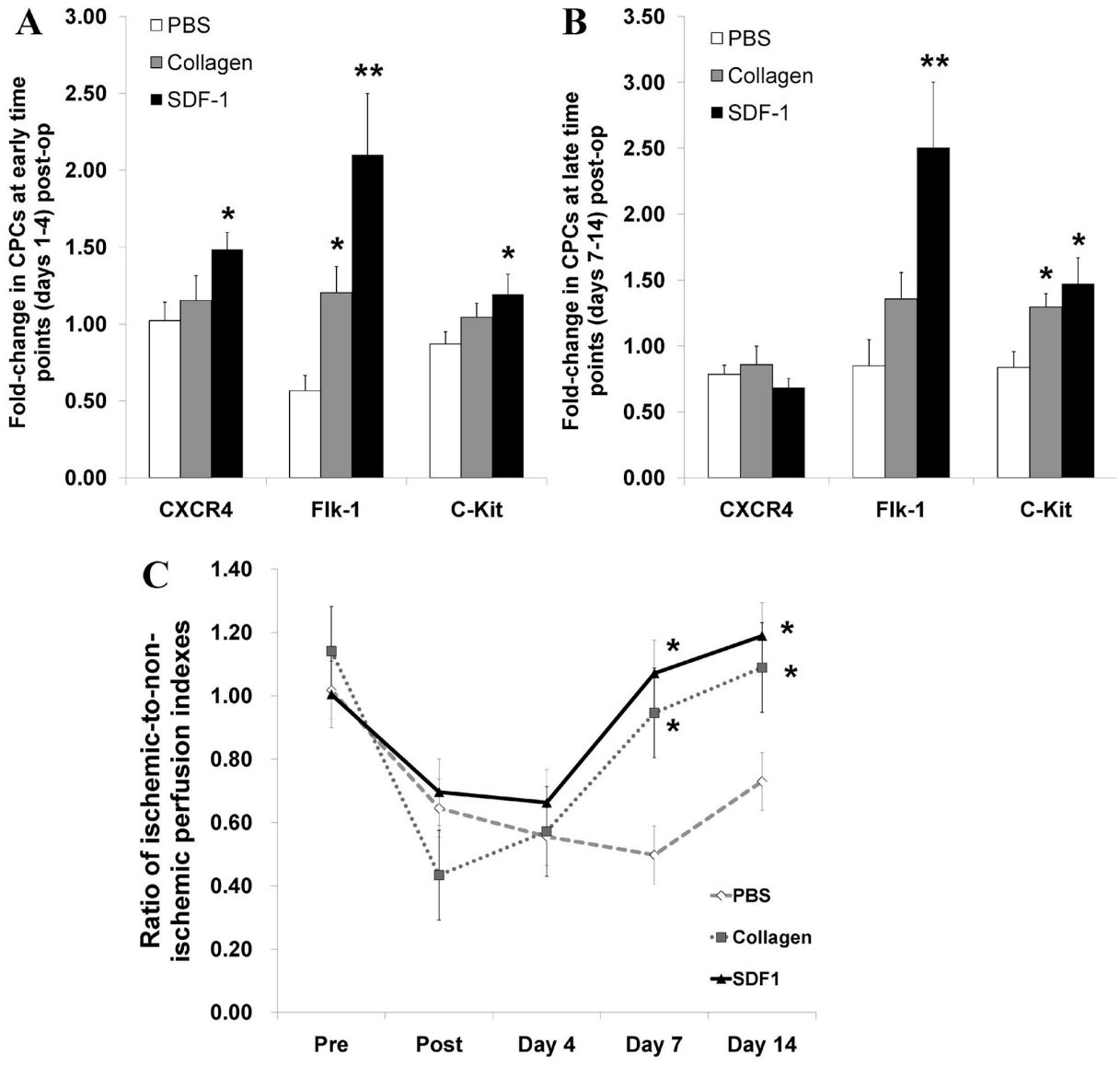
A
Fold-change in CPCs at early time points (days 1-4) post-op
PBS
Collagen
SDF-1
3.00
2.50
2.00
1.50
1.00
0.50
0.00
CXCR4
Flk-1
C-Kit
B
Fold-change in CPCs at late time points (days 7-14) post-op
3.50
C
Ratio of ischemic-to-non-ischemic perfusion indexes
1.40
1.20
1.00
0.80
0.60
0.40
0.20
0.00
Pre
Post
Day 4
Day 7
Day 14
SDF1

Arteriole Density of Ischemic Hindlimbs

Arteriole density in ischemic hindlimbs was not different between collagen and SDF-1 collagen matrices (P=0.9); however, both matrix and SDF-1 microsphere matrix treatments increased arteriole density compared to PBS by 67% (P=0.01) & 69% (P=0.02), respectively (Fig. 3-5A-E). Mean arteriole size was greater in the SDF-1 microsphere matrix treatment group compared to PBS-treated mice (P<0.05; Fig. 3-5B-E). There was also a trend for greater arteriole cross-sectional area with SDF-1 microsphere matrix treatment compared to collagen matrix (P=0.09), and for collagen matrix treatment compared to PBS (P=0.08; Fig. 3-5B).

Recruitment of Bone Marrow-Derived Cells to Treated Hindlimbs

SDF-1 microsphere matrix and collagen matrix treatments recruited 17.7- and 4.2-fold more GFP^+ cells to treated hindlimbs, compared to PBS (P=0.0007 and 0.02), respectively (Fig. 3-6A-D). There was a trend for SDF-1 microsphere matrix treatment to recruit more GFP^+ cells than collagen matrix alone (P=0.06; Fig. 3-6A).

Figure 3-5. Assessment of vasculature in treated hindlimbs. There was a trend for increased arteriole counts with matrix treatments (A). Larger arterioles were produced in animals receiving collagen or SDF-1 microsphere-matrix (SDF-1) treatments, with the SDF-1 microsphere-matrix treatment leading to the largest arterioles (B). C, D, E are representative images of arterioles (indicated by SMA^+, red), and counter stained with DAPI (blue). Scale bars=50μm. n=6-8 per group. $^{**}P \leq 0.05$; $^{*}0.05 < P < 0.10$.

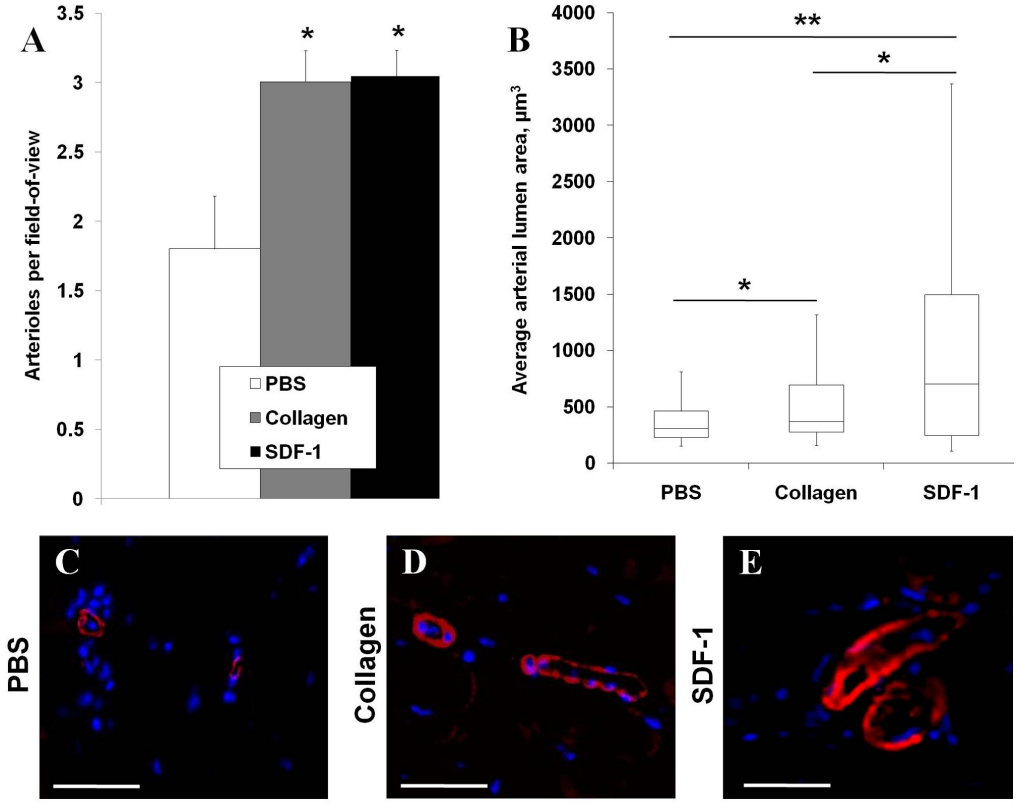
A
Arterioles per field-of-view
3.5
3
2.5
2
1.5
1
0.5
0
*
*
PBS
Collagen
SDF-1
B
Average arterial lumen area, µm³
4000
3500
3000
2500
2000
1500
1000
500
0
**
*
*
PBS
Collagen
SDF-1
C
PBS
D
Collagen
E
SDF-1

Figure 3-6. Recruited bone marrow-derived cells. More GFP^+ cells were engrafted in ischemic hindlimbs treated with collagen or SDF-1 microsphere-matrix (SDF-1), with a trend for more GFP^+ cells in the SDF-1 microsphere-matrix treatment, compared to matrix alone (A). Representative images of GFP^+ cells recruited to PBS- (B), collagen matrix- (C), or SDF-1 microsphere-matrix- (D) treated hindlimbs. Scale bars=100μm; n=6-8 per group. *$P \leq 0.02$ vs. PBS, $^{\dagger}P$=0.06 vs. collagen.

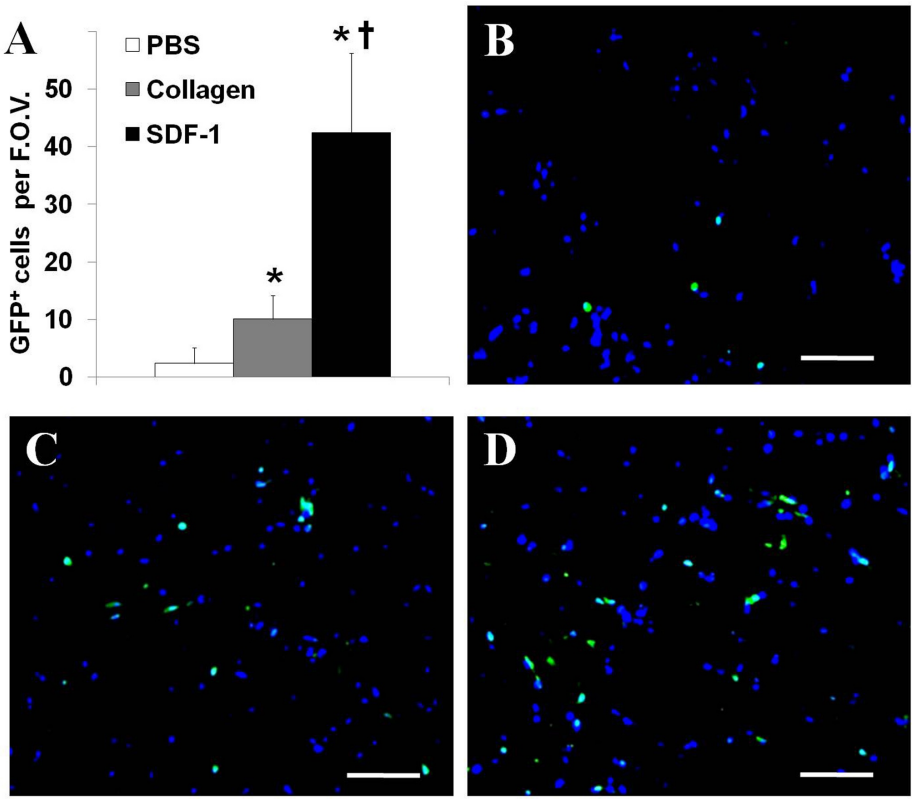
A
PBS
Collagen
SDF-1
GFP+ cells per F.O.V.
0
10
20
30
40
50
*
*†
B
C
D

Engraftment of CXCR4$^+$ Cells in Ischemic Hindlimbs

Overall, SDF-1 microsphere matrix treatment recruited 4.3- and 1.8-fold more CXCR4$^+$ cells to treated hindlimbs compared to PBS and collagen (P=0.0004 and 0.05; Fig. 3-7A-D). Separating the analysis of CXCR4$^+$ cells into those recruited from the marrow versus those recruited locally, SDF-1 microsphere matrix treatment recruited 4.9-fold more CXCR4$^+$GFP$^+$ (bone marrow-derived) and 4.5-fold more CXCR4$^+$GFP$^-$ (local) cells, compared to PBS and collagen (P=0.008 and 0.02; Fig. 3-7A). Collagen matrix alone also recruited 2.8-fold more CXCR4$^+$GFP$^+$ cells compared to PBS (P=0.03; Fig. 3-7A).

Figure 3-7. Localized $CXCR4^+$ cells. SDF-1 microsphere-matrix (SDF-1) treatment recruited more $CXCR4^+$ cells, from both bone marrow (GFP^+) and locally (GFP^-; A). Representative images of GFP^+ (green), $CXCR4^+$ (red), or GFP^+CXCR4^+ cells (yellow) in PBS- (B), collagen matrix- (C), or SDF-1 microsphere-matrix- (D) treated hindlimbs. Scale bars=200μm; *n*=6-8 per group. **P*<0.05 vs. PBS, ***P*<0.05 vs. all.

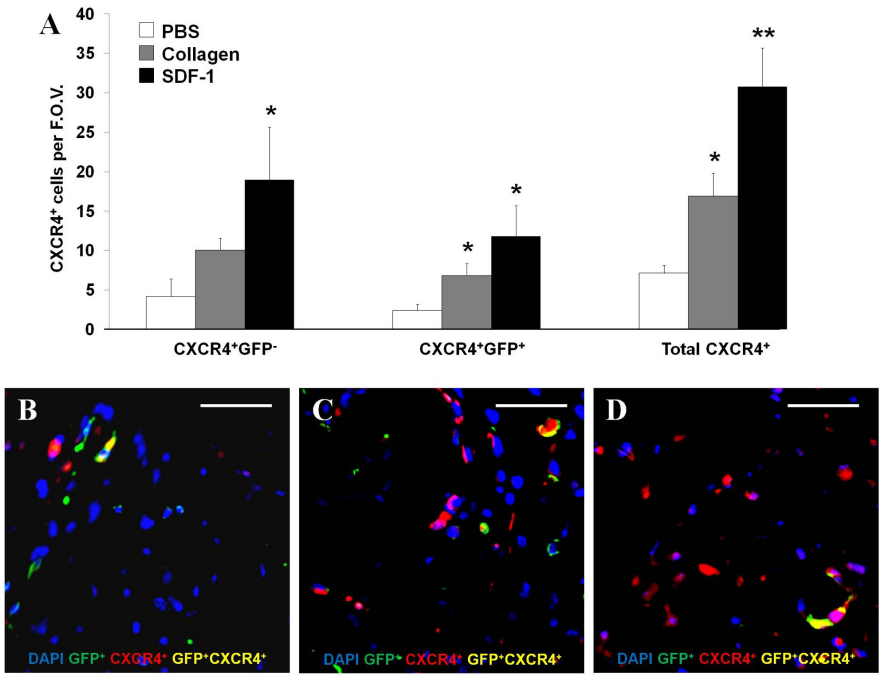
A
PBS
Collagen
SDF-1
CXCR4+ cells per F.O.V.
40
35
30
25
20
15
10
5
0
*
*
*
*
**
CXCR4+GFP-
CXCR4+GFP+
Total CXCR4+
B
C
D
DAPI GFP+ CXCR4+ GFP+CXCR4+
DAPI GFP+ CXCR4+ GFP+CXCR4+
DAPI GFP+ CXCR4+ GFP+CXCR4+

Cytokine Profiles

In the hindlimb (Fig. 3-8a), interleukin-1α (IL-1α; P=0.04) and monocyte inhibitory protein-3α (MIP-3α; P=0.04) were reduced, and vascular cell adhesion molecule-1 (VCAM-1; P=0.03) and insulin-like growth factor-1 (IGF-1; P=0.03) were increased with SDF-1 microsphere matrix treatment. In the serum (Fig. 3-8B): L-selectin was increased with SDF-1 microsphere matrix treatment (P=0.01) and reduced with collagen alone (P=0.01); basic fibroblast growth factor (bFGF) was increased with collagen alone (P<0.001) and with SDF-1 microsphere matrix treatment (P=0.02); and VCAM-1 was reduced with SDF-1 microsphere matrix treatment compared to collagen matrix (P=0.007) and PBS (P<0.001). For both serum and hindlimb, no significant differences between any treatments were observed for the following inflammatory cytokines: GM-CSF, TNF-α, IL-1β and IL-6 (all P>0.4).

Figure 3-8. Cytokine profiles. Observed differences in cytokines in hindlimb lysates (A) and serum (B), two weeks after treatment (n=5). *P<0.05.

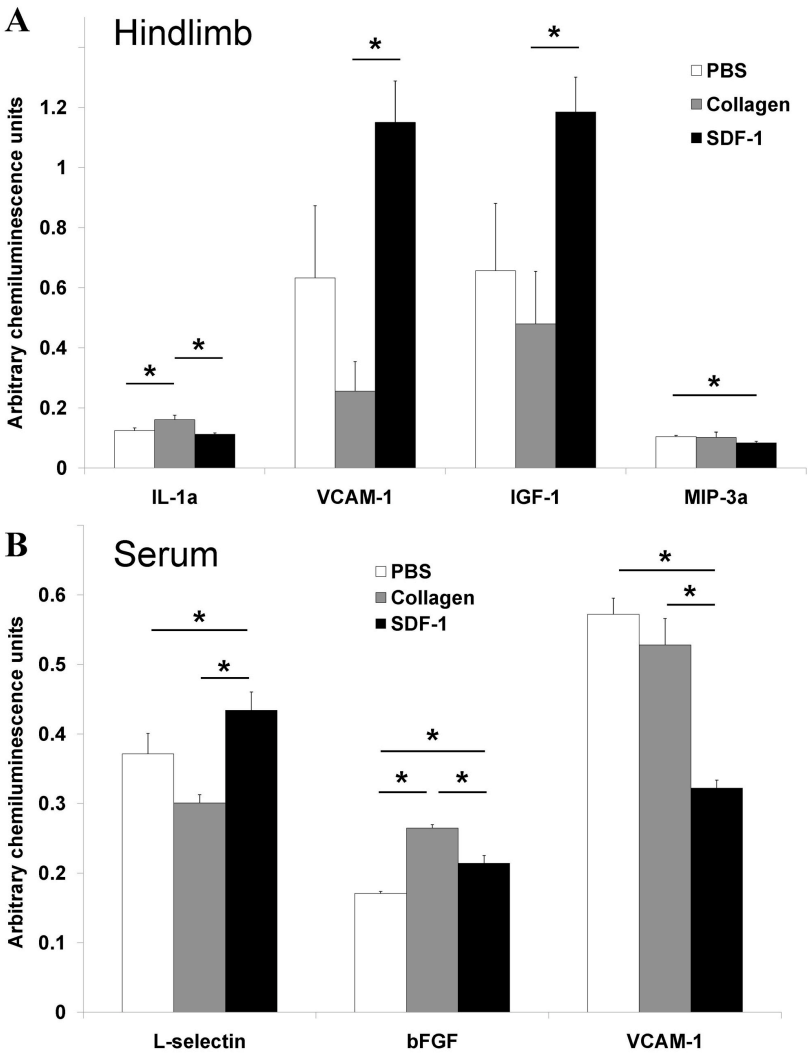
A
Hindlimb
PBS
Collagen
SDF-1
Arbitrary chemiluminescence units
0
0.2
0.4
0.6
0.8
1
1.2
IL-1a
VCAM-1
IGF-1
MIP-3a
B
Serum
PBS
Collagen
SDF-1
Arbitrary chemiluminescence units
0
0.1
0.2
0.3
0.4
0.5
0.6
L-selectin
bFGF
VCAM-1

Discussion

In this study, we demonstrated that the release of SDF-1 from alginate microspheres can be effectively prolonged by incorporation of the microspheres into a thermogelling collagen matrix. Released SDF-1 was bioactive, supported rapid adhesion and migration of CPCs, and also stimulated the mobilization of CPCs from bone marrow when applied to ischemic muscle. Both matrix alone and SDF-1-releasing matrix restored perfusion and improved arteriole density by 2 weeks, but the SDF-1 treatment best supported the growth of arterioles. SDF-1 microsphere matrix treatment also recruited more bone marrow-derived cells and local $CXCR4^+$ cells to the ischemic muscle, and altered levels of local angiogenic factors.

Incorporation of alginate microspheres into the collagen matrix increased the hydrogel's viscosity and reduced the time to gelation. This is thought to be mediated by the cross-linking reaction, whereby functional groups on collagen ($–NH_2$) and alginate (–COOH) are covalently bound by EDC/NHS (Mitra et al.), increasing the total number of cross-links within the material and enhancing its strength, as has been previously reported (Liu et al., 2008). An earlier onset of gelation is advantageous in a clinical setting, allowing for a reduction in the time required for stable material integration within host tissue. Additionally, a positive correlation between hydrogel viscosity and resistance to degradation has been noted (Yang et al., 2010), suggesting a better persistence *in vivo* of microsphere-containing hydrogels.

During the period of release, SDF-1 kinetics from matrix-embedded microspheres fit the Higuchi model of release whereby the initial drug concentration >> drug solubility in the matrix, swelling is negligible, perfect sink conditions are maintained and edge effects are

negligible, suggesting that diffusion is the primary mechanism of SDF-1 release (Higuchi, 1963). In contrast, microspheres alone initially demonstrated a burst release followed by a first order release of SDF-1. Although a burst-release effect was observed with microspheres alone, the embedding of microspheres in matrix was able to prolong the SDF-1 release by 10-fold. This observation can be explained by the properties of the microspheres and the collagen-hydrogel system. Hydrogels have an innate ability to retain small peptides (Cadee et al., 2002; Ruvinov et al.), and incorporation of peptide-containing microspheres into hydrogels has been shown previously to extend the release profile of the peptide (Kempen et al., 2008). SDF-1 bioactivity was maintained during the microsphere generation and cross-linking procedure; upon its release, SDF-1 augmented rapid adhesion of CPCs, as well as inducing chemotaxis of CPCs, rather than chemokinesis, indicating its ability to induce CPC homing towards a chemotactic gradient rather than the induction of random mobilization.

In the ischemic hindlimb study, marrow-mobilized cells expressing the SDF-1 receptor CXCR4 were increased in circulation of SDF-1 microsphere matrix-treated animals at early time points, but this effect was later lost. This can be explained by previous studies showing the eventual down-regulation of CXCR4 following cytokine-induced mobilization from the bone marrow (Kim et al., 2006). More specifically, CXCR4 expression is dose-dependent on SDF-1 levels; doses of $\leq$ 1ug in a mouse model have shown CXCR4 levels equivalent to controls that did not receive SDF-1 (Kimura and Tabata). Interestingly, higher doses of SDF-1 have the same effect, suggesting a potential negative feedback loop for the SDF-1/CXCR4 axis. Notably, SDF-1 microsphere matrix treatment also stimulated an early mobilization of flk-1^+ and c-kit^+ cells from the bone marrow into circulation, and maintained this effect up to 2 weeks post-treatment. CXCR4 is SDF-1's exclusive receptor and $CXCR4^+$

CPCs are reduced over time, mechanisms other than SDF-1 release are needed to explain the increase in mobilized CPCs expressing flk-1 and c-kit. We have previously shown that systemic transplantation of CPCs can induce a potent response from the host's CPCs (Suuronen et al., 2009). Additionally, this effect has been documented in humans, and CPC persistence in the circulation has been observed up to 1 year after cell transplantation (Turan et al.). Therefore, it is likely that the initiation of the SDF-1/CXCR4 mobilization and recruitment response by SDF-1 microsphere matrix treatment activates other endogenous progenitor cell mechanisms.

Ischemia was induced in all mice (average of 55% of normal perfusion). By one week post-treatment, animals that received matrix treatment (with or without SDF-1 microspheres) had hindlimb perfusion restored to baseline levels, which is similar to previous reports of matrix treatment for hindlimb ischemia (Suuronen et al., 2009). It has been previously demonstrated that an increase in perfusion is attributable to increased local vasculature (Kim et al.; Suuronen et al.), an observation that was seen in the current study; matrix treatments increased arteriole density in ischemic hindlimbs. It was hypothesized that SDF-1 microsphere matrix treatment would confer superior restoration of perfusion, but instead, the matrix-only treatment was equally effective. Kimura and Tabata also attempted to enhance neovascularization using an SDF-1-releasing hydrogel (Kimura and Tabata), and observed increased capillary density with SDF-1 treatment at 4 days post-treatment, which was abrogated by 10 days. Another SDF-1 release study did not show a difference in vascular density between SDF-1 and controls at 9 days post-treatment (Rabbany et al.). It may be that the addition of SDF-1 accelerates the regenerative response to collagen matrix treatment. This is supported by the observation that SDF-1 treatment increased the cross-sectional size

of arterioles. Cross-sectional area of new vasculature has been shown to increase over a period of 4 weeks (Ruvinov et al.), demonstrating that vessel area is indicative of vessel maturity. Therefore, it is plausible that SDF-1 treatment had an earlier effect on neovascularization, allowing for more rapid growth/maturation of arterioles, compared to both matrix and PBS treatments.

The SDF-1 microsphere matrix treatment recruited the most GFP^+ marrow-mobilized cells in our animal model. Other SDF-1-release studies have also shown recruitment of stem cells, positive for c-kit (Thevenot et al.; Zhang et al., 2007) expression. In particular, it was expected that SDF-1 treatment would increase the recruitment and engraftment of $CXCR4^+$ cells. Both the matrix and SDF-1 microsphere matrix treatments increased homing of bone marrow-derived $CXCR4^+$ cells to the treated hindlimbs (SDF-1 microsphere matrix treatment had the most pronounced effect), but the SDF-1 microsphere matrix treatment also demonstrated an improved recruitment of $CXCR4^+$ cells of non-bone marrow origin. Recently, it was shown that local pools of progenitor cells co-expressing CXCR4 and endothelial markers reside in tissues (Sandstedt et al.), suggesting a potential role in neovascularization. In our experiment, SDF-1 treatment may be recruiting a similar population, as evidenced by $CXCR4^+GFP^-$ staining. Microvascular endothelial cells have also been documented to express CXCR4 (Takagi et al., 2009), suggesting another CXCR4-expressing population that is possibly activated in treated hindlimbs. Regardless, $CXCR4^+$ fractions have been observed to be superior to whole $CXCR4^-$ fractions with respect to potential for invasion, neovascularization, and restoration of perfusion (Seeger et al., 2009).

Compared to controls, inflammatory cytokines (IL-1α and MIP-3α) were reduced in hindlimbs treated with SDF-1 microsphere matrix, a similar result to Thevenot *et al.*'s study.

The latter examined cytokine responses to SDF-1 delivery in a synthetic scaffold (Thevenot et al.); however, our results also suggest that the SDF-1 microsphere matrix supports a favorable environment for angiogenic activity through local factors, as evidenced by increased IGF-1 and VCAM-1 in hindlimb lysates. IGF-1 is a stimulator of angiogenesis (Su et al., 2003) and is cytoprotective (Li et al., 1997), and elevated IGF-1 is ideal for recovery. Pelosi *et al.* have shown that persistent IGF-1 expression accelerates the regenerative response and restores architecture and structure soon after skeletal muscle injury (Pelosi et al., 2007). VCAM-1 is a cell adhesion molecule expressed by endothelial cells. When VCAM-1 is solubilized and detected in serum, it is used as an indicator of dysfunctional endothelium (Balciunas et al., 2009). Our SDF-1 microsphere matrix treatment had significantly less circulating VCAM-1, further suggesting a vasculo-protective role of this therapy. Furthermore, both matrix treatments increased systemic bFGF, which is a potent angiogenic cytokine (Hosseinkhani et al., 2006).

Conclusion

In this study, we demonstrated that SDF-1 can be successfully encapsulated in an alginate microsphere system and further incorporated into an injectable matrix for non-invasive delivery. The treatment of ischemic mouse hindlimbs with SDF-1-releasing matrix enhanced progenitor cell mobilization and recruitment. Compared to collagen-only treatment, the addition of SDF-1 appears to confer an earlier effect on neovascularization, as suggested by greater arteriole maturity. These findings suggest that application of an SDF-1-releasing matrix constitutes a suitable therapy for prevalent myopathies with reduced perfusion, with the potential to augment progenitor cell mobilization and homing, as well as its ability to rapidly support neovascularization.

Acknowledgments

DK was supported by a Canadian Institutes of Health Research Canadian Graduate Scholarship; PZ is a recipient of the Lawrence Soloway Research Fellowship Award; YZ was supported by a Heart & Stroke Foundation of Ontario Doctoral Research Award; DTP was supported by a University of Ottawa Cardiology Research Endowment Fellowship; KM was supported by an Ontario Graduate Scholarship; DK and TS were supported by Heart & Stroke Foundation of Ontario Master's Studentships; JZ was supported by a Natural Sciences and Engineering Research Council of Canada postdoctoral fellowship. The authors would like to thank Suzanne Crowe for her flow cytometry expertise and Ann Fook Yang for assistance with SEM.

This work was supported by grant-in-aid T6793 from the Heart and Stroke Foundation of Ontario (to EJS), by grant MOP-77536 from the Canadian Institutes of Health Research (to MR and EJS), by a Natural Sciences and Engineering Research Council of Canada Research Tool and Instruments Grant (to XC), by a Canadian Stem Cell Network grant (to MG), and by Fondazione Roma and 7FP-Myoage (to AM). Funding sources did not have a role in experimental design, data management, or manuscript preparation.

CHAPTER 4. Injected matrix stimulates myogenesis and regeneration of mouse skeletal muscle after ischaemic injury

This chapter has been published in *European Cells & Materials*, as per the following citation:

D. Kuraitis, D. Ebadi, P. Zhang, E. Rizzuto, B. Vulesevic, D.T. Padavan, A. Al Madhoun, K.A. McEwan, T. Sofrenovic, K. Nicholson, S.C. Whitman, T.G. Mesana, I.S. Skerjanc, A. Musarò, M. Ruel and E.J. Suuronen (2012) Injected matrix stimulates myogenesis and regeneration of mouse skeletal muscle after ischaemic injury. *Eur Cell Mater* 22:109-23.

Notes on Chapter

Although the first study to develop novel methods for restoring perfusion to ischemic muscle in Chapter 3 was successful, the results were underwhelming. One of our previous studies explored the possibility of restoring perfusion using the same collagen matrix, but with the oligosaccharide sialyl lewisX (sLe^X) incorporated into the structure (Suuronen et al., 2009). Presentation of this ligand, which in theory will bind progenitors expressing the receptor L-Selectin, was hypothesized to augment the recruitment and retention of CACs. Enhancement with sLe^X dramatically improved rapid reperfusion and vascular density, and this was indeed accompanied by many more recruited and retained CACs, compared to unenhanced matrix or PBS controls. Further studies elucidated that the enhanced matrix has a strong affinity for progenitor phenotypes (CACs) when exposed to a heterogeneous population of PBMCs, and that when cells were exposed to it, the cell phenotype switched to one that was more pro-regenerative with regard to its paracrine secretion.

Biomaterial therapy must first address any relevant shortages of perfusion before further tissue regeneration can occur. Given the therapeutic success with the sLe^X-enhanced matrix, this study sought to further characterize its potential for application in an ischemic state, and therefore focused on the molecular, phenotypic and functional changes that occurred in the ischemic muscle, in addition to the effect of the material on perfusion. Additional physical characterization and *in vitro* studies were performed to assess the materials' inherent ability to augment myogenesis in order to offer a global hypothesis for the restoration of muscle observed *in vivo*.

Contributions of co-authors to results and/or manuscript:

D. Ebadi and A. Al Madhoun performed mESC cultures and subsequent analyses [Fig 4-2]

A. Al Madhoun performed qPCR on muscle explants [Fig. 4-4].

P. Zhang performed marrow transplantation, and assisted with flow cytometry and histological analysis [Figs. 4-6,7].

E. Rizzuto explanted soleus muscles and performed mechanical testing and analysis [Fig. 4-9]

B. Vulesevic and K. Nicholson assisted with cytokine arrays [Fig. 4-8].

D.T. Padavan performed compression testing, performed and analyzed water contact angle assessment [Fig. 4-1C-E].

K.A. McEwan performed rheological measurements [Fig. 4-1A,B].

S.C. Whitman was involved in planning the bone marrow transplantation procedure.

T.G. Mesana, I.S. Skerjanc, A. Musarò, M. Ruel and E.J. Suuronen were involved in experimental planning and manuscript editing.

Abstract

Biomaterial-guided regeneration represents a novel approach for the treatment of myopathies. Revascularization and the intramuscular extracellular matrix are important factors in stimulating myogenesis and regenerating muscle damaged by ischemia. In this study, we used an injectable collagen matrix, enhanced with sialyl Lewis^X (sLe^X), to guide skeletal muscle differentiation and regeneration. The elastic properties of collagen and sLe^X-collagen matrices were similar to those of skeletal muscle, and culture of pluripotent mESCs on the matrices promoted their differentiation into myocyte-like cells expressing Pax3, MHC3, myogenin and Myf5. The regenerative properties of matrices were evaluated in ischemic mouse hindlimbs. Treatment with the sLe^X-matrix augmented the production of myogenic-mediated factors insulin-like growth factor (IGF)-1, and IGF binding protein-2 and -5 after 3 days. This was followed by muscle regeneration, including a greater number of regenerating myofibers and increased transcription of Six1, M-cadherin, myogenin and Myf5 after 10 days. Simultaneously, the sLe^X-matrix promoted increased mobilization and engraftment of bone marrow-derived progenitor cells, the development of larger arterioles and the restoration of tissue perfusion. Both matrix treatments tended to reduce maximal forces of ischemic solei muscles, but sLe^X-matrix lessened this loss of force and also prevented muscle fatigue. Only sLe^X-matrix treatment improved mobility of mice on a treadmill. Together, these results suggest a novel approach for regenerative myogenesis, whereby treatment only with a matrix, which possesses an inherent ability to guide myogenic differentiation of pluripotent stem cells, can enhance the endogenous vascular and myogenic regeneration of skeletal muscle, thus holding promise for future clinical use.

Introduction

The capacity of adult tissues to regenerate in response to injury stimuli represents an important homeostatic process. Nevertheless, the complete regenerative program in cases of aging, extended injury, peripheral artery disease or pathological conditions is severely affected and it is precluded by fibrotic tissue formation and consequent functional impairment. It is likely that the restricted tissue repair program under pathological conditions is due to either progressive loss of stem cell populations or to missing signals that limit the damaged tissues to efficiently activate a regenerative program (Carosio et al., 2011). Despite major advances in medicine, current therapies do not yet allow for muscle regeneration to take place when needed. Attempts at stem cell therapy for these diseases have demonstrated experimental success; for instance, the transplantation of cultured circulating angiogenic cells (CACs) can restore perfusion in ischemic hindlimbs (Kuraitis et al., 2011a); embryonic stem cells can improve function and prolong life in a spinal muscular atrophy model (Corti et al., 2010); and, improvement of motor function following mesenchymal stem cell transplantation was demonstrated in a model of DMD (Li et al., 2011). Despite such promise, no optimal therapy has yet emerged, and the need for strategies to regenerate muscle remains considerable.

The limitations of stem cell therapy are partially attributed to the poor engraftment and persistence of transplanted cells (Suuronen et al., 2008). To address this, materials are being tested as stem cell delivery vehicles for the regeneration of muscle; in particular, components of the body's extracellular matrices may be advantageous for therapeutic application because cells already have a pre-disposition for recognizing them (reviewed in (Kuraitis et al., 2012c)). Other technical challenges of stem cell therapy may include: potential requirement

for co-administration of immunosuppressant drugs, time required for preparation of cells for transplantation, and unavailability of autologous cells. Therefore, as an alternateve, an acellular approach to tissue regeneration has the potential to circumvent the risks and demands of these limitations. Recent studies have focused on the ability of implantable materials to augment tissue regeneration after ischemic damage by the release of stem cell-activating growth factors (Borselli et al., 2010; Kuraitis et al., 2011b; Saif et al., 2010). Another strategy, one that does not rely on having to control the release of growth factors, may be to provide the tissue with a healthy cell-supportive environment by implanting a material that can mediate and augment the body's natural responses.

In designing such a biomaterial, it may be vital to consider the importance of vasculature and the extracellular matrix in the muscle regeneration process. Specifically, revascularization and the provision of an adequate blood supply represent major limiting parameters for a successful therapeutic approach at regenerating muscle damaged by ischemia (Grounds, 2008a; Ko et al., 2007). Regenerative myogenesis has been characterized by increased transcription of the myogenic regulatory factors (MRFs) MyoD, Myf5 and myogenin (Sabourin and Rudnicki, 2000), and may be augmented by the activation and maturation of local myocyte progenitors, termed satellite cells, often identified by Pax7 expression (Parise et al., 2006). In addition, appropriate adaptive changes in the intramuscular extracellular matrix can enhance the potential of muscle to recover and/or regenerate from damage (Kovanen, 2002). Notably, type I collagen is the predominant component of the skeletal muscle's extracellular matrix (San Antonio and Iozzo, 2006), and has been used for muscle cell differentiation in myoblast cell culture and in grafts (Kroehne et al., 2008). Collectively, these findings suggest that a collagen-based material that can

promote blood vessel growth may be an ideal candidate treatment for promoting skeletal muscle regeneration.

We previously reported on a type I collagen-derived matrix that contained the oligosaccharide sialyl Lewis^X (sLe^X), a ligand for the receptor L-selectin (Suuronen et al., 2009). L-selectin, a receptor for sLe^X, is expressed on the surface membrane of circulating angiogenic cells (CACs), and has a role in regulating their homing and adhesion (Biancone et al., 2004). When applied in a rat model of muscle ischemia, the sLe^X-matrix increased the number of c-kit$^+$, CXCR4$^+$ and VEGFR2$^+$ CACs, augmented blood vessel regeneration and restored perfusion, while not eliciting a foreign body or harmful immune response (Suuronen et al., 2009). Given the importance of vasculature and the extracellular matrix in muscle regeneration, and since the sLe^X-matrix can promote neovascularization and its composition is based on type I collagen, we hypothesized that it may possess the ability to stimulate regenerative myogenesis.

In this study, we characterized the mechanical properties of the sLe^X-matrix (which may be contributing factors towards its regenerative effects), and its ability to promote differentiation of mouse embryonic stem cells into a myogenic lineage *in vitro*. *In vivo*, a mouse hindlimb ischemia model was used to temporally investigate the ability of the sLe^X-matrix to induce bone marrow and local tissue responses for myogenesis and vasculogenesis in ischemic skeletal muscle. The results suggest that the provision of a vascularized matrix environment can promote regenerative myogenesis in ischemic muscle, supporting the sLe^X-matrix as a promising future therapy for muscle diseases.

Materials & Methods

Unless otherwise stated, all materials and reagents were obtained from Sigma-Aldrich (Oakville, Canada).

Matrix preparation

As previously described (Suuronen et al., 2009), 1mM sLe^X (Cedarlane Laboratories, Hornby, Canada) was prepared in 0.1M 2-(*N*-morpholino) ethanesulfonic acid (MES) buffer, at pH 5.0, containing 1:1 (molar equivalent) cross-linking mixture of *N*-ethyl-*N*-(3-dimethylaminopropyl) carbodiimide and N-hydroxysuccinimide (EDC/NHS; 13mM). This mixture was subsequently mixed on ice with 1% porcine type I atelocollagen (w/v; Nippon Ham, Tskuba, Japan) with 40% (w/v) chrondroitin sulfate-C (CS-C; Wako Chemicals, Osaka, Japan) and thoroughly mixed, then diluted with PBS. The final concentration of each component was: 0.59% collagen (w/v), 2.35% (CS-C) and 0.1mM sLe^X. The final pH was adjusted to 7.2-7.4 using 1N NaOH. Collagen-only matrices were prepared identically, but without sLe^X in the mixture. For *in vitro* use, 150µl of each matrix was evenly spread into a well of a 6-well culture plate (BD Biosciences, Mississauga, Canada) using a cell scraper, resulting in an approximate thickness of 6 mm. Materials were allowed 20 minutes at 37 °C to solidify. After gelation and hydration with media or PBS, the matrices display little affinity for TCPS and are easily removed. For *in vivo* application, materials were kept on ice and when required, 80µl was rapidly transferred to a syringe and subsequently injected.

Compression testing

Unconfined compression tests were performed using an MTS Bionix 858 servo-hydraulic material-testing system (MTS, Bellevue, USA) equipped with a 5kg load cell. Matrices (± sLe^X) were swelled for 24h in dPBS at 37°C. Samples were cut using an 8 mm diameter

punch, measured for thickness and placed inside of a plexiglass tank filled with dPBS for 1h prior to testing at 37°C. Samples were then placed between two non-porous stainless steel plates. Crosshead position and load were recorded using the Instron Wavemaker Software (version 7.0.0, Instron) at a crosshead-speed of 50%-per-minute and strained to a maximum of 20% strain. Each material was tested with *n*=5. Data was fitted to a stress-strain, 5-parameter double exponential growth model, as described (Millon et al., 2009):

$\sigma = y_0 + a*\exp(b*\varepsilon)+c*\exp(d*\varepsilon)$ Equation (1),

where σ is stress, ε is strain, and y_0, a, b,c and d are curve-fitting parameters. The elastic modulus, as a function of strain was calculated by differentiating Equation (1),

$\sigma' = a*b*\exp(b*\varepsilon) + c*d*\exp(d*\varepsilon)$ Equation (2),

where σ' is the elastic (tangent) modulus, ε is strain, and a, b, c and d are curve-fitting parameters. Elastic moduli are reported in kPa for the linear elastic region of the curves, which is the slope of the fitted curve in the linear region.

Water contact angle assessment

Contact angle measurements were performed on a VCA Optima contact angle system that relies on the deformation of drops or bubbles by gravity. The instrument equipped with a motorized syringe allows a water drop (5ul) to be suspended from a syringe of known radius. The drop is held up initially by surface tension but soon is deformed by gravity. Matrices were swelled for 24h in dPBS at 37°C. Samples were cut using a 4mm diameter punch, placed on the instrument's platform and tested immediately. Contact angle measurements were analyzed using VCA Optima Image Analysis software (*n*=6 for each material).

Rheology

Measurements of gelation time and viscosity were performed using a Brookfield R/S Plus Rheometer and a CC-3-50-2 R/S Spindle (Brookfield, Middleboro, USA), as previously described (Deng et al., 2010). The maximum viscosity η_{max} and the time required to reach η_{max} (T_{max}) were recorded for collagen- and sLe^X-matrices (n=5 each).

Mouse embryonic stem cell culture

D3 mouse embryonic stem cells (mESCs) were grown and differentiated as previously described (Kennedy et al., 2009). Briefly, the cells were aggregated at a density of $4x10^4$ cells/ml for 2 days in hanging drops and 5 days in non-tissue culture plates (Fisher Scientific, Ottawa, Canada). On day 7, the embryoid bodies were transferred to standard TCPS plates or tissue culture plates coated with either collagen or sLe^X-matrix. At the same time, some aggregates were transferred to coverslips coated with 0.1% gelatin (Fisher Scientific), collagen or sLe^X-matrix for later immunofluorescence analysis. On day 10, the medium (DMEM High Glucose + 15% FBS + 1% non-essential amino acids + 1% pen-strip + 0.8% beta-mercaptoethanol) was changed to a low serum formulation (DMEM-F12 + 1% pen-strep + 1% N2 Supplement (Invitrogen)) and the cells were allowed to grow for 5 more days. On day 15, the cells were harvested from the TC plates and fixed on coverslips. All experiments were performed in duplicate, with n=6.

RNA extraction, cDNA synthesis and quantitative PCR

Total RNA was extracted from cells and tissues using the RNeasy Kit (Qiagen Inc., Streetsville, Canada) following the manufacturer's protocol. The first strand of cDNA was synthesized from 1μg RNA by reverse transcription using QuantiTect Reverse Transcription Kit (Qiagen Inc.). qPCR reactions were performed as previously described (Savage et al.,

2009) using the primer sequences in Table 4-1. The reactions and data analysis were performed on an Epgradien S system (Eppendorf, Hamburg, Germany) using RealPlex version 2.2 software (Eppendorf). Relative gene expression was calculated using the comparative Ct method as described previously (Savage et al., 2009). Results for *in vitro* and *in vivo* tissue work were expressed as a ratio to β-actin and GAPDH, respectively. *In vitro* results were compared to results obtained on TCPS; *in vivo* results were compared to each animal's untreated, contralateral limb.

Table 4-1 – qPCR primer sequences used for analysis of murine transcripts in both tissue lysates and embryonic stem cell cultures.

GENE	FORWARD PRIMER, 5' to 3'	REVERSE PRIMER, 5' to 3'
GAPDH	TCGGTGTGAACGGATTTG	GGTCTCGCTCCTGGAAGA
M-cadherin	CATCCCACCCATTAGTGTGTC	TCCCAGTGAACTTGTCGATAGA
MHC3	GCATAGCTGCACCTTTCCTC	GGCCATGTCCTCAATCTTGT
MHC7	GATGAGCAAGCCCTGGGCAGTC	TCAGAGCGCAGCTTCTCCACCT
Myf5	CCTGTCTGGTCCCGAAAGAAC	GACGTGATCCGATCCACAATG
MyoD	CCCCGGCGGCAGAATGGCTACG	GGTCTGGGTTCCCTGTTCTGTT
Myogenin	GCAATGCACTGGAGTTCG	ACGATGGACGTAAGGGAGTG
Pax3	TTTCACCTCAGGTAATGGGACT	GAACGTCCAAGGCTTACTTTGT
Pax7	CTCAGTGAGTTCGATTAGCCG	AGACGGTTCCCTTTGTCGC
Six1	TAACTCCTCCTCCAACAAGCA	CGAGTTCTGGTCTGGACTTTG
β-actin	AAATCGTGCGTGACATCAAA	AAGGAAGGCTGGAAAAGAGC

Western blotting

Cells were harvested for total protein extract with modified RIPA buffer (50mM Tris-HCl, pH 7.4, 1% NP-40, 0.25% Na-deoxycholate, 150mM NaCl, 1mM EDTA, 1mM PMSF) with a protease inhibitor cocktail (Roche, Laval, Canada). Protein was separated on a 10% SDS PAGE gel in a 1× Running Buffer and transferred to an Immunoblot PVDF-membrane (BioRad, Saint-Laurent, Canada). Anti-Pax3 (1:300, R&D Systems) was used and visualized with HRP-conjugated secondary antibodies. Blots were enhanced using Western Blot Signal Enhancer (Fisher Scientific) before blocking with 5% Milk in TBST.

Immunofluorescence

mESCs were fixed in cold methanol and incubated with mouse anti-myosin heavy chain (MHC) monoclonal antibody MF20 (Developmental Studies Hybridoma Bank) overnight at 4°C. Goat anti-mouse IgG (H+L) Cy3-linked secondary antibody (Jackson ImmunoResearch Laboratories, West Grove, USA) was used to visualize MHC3 protein expression. Hoechst dye was used for nuclear staining. Images were acquired with an Olympus BX50 microscope using Image Pro Plus. Fusion index was reported as the percentage of nuclei per field-of-view (FOV) that are in multi-nucleated cells, indicating that cell fusion has occurred.

Animal model

All procedures were performed with approval of the University of Ottawa Animal Care Committee, in compliance with the National Institute of Health's Guide for the Care and Use of Laboratory Animals. To investigate the endogenous bone marrow response, a green fluorescent protein (GFP) bone marrow transplantation (BMTx) was performed, as previously described (Whitman et al., 2004). Briefly, 8-9 week-old female C57BL/6J mice (Jackson Laboratories, Bar Harbor, USA) were irradiated with a total of 900 rads from a

cesium source, delivered 3 hours apart in 2 equal doses. Donor bone marrow cells (7×10^6) from a transgenic GFP mouse (C57BL/6-Tg(CAG-EGFP)10sb/J; Jackson Laboratories) were injected into the tail vein of irradiated recipient mice in a total volume of 150µl dPBS. Six weeks after BMTx, proximal femoral arteries in left hindlimbs were ligated, as described (Limbourg et al., 2009), using 4.0 silk thread, under 2% isoflurane. Gastrocnemius muscles, downstream of the ligation site, subsequently received 80 µl injection of: dPBS (*n*=9), collagen matrix (*n*=8), or sLe^X-matrix (*n*=8), using a 27-gauge needle (BD Biosciences) in 3 equivolumetric injections spaced throughout the muscle. Animals were sacrificed on day 14. To further characterize the myogenic response without the effects of a BMTx, the same procedure was performed on wild-type C57BL/6J mice without a BMTx, and animals were sacrificed on day 3 or day 10 (*n*=6 for all treatments per time point). Additional age-matched, untreated animals (no ligation surgery or treatment) were sacrificed as baseline controls (*n*=6).

Flow cytometry

Blood samples (~100µl) were procured from the right saphenous veins on days 0 (pre-operative/baseline), 1, 4, 7 and 14 post-operatively. As previously described (Suuronen et al., 2009), CACs were isolated using density-gradient centrifugation on Histopaque 1077 and immediately stained with the following antibodies: anti-c-kit (Southern Biotech, Birmingham, USA), anti-CXCR4 (BD Biosciences, Mississauga, Canada) and anti-flk-1 (eBioscience, San Diego, USA). Cells were analyzed with a FACSAria flow cytometer (BD Biosciences). Isotype, fluorochrome-matched immunoglobulin antibodies were used as controls. CAC expression of a particular antigen is presented as relative to its baseline value (at day 0).

Laser Doppler

Perfusion was assessed using laser Doppler pre-operatively (baseline) and on days 4 and 14, as previously described (Kuraitis et al., 2011a). Briefly, under 2% isoflurane, a multi-fiber needle probe (8 separate collecting fibers; Moor Instruments, Axminster, UK) was used to evaluate perfusion in both treated and untreated hindlimbs. Data are reported as perfusion indexes, calculated as a ratio of perfusion in treated:untreated hindlimbs.

Immunohistochemistry

Gastrocnemius muscles from BMTx mice were collected and fixed overnight in 4% paraformaldehyde before paraffinization. All samples were analyzed in cross-section. Samples were de-paraffinized and hydrated with sequential washes in toluene and decreasing concentrations of ethanol. Antigen retrieval was performed using boiling citrate buffer (pH 5.6). All staining was performed in PBS containing 10% normal horse serum (Vector Laboratories, Burlington, Canada). The following antibodies were used: anti-α-SMA (pre-diluted, Abcam, Cambridge, USA), anti-GFP (1:100; Abcam), and anti-CXCR4 (1:50; Abcam). Hindlimbs from non-BMTx mice were collected and placed in OCT solution before being frozen in liquid nitrogen. Tissue sections were stained with anti-active caspase-3 antibody (1:50; Abcam), and myofiber borders were visualized using wheat germ agglutinin-Texas Red (Invitrogen, Burlington, Canada), following the manufacturer's protocol. For all analyses: sections were 5μm in thickness; mounting medium with DAPI (Vector Laboratories) was used to visualize nuclei; and measurements and cell counts were determined from 6 random microscopic FOV, taken by a blinded observer with a Zeiss AxioObserver Z1 microscope and visualized with Axiovision. Counts were averaged from

two blinded observers. The cross-sectional area (CSA) of arterioles was determined using Image Pro Plus.

Cytokine arrays

As previously described (Kuraitis et al., 2011a), hindlimbs were lysed under liquid nitrogen, and cytokine arrays (Raybiotech, Norcross, USA) were performed according to the manufacturer's recommendations. Custom cytokine arrays were used to analyze the protein levels of basic fibroblast growth factor (bFGF), insulin-like growth factor-I (IGF-I), IGF binding proteins -2 and -5 (IGFBP-2, -5), interleukin-10 (IL-10), L-selectin, P-selectin, stromal cell-derived factor-1α (SDF-1α), tissue inhibitor of matrix metalloproteinase-2 (TIMP-2), tumor necrosis factor-α (TNFα), vascular cell adhesion molecule-1 (VCAM-1), and vascular endothelial growth factor (VEGF). Arrays were performed with n=5 for each group evaluated.

Functional assessment of treated muscle

A subset of mice that received PBS or one of the matrix treatments into the ischemic hindlimb (n=6 per group) were sacrificed at day 10 for functional assessment of the treated muscle. Untreated wild-type animals were included as controls. Soleus muscles were carefully isolated and maintained in a continuously oxygenated Krebs-Ringer bicarbonate buffer solution. One end of the muscle was linked to a fixed clamp and the other end to the lever arm of an Aurora Scientific Instruments 300B actuator/transducer system. Muscles were electrically stimulated via two platinum electrodes and cross-sectional area, twitch force, maximum force, power decrease and time to fatigue were recorded as previously described (Del Prete et al., 2008). Cross-sectional area measurements allowed for calculation of specific force values.

To assess the functional recovery of treated muscles, animals were subjected to a forced treadmill protocol. They were conditioned to the treadmill process for 1 week prior to final testing at an incline of 0º for 5min at 5m/s and 5min at 10m/s. Animals that did not maintain the treadmill speed received a shock of 0.5mA. The maximal test of exhaustion was modified from Ferreira *et al*. (Ferreira et al., 2008). In brief, the treadmill speed increased every 3 minutes at a rate of 3m/min. Animals were removed from the treadmill when they could no longer manage to return to the treadmill from the shock platform. Total distance and speed at which exhaustion occurred were recorded (n=5).

Statistical analysis

Comparisons between multiple groups were performed using a one-way analysis of variance with Tukey's post-hoc test. Comparisons between repetetitive stimulation in power measurements were performed using a two-way analysis of variance with Bonferroni's post-hoc test. Comparisons between two groups were performed using a 2-tailed student's *t*-test. (SPSS; IBM, Somers, USA). Unless otherwise stated, values are expressed as means ± standard error. *P*-values of < 0.05 were considered statistically significant.

Results

Mechanical properties of the matrices are similar to those of skeletal muscle

It is known that a substrate's mechanical properties (such as stiffness) are important for regulating the development and maintenance of muscle (Engler et al., 2004; Engler et al., 2006). Therefore, the physical properties of sLe^X-matrix and collagen-only matrix were tested to determine if these fell within the range considered favorable for the support of

skeletal muscle. Rheological assessment revealed that the addition of sLe^X to the collagen matrix did not alter the time to gelation at 37ºC (P=0.7; Fig. 4-1A), nor did it change the viscosity of the material upon gelation (P=1.0; Fig. 4-1B). Both matrices (with and without the addition of sLe^X) displayed a gradual increase in stiffness and showed a linear stress-strain response up to 12% strain, followed by a non-linear response (Fig. 4-1C). In this linear region, the elastic modulus (σ') for the collagen matrix was 5.85±0.06 kPa. Incorporation of sLe^X into the matrix increased the modulus to 7.51±0.07 kPa (p=0.013). These moduli are similar to the range of native skeletal muscle elasticity (Engler *et al*., 2006). Water contact angles were not measurable on the collagen matrix (Fig. 4-1D), due to its extreme hydrophilicity and water content; however, the addition of sLe^X generated areas on the matrices where contact angle was measured at 48.1°±3.2, indicating the presence of less hydrophilic areas within the matrix (Fig. 4-1E). To summarize, our mechanical analysis revealed that the elastic moduli of the matrices are similar to that of skeletal muscle.

Figure 4-1 Characterization of matrices' mechanical properties. (A) Average viscosity upon gelation (η_{MAX}, Pa·s), and (B) average time to gelation (T_{MAX}, s) measurements for the collagen matrix and the sLe^X-matrix. (C) Stress-strain curves for the 2 matrices at 20% strain and a 50%/min strain rate. (D, E) Representative images of water contact angle (θ) for collagen (D) and sLe^X-matrix (E); water contact angle of θ=46° is shown. Histograms in A and B represent data from n=4 different samples, and in C are from n=5 different samples. Water contact angle images in D and E are representative of n=6 separate samples per group.

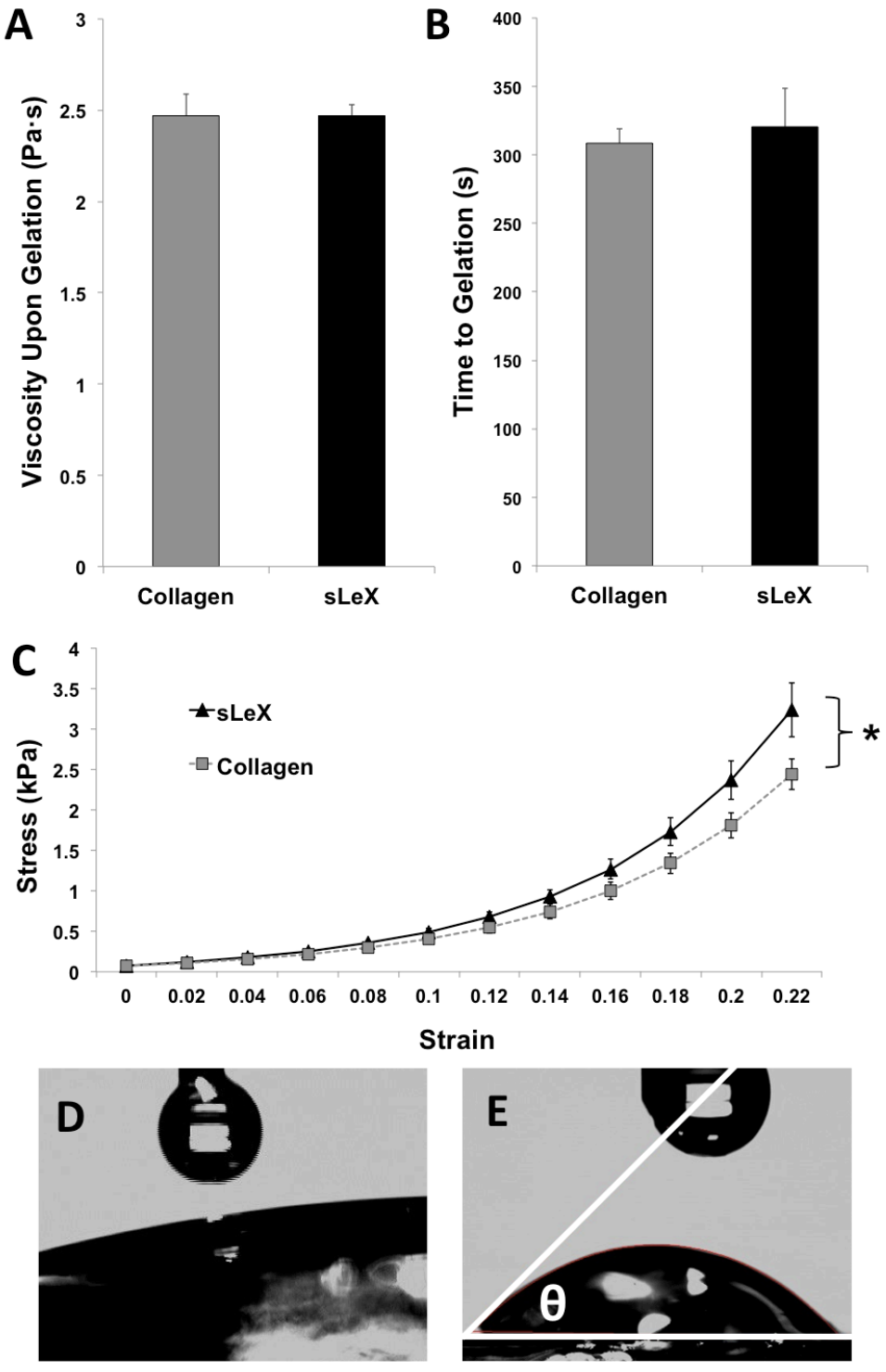
A
Viscosity Upon Gelation (Pa·s)
3
2.5
2
1.5
1
0.5
0
Collagen
sLeX
B
Time to Gelation (s)
400
350
300
250
200
150
100
50
0
Collagen
sLeX
C
Stress (kPa)
4
3.5
3
2.5
2
1.5
1
0.5
0
sLeX
Collagen
*
0
0.02
0.04
0.06
0.08
0.1
0.12
0.14
0.16
0.18
0.2
0.22
Strain
D
E
θ

Matrices facilitate myogenic differentiation of murine embryonic stem cells

To study the myogenic properties of the matrices, we compared the differentiation of murine embryonic stem cells (mESCs) on the sLe^X-matrix versus collagen-only matrix and tissue culture polystyrene (TCPS) substrates over a period of 8 days, after 7 days of embryoid body formation. The culture of mESCs on collagen and/or sLe^X-matrix increased mRNA levels for factors involved in myogenic progenitor formation, myogenic regulation, and final muscle development (Fig. 4-2A-H). Collagen matrix and sLe^X-matrix increased mRNA levels of Pax3 ($P<0.03$; Fig. 4-2C), MHC3 ($P<0.05$; Fig. 4-2D), myogenin ($P\leq0.1$; Fig. 4-2E) and troponin-C ($P<0.05$; Fig. 2H). Only culture on collagen matrix increased Pax7 mRNA levels ($P=0.02$; Fig. 4-2B) and Myf5 ($P=0.01$; Fig. 4-2F). Differences in mRNA were not noted for Six1 (Fig. 4-2A) or MyoD (Fig. 4-2G). An increase in the protein level of Pax3 in cells cultured on either matrix was detected by Western blotting (Fig. 4-2I). The fusion index was greater for both matrix treatments (Fig. 4-2J). Immunofluorescence staining demonstrated increased MHC protein in mESCs cultured on matrix versus TCPS (Fig. 4-2K-M). These results demonstrate that the matrices enhanced skeletal myogenesis in mESCs, indicated by the upregulation of skeletal muscle markers.

Figure 4-2 Matrices augment myogenic differentiation of murine embryonic stem cells. (A-H) mESCs were differentiated for 8 days on collagen matrix or sLe^X-matrix (after 7 days of EB formation) and mRNA levels for several myogenic factors were measured by q-PCR, and compared to culture on tissue culture polystyrene plates (TCPS). The y-axis for all graphs represents the fold-difference relative to TCPS. (I) Pax3 protein expression in mESCs differentiated on the 3 substrates was measured by Western blot. Myocyte fusion was increased in both matrix treatments (J). (K-M) Hoechst staining (blue) and immunofluorescence staining for MHC (red) in differentiated mESCs. Scale bars=180μm. *$P<0.05$ and $^{\dagger}0.05<P<0.1$ vs. TCPS. Results are from 2 (n=6 total per group; in duplicate for A-G) independent experiments.

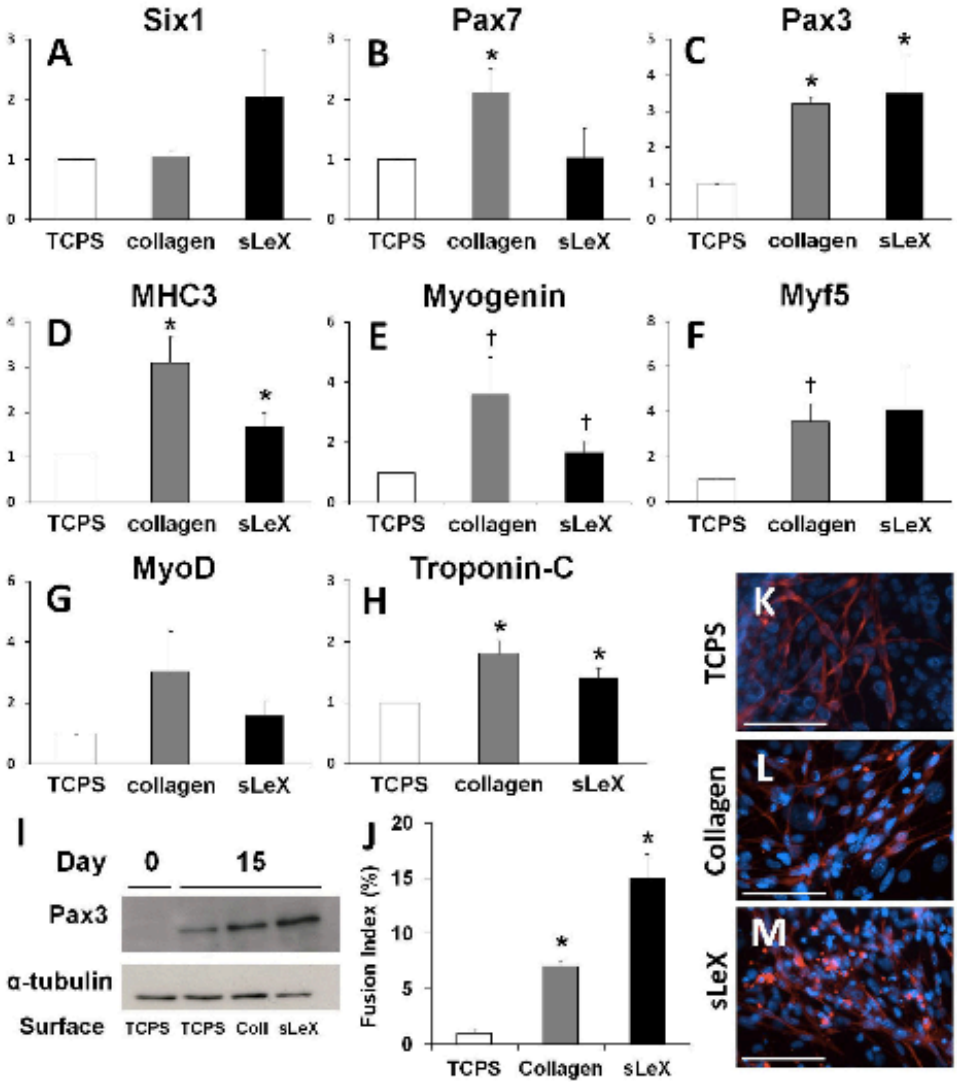
Six1
A
TCPS collagen sLeX
Pax7
B
*
TCPS collagen sLeX
Pax3
C
*
*
TCPS collagen sLeX
MHC3
D
*
*
TCPS collagen sLeX
Myogenin
E
†
†
TCPS collagen sLeX
Myf5
F
†
TCPS collagen sLeX
MyoD
G
TCPS collagen sLeX
Troponin-C
H
*
*
TCPS collagen sLeX
I
Day 0 15
Pax3
α-tubulin
Surface TCPS TCPS Coll sLeX
J
Fusion Index (%)
20
15
10
5
0
*
*
TCPS Collagen sLeX
K
TCPS
L
Collagen
M
sLeX

Myocyte regeneration is enhanced 10 days post-matrix treatment

Regenerative myogenesis was quantified in sections of hindlimb muscle by the number of myocytes with centralized nuclei, which represent young myocytes under 1-month of age (Sun et al., 2009). Data is reported as the percentage of myocytes with centralized nuclei (termed regenerating myocytes). At day 14, the sLe^X-matrix-treated animals had 8.1-fold more regenerating myocytes, compared to PBS (P=0.005; Fig. 4-3A). To better understand the myogenic regenerative process of the ischemic muscle in response to our treatment temporally, additional mice were evaluated 3 and 10 days after treatment. At day 3, mice did not show any differences in regenerating myocytes between treatment groups (P=0.8; Fig. 4-3A-D). However, at day 10, the sLe^X-matrix treatment significantly increased the regenerating myocyte number by 4.5-fold compared to the PBS group (P=0.02; Fig. 4-3A, E, G).

Similarly, differences in the mRNA levels of several skeletal muscle markers in ischemic hindlimbs were not noted between treatment groups at day 3. The exception was Pax7 (marker for skeletal muscle satellite cell), which was greatest in PBS-treated animals compared to treatment with collagen matrix (13.9-fold; P=0.007) or with sLe^X-matrix (6.1-fold; P=0.02; Fig. 4-4A). However, at day 10, matrices induced the transcription of several myogenic factors (Fig. 4-4B), compared to PBS. Specifically, treatment with sLe^X-matrix upregulated the hindlimb tissue mRNA levels of the MRFs MyoD (3.7-fold; P=0.06), myogenin (8.1-fold; P=0.007) and Myf5 (3.4-fold; P=0.007), as well as Six1 (2.1-fold; P=0.04), and the satellite cell markers Pax7 (8.5-fold; P=0.06) and M-cadherin (3.5-fold; P=0.01). There was a favourable trend for collagen matrix treatment to upregulate the muscle differentiation marker MHC3 (3.2-fold; P=0.06), the MRF Myf5 (1.6-fold; P=0.09), and

Six1 (2.3-fold; *P*=0.1). Overall, both matrices increased the transcription of myogenic genes. Although no differences were detected between the 2 matrices, only treatment with sLe^X-matrix resulted in significantly elevated levels of some of these genes compared to PBS, and only the sLe^X-matrix treatment increased the number of new myocytes.

Figure 4-3 Regenerative myogenesis is enhanced after treatment with sLe^X-matrix. (A) The number of regenerating myocytes (identified by centralized nuclei) per FOV in hindlimb muscle sections in non-BMTx model, 3 and 10 days after treatment, and in the BMTx model, 14 days after treatment. (B-G) Double immunofluorescent staining for nuclei (DAPI) and myocyte borders (wheat germ agglutinin-Texas Red (red)) in early- (day 3; B-D) and late- (day 10; E-G) stage cross-sections of hindlimb muscle (non-BMTx model). Scale bars=50μm. $^{**}P \leq 0.01$ vs. PBS of the same day. Results are representative of n=8-9 (BMTx model) and n=6 (non-BMTx model) separate mice per treatment group per time point.

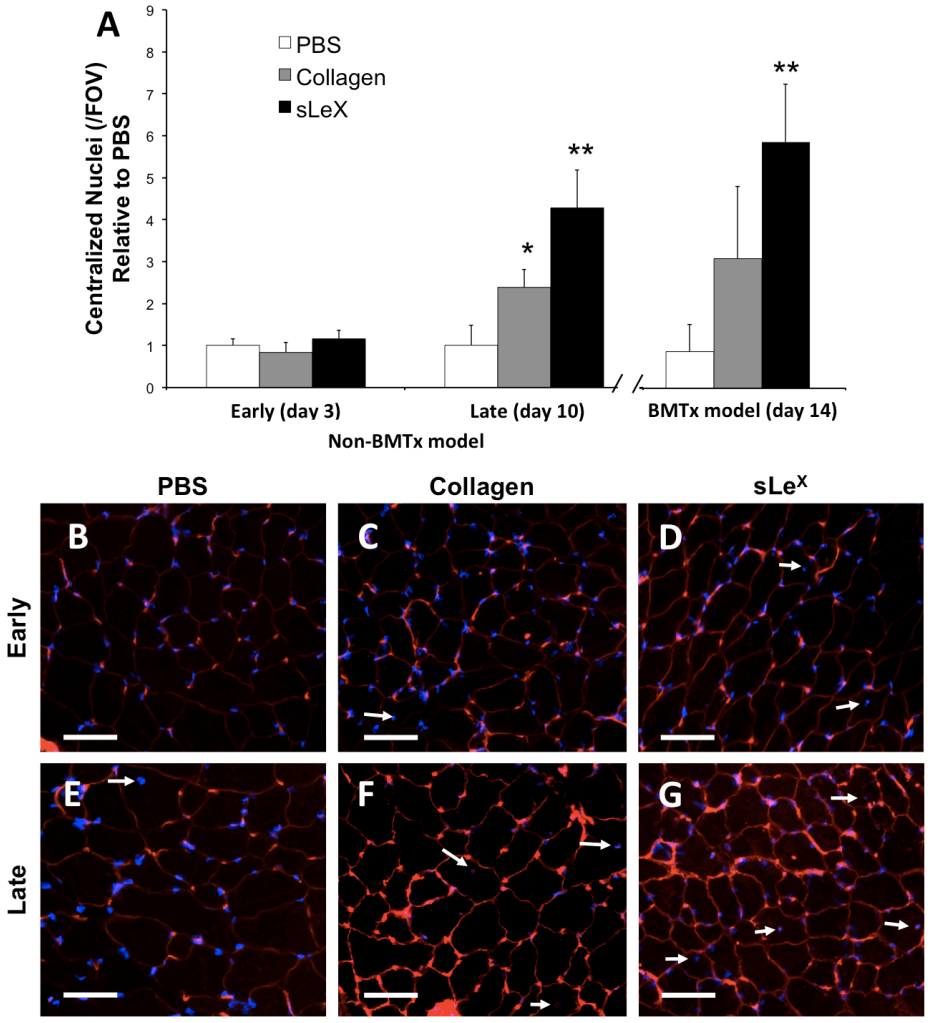
A
PBS
Collagen
sLeX
Centralized Nuclei (/FOV)
Relative to PBS
0
1
2
3
4
5
6
7
8
9
*
**
**
Early (day 3)
Late (day 10)
BMTx model (day 14)
Non-BMTx model
PBS
Collagen
sLeX
Early
Late
B
C
D
E
F
G

Figure 4-4 Treatment with sLe^X-matrix increases the transcription of myogenic factors in the hindlimb muscle. (A) qPCR analysis of myogenic transcripts in hindlimb tissue at 3 days after treatment (non-BMTx model). (B) qPCR analysis of myogenic transcripts in hindlimb tissue at 10 days after treatment (non-BMTx model). The y-axis for all graphs represents the fold-difference relative to the untreated, contra-lateral limb. $^{\dagger}0.05<P<0.1$ vs. PBS; $^{*}P<0.05$ vs. PBS. Results are from n=6 different mice per group per time point.

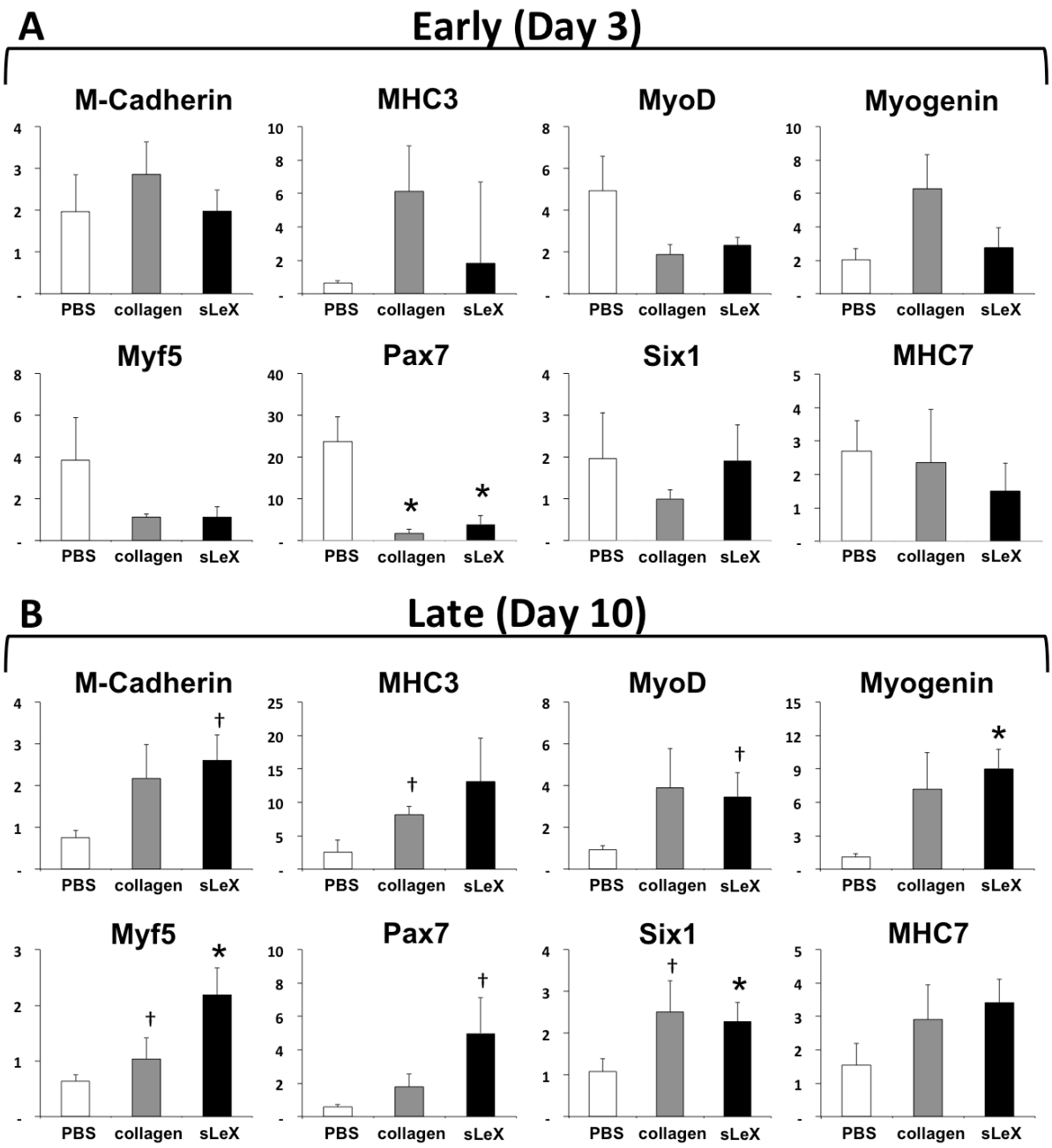
A
Early (Day 3)
M-Cadherin
MHC3
MyoD
Myogenin
Myf5
Pax7
Six1
MHC7
PBS
collagen
sLeX
*
B
Late (Day 10)
M-Cadherin
MHC3
MyoD
Myogenin
Myf5
Pax7
Six1
MHC7
†
*

Cytoprotection is conferred by matrices

The level of ischemia-induced apoptosis, as determined by positive staining for active caspase-3, was assessed in hindlimbs. At day 3, hindlimbs of PBS and collagen matrix treatments had 1.47- (P=0.01) and 1.51-fold (P=0.01) more apoptotic cells, respectively, than those treated with sLe^X-matrix (Fig. 4-5A). Later, at day 10, there was no longer a difference in local apoptosis between the two matrix treatments, but PBS-treated hindlimbs maintained more apoptotic cells than those which received collagen matrix (by 2.1-fold; P=0.02) or sLe^X-matrix (by 3.4-fold; P=0.0002; Fig. 4-5A-D). From day 3 to day 10, the number of apoptotic cells in sLe^X-matrix-treated hindlimbs did not change (P=0.4), but a reduction (0.6-fold) was observed for collagen matrix treatment (P=0.02). A trend for increased apoptosis (by 1.4-fold) was observed for the PBS treatment (P=0.07).

Figure 4-5 Reduced apoptosis is observed in hindlimbs treated with sLe^X-matrix. (A) The number of apoptotic cells (positive for active caspase-3) per FOV in hindlimb muscle sections at 3 and 10 days post-treatment (normalized to PBS). (B-D) Double immunofluorescence for the detection of active caspase-3 (green) and nuclei (DAPI) in hindlimb muscle sections. Scale bars=30μm. *$0.05<P<0.1$ vs. collagen; **$P<0.05$ vs. all others; $^{\#}0.05<P<0.1$ between days 3 and 10; $^{\#\#}P<0.05$ between days 3 and 10. Results are from n=6 different mice per group per time point.

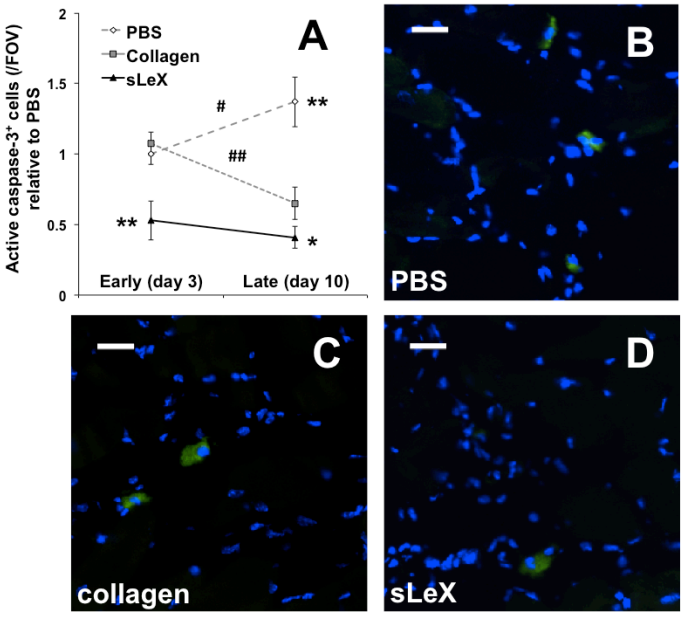
A
PBS
Collagen
sLeX
Active caspase-3+ cells (/FOV) relative to PBS
2
1.5
1
0.5
0
#
##
**
**
*
Early (day 3)
Late (day 10)
B
PBS
C
collagen
D
sLeX

Treatment with sLe^X-matrix improves arteriogenesis and restores perfusion

The same hindlimb ischemia model was used to assess matrix effects on vascular regeneration, but using a bone marrow transplantation (BMTx) model. We have previously demonstrated that an injectable matrix can restore perfusion to ischemic muscle (Suuronen et al., 2009), and wanted to identify the role of bone marrow-derived progenitors in this phenomenon. Bone marrow reconstitution was performed using donor bone marrow cells from a transgenic green fluorescent protein (GFP) mouse, so that the mobilized bone marrow cells could be tracked using immunohistochemistry and flow cytometry. Laser Doppler analysis demonstrated that the ligation surgery reduced perfusion in the hindlimb by approximately 50%. Four days after ligation surgery and treatment injection, there was no difference in perfusion among the treatment groups (Fig. 4-6A; P=0.6). At day 14, sLe^X-matrix treatment restored perfusion to a level that was 85% greater than the PBS group (P=0.01), and 24% greater than the collagen matrix group (P=0.03; Fig. 4-6A).

Although hindlimb arteriole density (determined by immunofluorescence with α-smooth muscle actin (SMA)) did not differ between matrix treatments (P=0.7), it was increased in both the sLe^X-matrix and collagen matrix groups by 1.8- (P=0.01) and 1.7-fold (P=0.01), respectively, compared to PBS treatment (Fig. 4-6B-E). Upon examination of arteriolar size, the mean cross-sectional area of arterioles of sLe^X-matrix-treated animals was 3.2- and 5.2-fold greater than that of the collagen matrix (P=0.01) and the PBS-treated animals, respectively (P=0.003; Fig. 4-6F). A trend for increased arteriolar area by 1.6-fold was observed for treatment with collagen matrix compared to PBS (P=0.08). To summarize, the sLe^X-matrix induced the formation of arterioles of greater size, accompanied by a greater restoration of blood flow.

Figure 4-6 The sLe^X-matrix improves perfusion of ischemic hindlimbs and augments arteriole formation. (A) Hindlimb perfusion measured by laser Doppler analysis up to 2 weeks after treatment with PBS, collagen or sLe^X-matrix. (B-D) Double immunofluorescence images of hindlimb muscle for α-SMA (red) and nuclei (DAPI). (E) The number of arterioles quantified in hindlimb muscle sections. (F) Assessment of the average arteriolar lumen size (area) in hindlimb muscle. Scale bars=125μm. *P<0.05 vs. PBS; **P≤0.01 vs. all others. Results represent data from n=8-9 separate mice per group.

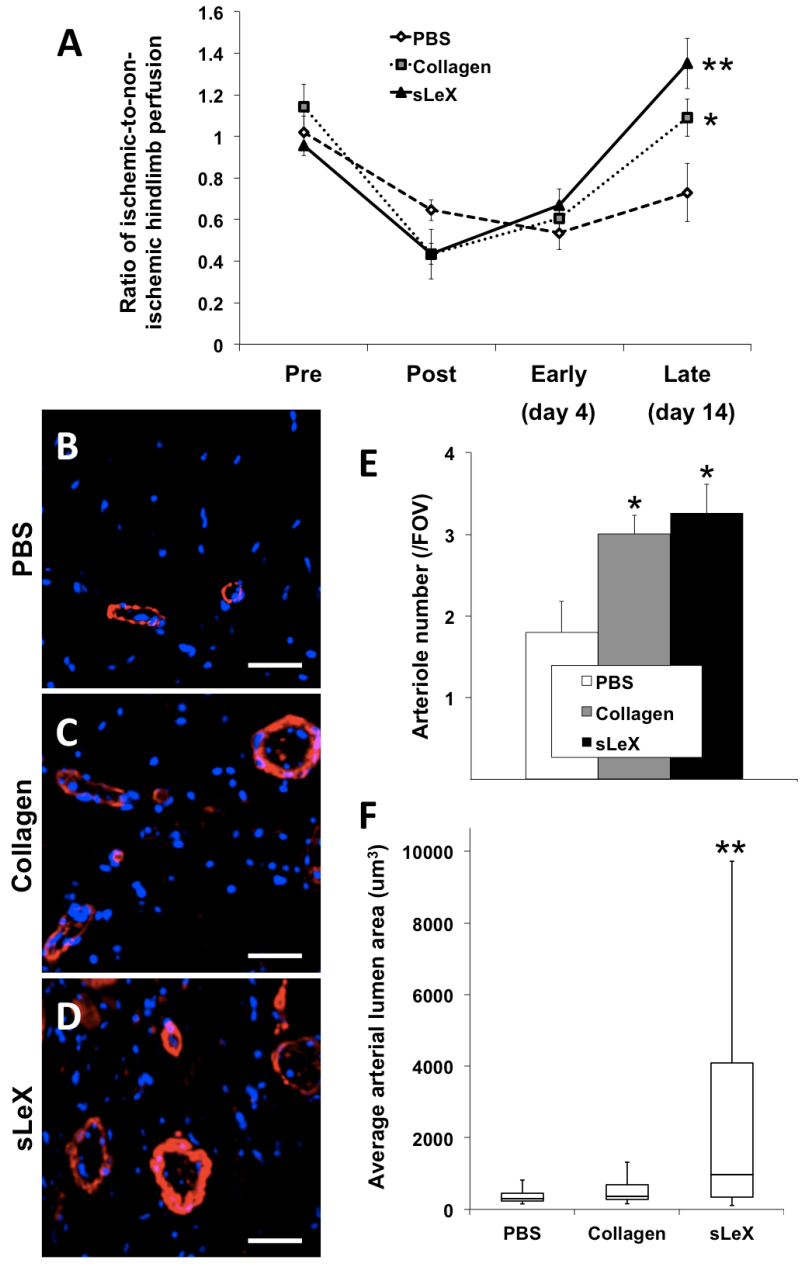
A
Ratio of ischemic-to-non-ischemic hindlimb perfusion
1.6
1.4
1.2
1
0.8
0.6
0.4
0.2
0
PBS
Collagen
sLeX
**
*
Pre
Post
Early (day 4)
Late (day 14)
B
C
D
PBS
Collagen
sLeX
E
Arteriole number (/FOV)
4
3
2
1
*
*
PBS
Collagen
sLeX
F
Average arterial lumen area (um3)
10000
8000
6000
4000
2000
0
**
PBS
Collagen
sLeX

The sLe^X-matrix mobilizes CACs from bone marrow

Marrow-derived progenitor cells (GFP$^+$ cells) that were mobilized to the circulation were characterized by flow cytometry using antibodies for the CAC markers c-kit, flk-1 and CXCR4. At early time points after intramuscular delivery of the treatment (days 1-4), the sLe^X-matrix increased GFP$^+$c-kit$^+$ cells in the circulation by 1.4-fold, compared to PBS (Fig. 4-7A; *P*=0.001). Both collagen and sLe^X-collagen matrices increased the frequency of GFP$^+$flk-1$^+$ cells by 2.1- and 2.3-fold, respectively (Fig. 7A; *P*=0.03, 0.006). At later time points (days 7-14), continued effects of the sLe^X-collagen matrix treatment on bone marrow cell mobilization were observed (Fig. 4-7A). Specifically, the sLe^X-matrix treatment increased circulating GFP$^+$CXCR4$^+$ cells compared to both PBS (1.7-fold; *P*=0.04) and collagen matrix (1.5-fold; *P*=0.02) treatments. In addition, sLe^X-matrix treatment increased GFP$^+$flk-1$^+$ cells by 2.3-fold (*P*=0.001) compared to PBS, and by 1.4-fold (*P*=0.02) compared to collagen matrix. Collagen matrix and sLe^X-matrix increased GFP$^+$c-kit$^+$ cells by 1.5-fold (*P*=0.03) and 2.1-fold (*P*=0.0001), respectively, compared to PBS. Overall, these results demonstrate the ability of the sLe^X-matrix to increase the mobilization of CACs from the bone marrow.

Matrix treatment increases marrow-derived and local CXCR4$^+$ cell recruitment to the ischemic hindlimb

Following bone marrow cell mobilization into the circulation, we investigated the effect of the different treatments on recruiting mobilized GFP$^+$ cells from the circulation to the ischemic hindlimb muscle. After 2 weeks, the sLe^X-matrix treatment resulted in the greatest recruitment and engraftment of bone marrow cells in the hindlimb muscle, which was 5.6- (*P*=0.004) and 2.5-fold (*P*=0.02) more than the PBS and collagen matrix treatments,

respectively (Fig. 4-7B-E). The collagen matrix also increased the number of engrafted GFP^+ cells by 2.3-fold (P=0.02), compared to PBS (Fig. 4-7E). Immunostaining did not demonstrate any GFP^+ cell incorporation into vasculature, nor into myocytes.

The importance of CXCR4 expression for neovascularization has been previously shown (Borselli et al., 2010; Grounds, 2008a; Seeger et al., 2009); therefore, we sought to characterize $CXCR4^+$ cells in the present study. Both sLe^X-matrix and collagen matrix treatments increased total counts of $CXCR4^+$ cells in treated hindlimbs compared to PBS (Fig. 4-7F-I), by 3.3- (P=0.002) and 2.4-fold (P=0.03), respectively. Notably, the sLe^X-matrix recruited more non-marrow derived $CXCR4^+$ cells (by 9.2-fold; likely from the local tissue since they lack GFP expression), compared to the PBS group (P=0.02). Therefore, recruitment/engraftment of both bone marrow-derived CACs and local angiogenic cells were greatest with the sLe^X-matrix treatment.

Figure 4-7 Mobilization and recruitment of bone marrow CACs and local cells are improved by sLe^X-matrix treatment. (A) Levels of GFP$^+$ circulating cells (relative to day 0 baseline) expressing CXCR4, flk-1 and c-kit measured by flow cytometry at 1-4 and 7-14 days after treatment with PBS, collagen or sLe^X-matrix. (B-D) Double immunostaining of hindlimb muscle for recruited GFP$^+$ marrow cells (green) and nuclei (DAPI). (E) Numbers of GFP$^+$ cells per FOV in hindlimb muscle. (F) Numbers of local (GFP$^-$), marrow (GFP$^+$), and total CXCR4$^+$ cells per FOV in hindlimb muscle. (G-I) Triple immunostaining of hindlimb muscle for recruited GFP$^+$ marrow cells (green), CXCR4 (red) and nuclei (DAPI). Scale bars=50μm. *P<0.05 vs. PBS; **P<0.05 vs. all others; $^\dagger P$<0.05 vs. baseline. Results represent data from n=8-9 separate mice per group.

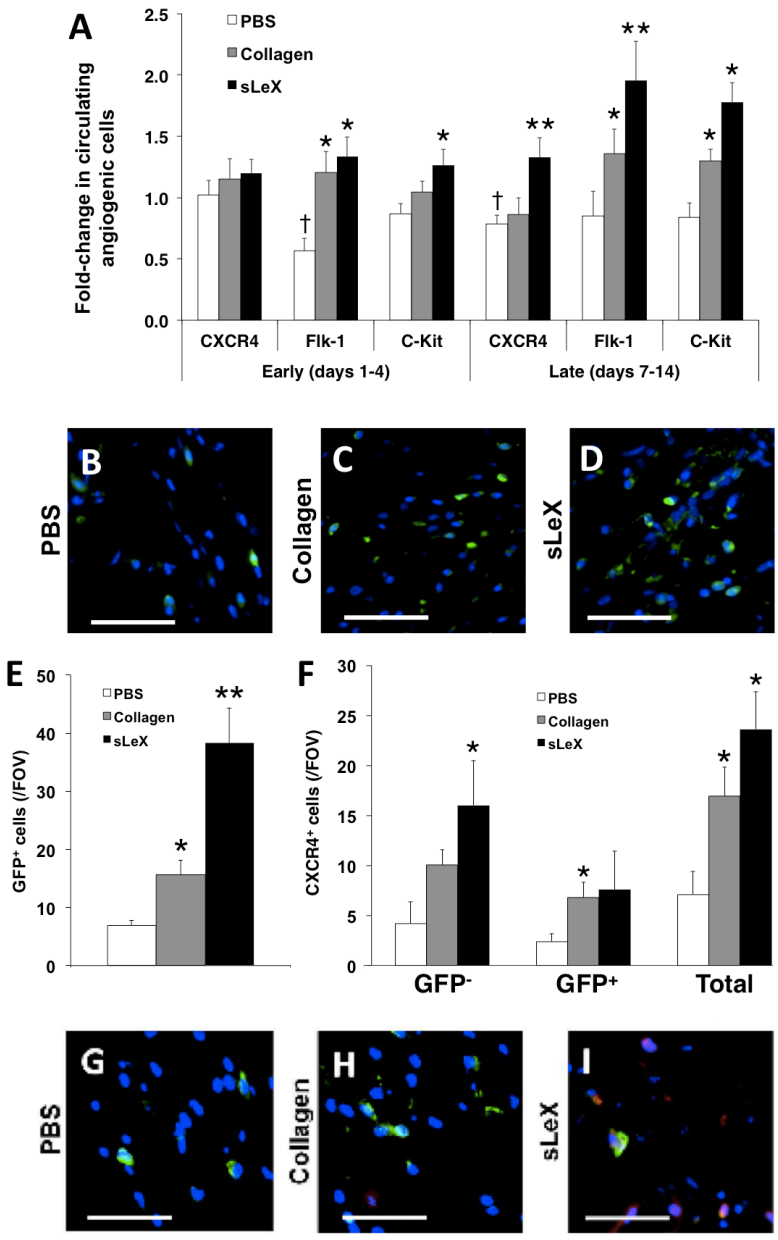
A
Fold-change in circulating angiogenic cells
PBS
Collagen
sLeX
CXCR4
Flk-1
C-Kit
Early (days 1-4)
Late (days 7-14)
B
C
D
PBS
Collagen
sLeX
E
GFP+ cells (/FOV)
F
CXCR4+ cells (/FOV)
GFP-
GFP+
Total
G
H
I

Matrix treatments augment protein levels of regenerative factors and cytokines

To explore potential mechanisms for the observed myogenic and vascular regeneration, we used a mouse-specific antibody array to assess protein levels of cytokines in the ischemic tissue in the non-BMTx model. A summary of differences in the levels of various cytokines in the hindlimb is presented in Fig. 8 (differences with $P<0.05$ are indicated). Animals that received neither the ligation surgery nor an injected treatment served as baseline controls. Myogenic-mediated factors assessed included IGF-1 and IGFBPs. At day 3, the sLe^X-matrix greatly increased local IGF-1 (17.9-fold versus baseline). Similarly, IGFBP-2 and -5 levels were increased with sLe^X-matrix treatment versus all other treatments at the early time point (≥2.1- and ≥1.4-fold, respectively).

In the analysis of angiogenic cytokines, notably, only the sLe^X-matrix treatment increased hindlimb VEGF levels (2.3-fold versus baseline; ≥1.8-fold versus other treatments). In addition, bFGF was upregulated in both matrix treatments early on (versus baseline at day 3), and this upregulation was maintained later on (versus baseline and ≥4.2-fold versus PBS at day 10). VCAM-1 was increased for all treatments at the 3- and 10-day time point; however, matrix treatments increased VCAM-1 levels by ≥2.2-fold versus PBS early on (day 3). At 10 days, only limbs treated with PBS had a lasting increase in the anti-angiogenic and anti-remodeling protein TIMP-2 (5.4-fold vs. baseline). Matrices promoted greater levels of IL-10 (anti-inflammatory cytokine) in the ischemic muscle (by ≥1.8-fold), compared to PBS-injected hindlimbs. Overall, both matrices increased local anti-inflammatory and angiogenic cytokines, but the sLe^X-matrix treatment had the most profound effect of increasing both myogenic and vasculogenic cytokine production.

Figure 4-8 Matrix treatment augments the protein levels of regenerative cytokines in ischemic hindlimb muscle. Histograms represent protein levels of cytokines, relative to baseline controls (animals that did not receive ligation surgery or treatment) in hindlimb muscle tissue samples at 3 and 10 days after treatment with PBS, collagen or sLe^X-matrix (non-BMTx model). Pro-vasculogenic (bFGF, TIMP-2, VCAM-1, VEGF), pro-myogenic (IGF-I, IGFBP-2, IGFBP-5), chemotactic (SDF-1α, VEGF) and immunomodulatory (IL-10, L-Selectin, P-Selectin, TNFα) cytokines were evaluated. The y-axis for all graphs represents arbitrary chemiluminescence units. $^{\dagger}P<0.05$ vs. baseline; $*P<0.05$ vs. PBS; $**P<0.05$ vs. all others at the indicated time point. Histograms represent data n=5 different mice per group per time point.

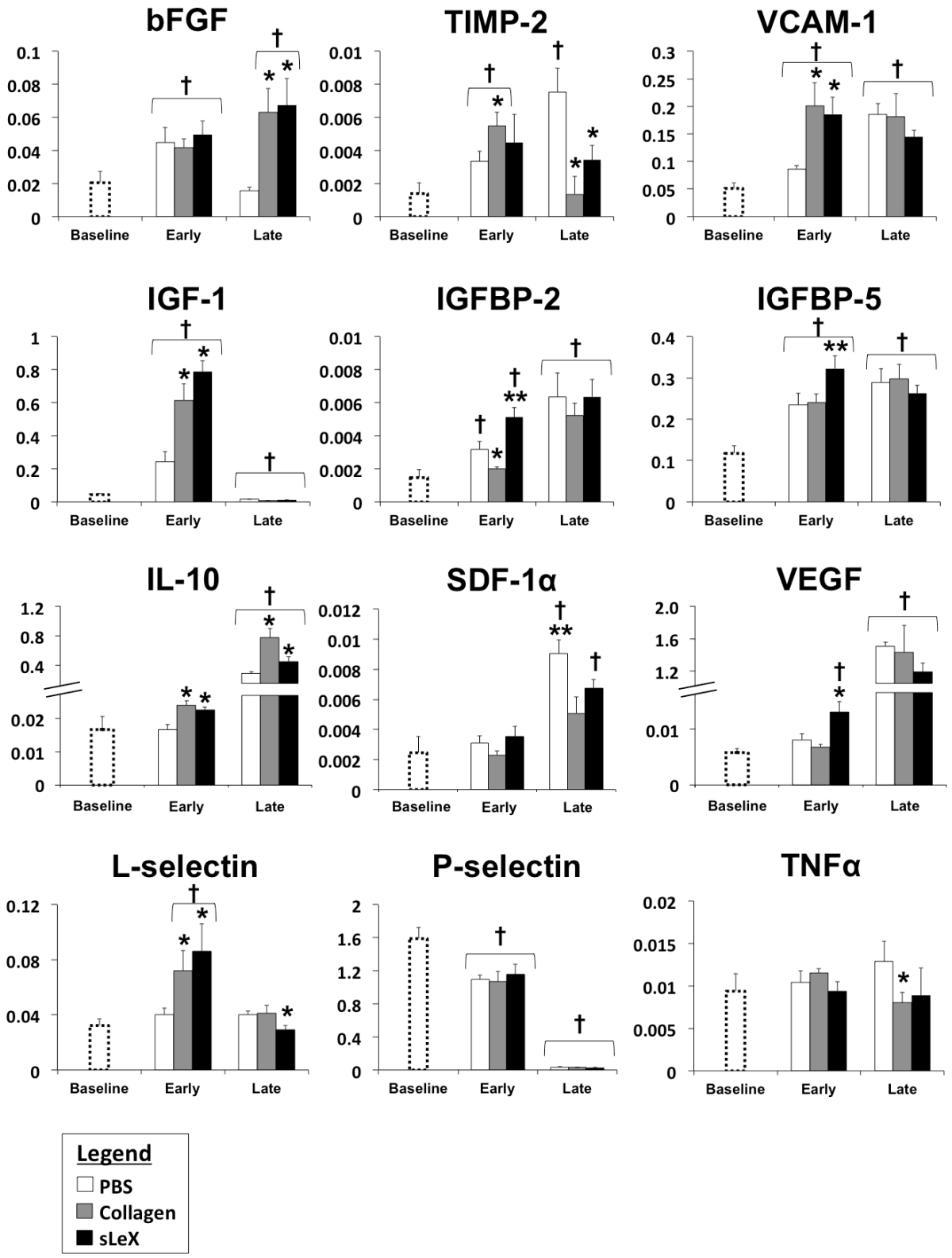
bFGF
TIMP-2
VCAM-1
IGF-1
IGFBP-2
IGFBP-5
IL-10
SDF-1α
VEGF
L-selectin
P-selectin
TNFα
Baseline
Early
Late
Legend
PBS
Collagen
sLeX

Matrix treatment affects muscle function

For the first 8 shortenings, soleus power was reduced in all treated animals, compared to wild-type ($P<0.05$; Fig. 4-9A). The soleus muscle from PBS- and collagen matrix-treated mice fatigued more rapidly than wild-type soleus (51.0±5.7s and 53.3±5.4s versus 71.2±4.2s, respectively; $P\leq0.03$; Fig. 4-9B), whereas no difference in the time to fatigue was observed in sLe^X-matrix-treated muscles (64.0±4.1s) compared to wild-type controls. Only treatment with the collagen matrix changed the soleus twitch and specific forces compared to wild-type controls; specific force was reduced (172.1±10.8 versus 214.0±12.7 mM; $P=0.03$; Fig. 4-9C) and twitch force was reduced (25.4±1.4 versus 38.9±4.5 mM/mm^2; $P=0.01$; Fig. 4-9D). The sLe^X-matrix-treated muscles only trended towards a reduction in twitch force ($P=0.1$; Fig. 4-9D).

Figure 4-9 *Ex vivo* analysis of explanted soleus muscle function. Power was reduced in all ligated soleus muscles, compared to wild-type controls (A). Time to fatigue was unaffected with sLe^X-matrix treatment, but reduced in PBS controls and collagen matrix treatment (B). Specific force (C) and specific twitch force (D) were reduced with collagen matrix treatment. *$P \leq 0.03$ vs. wild-type; **$P < 0.05$ for wild-type vs. all other treatments.

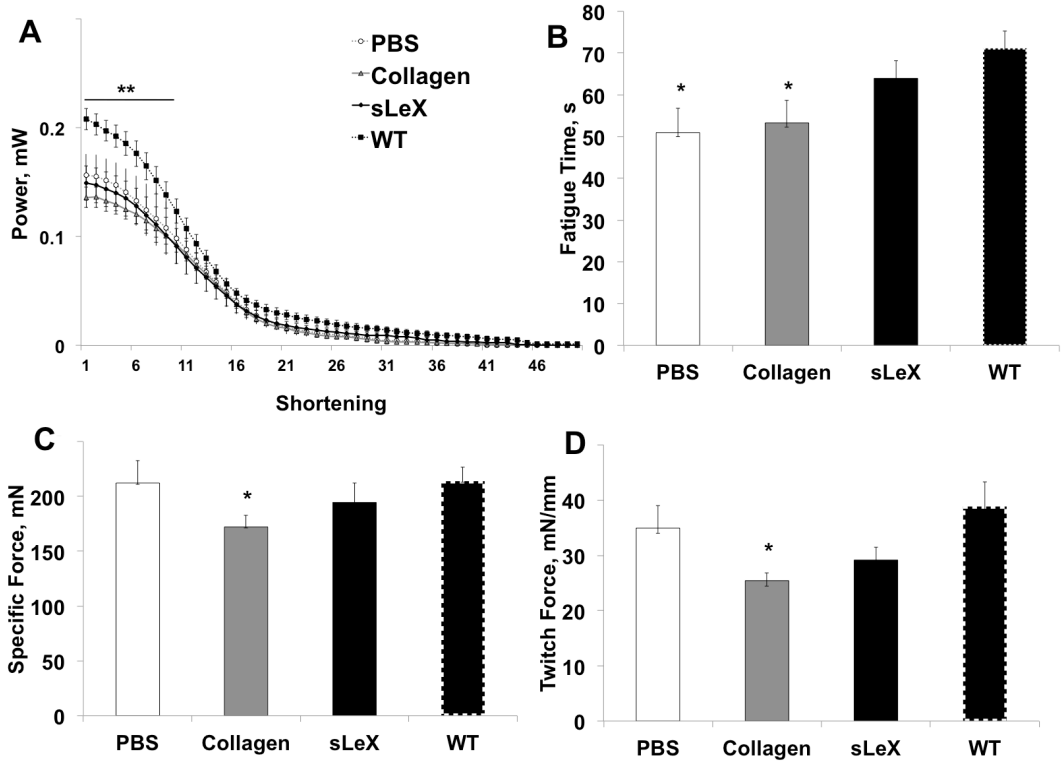
A
PBS
Collagen
sLeX
WT
**
Power, mW
0
0.1
0.2
1
6
11
16
21
26
31
36
41
46
Shortening
B
Fatigue Time, s
0
10
20
30
40
50
60
70
80
*
*
PBS
Collagen
sLeX
WT
C
Specific Force, mN
0
50
100
150
200
*
PBS
Collagen
sLeX
WT
D
Twitch Force, mN/mm
0
10
20
30
40
*
PBS
Collagen
sLeX
WT

The sLe^X-matrix ultimately supports *in vivo* functional recovery

The sLe^X-matrix-treated mice that were forced to run until exhaustion were able to run significantly greater lengths, compared to PBS- and collagen matrix-treated animals (553m versus 401m and 433m, respectively; $P \leq 0.009$; Fig. 4-10A). Exhaustion also occurred at higher speeds for sLe^X-matrix-treated mice (31.8m/s) versus PBS- (25.8m/s) and collagen matrix-treated (27m/s) animals ($P \leq 0.02$; Fig. 4-10B). Differences in running abilities were not observed between PBS and collagen matrix treatments.

Figure 4-10 sLe^X-enhanced matrix allows for functional recovery in a unilateral model of hindlimb ischemia. When forced to run on a treadmill, animals treated with sLe^X-matrix ran significantly further (A; $P \leq 0.009$) and at greater speeds (B; $P \leq 0.02$) than PBS- or collagen matrix-treated animals.

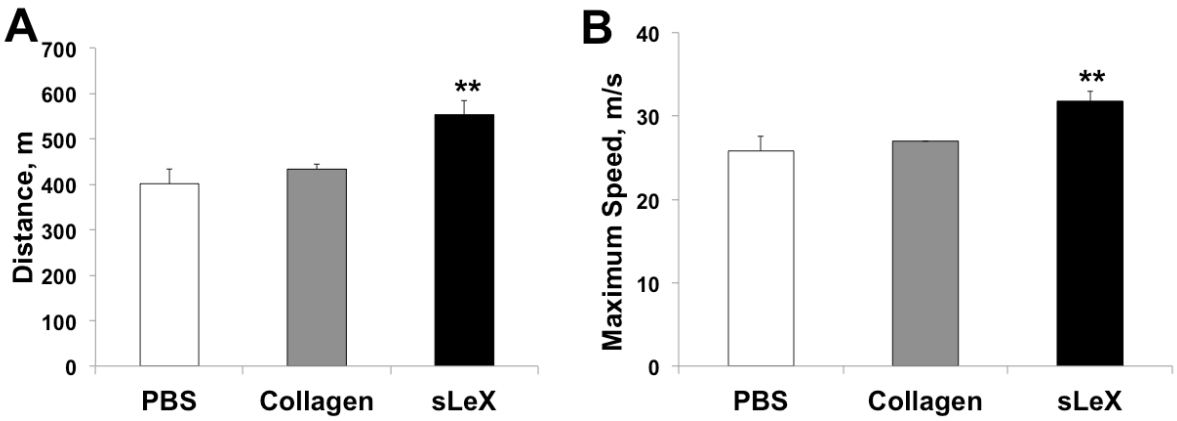
A
Distance, m
700
600
500
400
300
200
100
0
**
PBS
Collagen
sLeX
B
Maximum Speed, m/s
40
30
20
10
0
**
PBS
Collagen
sLeX

Discussion

The need for biomaterials to act as *de novo* environments *in vivo* for stem cell and regenerative responses has been identified (Kuraitis et al., 2012c; Rossi et al., 2010). In the present study, we demonstrated that the treatment of hindlimb ischemia with a sLe^X-collagen matrix can augment bone marrow and local cell responses, to improve neovascularization and regenerative myogenesis of skeletal muscle. Notably, the sLe^X-matrix demonstrated an inherent ability to: 1) physically mimic skeletal muscle; 2) augment pluripotent mESC differentiation towards a muscle lineage; 3) stimulate skeletal muscle regeneration; 4) augment the mobilization and recruitment of marrow-derived progenitor cells; and 5) regulate the temporal expression of cytokines involved in both the muscular and vascular regenerative processes.

The culture of mESCs on our materials as a substrate resulted in increased differentiation towards a myogenic lineage compared to the standard ESC-to-myocyte culture protocol (which uses TCPS). ESC cultures were performed to assess the matrices' inherent ability to guide pluripotent progenitors towards a myocytic lineage. At day 15, mESCs cultured on matrices expressed greater levels of Pax3 and Pax7 (myogenic progenitor marker), Myf5 and myogenin (MRFs), and MHC3 (final muscle differentiation marker) versus culture on TCPS. Therefore, culture on the matrices promoted a more efficient differentiation pathway in mESCs that produced a premyogenic progenitor population, and enhanced MRF expression and terminal differentiation. Given that ESCs are pluripotent and have the capacity to differentiate into cells of any lineage (Guan et al., 1999), it is significant that the collagen-based matrix appears to have an inherent ability to direct mESC differentiation towards a

Pax3/7^{+ve} progenitor population and skeletal myogenesis. The generation of Pax3/7^{+ve} muscle progenitor cells is noteworthy, as these cells would be valuable in replenishing the satellite cell niche (Kuang et al., 2007; Montarras et al., 2005) in therapies targeted at treating muscle diseases, and Pax3/7 induce skeletal myogenesis in stem cells (Ridgeway and Skerjanc, 2001; Seale et al., 2004). These results suggest that the collagen-based matrices could serve a two-fold purpose: 1) to provide an injectable biomaterial for the promotion of endogenous regenerative myogenesis; and 2) to enhance and enrich populations of myogenic lineage cells for transplantation.

It is known that mechanical properties of a cell's extracellular environment, and in particular the elasticity of the cell's substrate, are key regulating factors in the differentiation of cells (Engler et al., 2006). *Ex vivo*, cells appear to differentiate towards phenotypes that would naturally be found on similar substrates, such as neural differentiation on very soft materials and osteogenic differentiation on very hard materials. A substrate with an elastic modulus range of 6.5–17 kPa appears ideal for maximal myotube differentiation (Engler et al., 2004). Similarly, a range of 8–17 kPa induces a myoblast-like morphology in mesenchymal stem cells and a marked increase in the myogenic transcription factor MyoD (Engler et al., 2006). Unstimulated skeletal muscle has a range of 10-20 kPa (Engler et al., 2006). Although these examples used atomic force microscopy, which may overestimate the moduli values, the elasticity values of our matrices (5.85 and 7.51 kPa) obtained using compression testing are quite similar. This suggests that the matrices' elasticity may play a role in the observed myogenesis. Furthermore, the statistical difference between matrices' elastic moduli may be one of the key reasons for the increased emergence of myocytic lineages on the sLe^{X}-matrix. It is not likely that the matrices' rheological properties

contributed to the observed differences in myogenesis, since viscosity and time to gelation between the two materials were very similar. However, the addition of sLe^X to the collagen matrix made regions of the material less hydrophilic. The degree of hydrophilicity is another key property for cell interaction, as slight changes in a material's hydrophilicity have been shown to have dramatic effects on cellular adhesion and spreading (Derkaoui et al., 2010; Elliott et al., 2007), and this may be involved in the observed differences in mESC phenotypes.

Pelosi *et al.* have demonstrated that in wild-type mice, the onset of skeletal muscle regeneration begins around 10 days after injury (Pelosi et al., 2007). In the present study, at 3 days post-treatment, very few regenerating fibres were apparent and we observed no differences between treatments. However, at day 10, mice treated with sLe^X-matrix displayed an increase in the number of regenerating fibres, and the same effect was observed at 14 days in the BMTx model. In parallel, the sLe^X-matrix did not increase the hindlimb levels of myogenic mRNA transcripts at day 3, but at day 10 it had induced an upregulation of transcripts of genes that are known to have active roles in directing myogenesis, such as M-cadherin (Donalies et al., 1991), Myf5 (Gayraud-Morel et al., 2007; Rudnicki et al., 1993), MyoD (Rudnicki et al., 1993), myogenin (Nabeshima et al., 1993), Pax7 (McGeachie and Grounds, 1987) and Six1 (Liu et al., 2010). Interestingly, animals receiving the PBS control demonstrated a greater abundance of Pax7 transcripts at day 3, compared to both matrices. Pax7 is indicative of skeletal precursor satellite cells, and after injury, the normal response for satellite cells is to synthesize new DNA and proliferate after 18 h, peaking at 3 days and gradually reducing afterwards (McGeachie and Grounds, 1987). Our results suggest that PBS-treated animals experienced this phenomenon, and that matrix treatment may have

delayed it. Despite this delay, the sLe^X-matrix was superior in inducing regenerative myogenesis over the longer term.

In our previous report, we noted that the sLe^X-matrix could increase the number of CACs in the circulation (Suuronen et al., 2009). In the present study, using a GFP^+ marrow transplant and hindlimb ischemia model, we demonstrated that c-kit^+, flk-1^+ and $CXCR4^+$ CACs were increased in animals with sLe^X-matrix-treated hindlimbs at early time points (days 1-4) after treatment. The circulating cells analyzed were positive for GFP expression, indicating bone marrow origin of the responding cells. Greater numbers of these cells persisted in the circulation of sLe^X-matrix-treated animals by 2 weeks post-application.

The analysis of hindlimb tissue sections revealed that the sLe^X-matrix was superior at recruiting marrow-derived (GFP^+) and $CXCR4^+$ cells to the treated muscle tissue. Notably, the number of $CXCR4^+$ cells of non-marrow origin (GFP^-) was greater in hindlimbs treated with sLe^X-matrix than in the other groups, suggestive of an enhanced local cell response with this treatment. It is well-known that marrow-derived CACs are therapeutic and may augment reperfusion (Abdel-Latif et al., 2007). Recently, the role of $CXCR4^+$ fractions of CACs has been highlighted (Seeger et al., 2009): compared to $CXCR4^-$ fractions, $CXCR4^+$ cells display a more potent ability to migrate, as well as a superior ability to augment neovascularization and to secrete pro-vasculogenic cytokines. This suggests that $CXCR4^+$ cells are a highly therapeutic fraction of CACs with a strong homing ability, which is particularly important in the response to ischemic damage and support of neovascularization.

By 2 weeks, the sLe^X-matrix improved the perfusion of ischemic hindlimbs compared to PBS and collagen matrix treatments, although both matrices increased hindlimb arteriole density to similar levels. In contrast, we have previously observed increased arteriole density

with sLe^X-matrix compared to collagen matrix treatment (Suuronen et al., 2009). Despite being another hindlimb ischemia model, there were key differences between the current study and our 2009 study that may have altered the physiological responses to the material's application: rat versus mouse model; BMTx versus non-BMTx; young (rats) versus older (mice). In this study, the sLe^X-matrix was able to induce the formation of arterioles of greater size, possibly contributing to greater blood flow. This may be indicative of more mature and/or strengthened arterioles, since the size (cross-sectional area) in newly developing vasculature was recently shown to increase over time, up to a period of 4 weeks (Ruvinov et al., 2011). The differentiation of GFP^+ marrow-derived cells into cells of the vasculature was not observed. The differentiation of CACs into vascular cells is a topic of intense debate (Klein et al., 2010) and the potential for vascular transdifferentiation of CACs is not yet clear. It is more likely that the increased engraftment of GFP^+ marrow cells in the sLe^X-matrix treated hindlimbs contributes to a greater paracrine mechanism (higher levels of angiogenic cytokines were observed), which then induces a superior local cell response (supported by the observation that greater numbers of non-marrow derived (GFP^-) $CXCR4^+$ cells were present in sLe^X-matrix treated muscle). Furthermore, it was recently highlighted that the expression of L-selectin (the receptor for sLe^X) greatly enhances the *in vivo* migration and retention of transplanted cells into ischemic myocardium (Bernal et al., 2011). Therefore, the presentation of sLe^X may also contribute to the retention of therapeutic cells in the ischemic muscle.

A time course analysis of cytokines indicated the simultaneous signaling for vascular and muscular regeneration and also corroborated the myogenic and vasculogenic results that were observed. IGF-1, a potent initiator of skeletal myogenesis (Pelosi et al., 2007), displayed the

greatest increase with sLe^X-matrix treatment at day 3 post-treatment. Similarly, an increase in IGF binding proteins IGFBP-2 and -5, in response to sLe^X–matrix treatment, was observed only at the 3 day time point. The family of IGFBPs (1 through 5) have implicated and overlapping roles in regulating myogenesis (Duan et al., 2010); however, a knock-out of multiple members has shown reduced skeletal muscle size, implicating their role in the growth and homeostasis of skeletal muscle (Ning et al., 2006). IGFBP-5 is perhaps the most potent family member for myogenesis. Its expression increases greatly in differentiating myoblasts (Bayol et al., 2000) and in the presence of IGF-1, it can augment the myogenic actions of IGF-1, indicated by greater myogenin expression and fusion of myoblasts into myotubes (Ewton et al., 1998; Musaro and Rosenthal, 1999). Vasculogenic cytokines were also assessed. The matrix-induced production of bFGF, a molecule able to stimulate reperfusion of ischemic muscle (Boodhwani et al., 2008), was observed at the same time when matrices demonstrated improved perfusion, while concurrently, the level of an inhibitor of angiogenesis, TIMP-2 (Koike et al., 2003), was reduced. Another indicator of neovascularization, VCAM-1 (Martin et al., 2005), was also increased with matrix treatment. Together, with the transcriptional and morphological evidence of myogenesis, it is believed that sLe^X-matrix induced local paracrine signaling, which is responsible for the later initiation of regenerative events that manifest as amplified vasculogenesis, followed by myogenesis, at around 10 days. This concept is supported by findings which demonstrate that when vascularization is present, there is a greater functional enhancement of regenerating muscle (Koffler et al., 2011).

PBS treatment led to the greatest local level of SDF-1 (at the late time-point), a chemoattractant for CXCR4-expressing cells. Interestingly, more $CXCR4^+$ cells were

observed in the circulation and engrafted into muscle after matrix treatment, despite the greater concentration of SDF-1 in the PBS-treated hindlimbs (at 10 days). Greater levels of SDF-1 were expected with matrix treatment; however, serum SDF-1 levels were not measured. If elevated, serum SDF-1 could explain the increase in mobilized and engrafted $CXCR4^+$ CPCs in matrix-treated tissue. Furthermore, local SDF-1 expression in response to ischemic injury is maintained over longer periods in older mice (~18mo) compared to the response in younger mice (3mo), which peaks at day 3 (Wang et al., 2011). This suggests that increased SDF-1 levels may persist in tissue that is less efficient at recovering from perfusion defects; under this scenario, the PBS-treated hindlimb muscle, in which perfusion was not restored, would maintain an elevated local SDF-1 concentration compared to the reperfused matrix-treated hindlimbs. Also, SDF-1-CXCR4 responses may not be linear, whereby a threshold concentration of SDF-1 is reached, resulting in a plateau of the CXCR4 response (Kimura and Tabata, 2010), and therefore the elevated SDF-1 levels seen with PBS treatment may be ineffective at activating $CXCR4^+$ cells over the long-term. Other chemokines, such as VEGF, were upregulated with sLe^X-matrix treatment. When VEGF, known as a progenitor cell activator and homing factor, and as an angiogenic cytokine, is produced locally by transplanted muscle-derived stem cells, enhanced myogenesis occurs in addition to increased angiogenesis (Deasy et al., 2009), underscoring the importance and role of local VEGF production in injured muscle. Furthermore, both matrix treatments augmented the level of IL-10, a known cytoprotective cytokine that is endogenously upregulated after an ischemic episode (Frangogiannis et al., 2000; Hayward et al., 1997). IL-10 has also recently been associated with improved muscle regeneration, based on its ability to inhibit the cytotoxic M1 macrophage phenotype (Villalta et al., 2011). We assessed the potential of these

materials to elicit a harmful inflammatory response by monitoring TNF-α. Similar to our previous study, the matrix application did not induce TNF-α expression (Suuronen et al., 2009), highlighting the material's biocompatibility.

It is known that ischemic injury reduces the maximal forces in soleus muscle (Vignaud et al., 2010) and that this leads to fibre death and subsequent regeneration. Power measurements showed that all ischemic solei were less efficient; however, the small changes in maximal (specific and twitch) forces observed in our model were surprising, but perhaps attributable to the relatively mild degree of ischemia that was induced. Statistically, both matrix treatments reduced specific maximal forces, but the reductions observed with sLe^X-matrix were less severe when compared to control animals. Despite these reductions in matrix-treated solei, it has been shown that regenerating soleus muscle exhibits reduced maximal forces, compared to soleus in a non-regenerative state (Esposito et al., 2007), suggesting regeneration is occurring in matrix-treated muscles. Given that ischemic injury initiates major changes in ECM composition (Roy et al., 2006), together with the observed changes in ECM-modulating proteins in this study and others (Kuraitis et al., 2011b; Suuronen et al., 2009), we believe that muscle regeneration and ECM turnover leads to the observation of reduced maximal forces. Moreover, the reduction in specific force is probably due to the fact that the matrix increases the number of regenerating fibers, which do not contribute to force generation. We can envision that the regenerating fibers, once they complete the maturation program, will significantly contribute to an increase in muscle strength. Despite the loss of force, this did not translate into reduced function *in vivo* for mice with ischemic hindlimbs treated with sLe^X-matrix, which experienced improved mobility (ran further and faster on a treadmill). Arguably the most important parameter measured, sLe^X-matrix treatment allowed

for functional restoration of ischemic hindlimbs. This result was supported by the *ex vivo* observation that sLe^X-matrix treatment improved muscle endurance, compared to both PBS- and collagen matrix-treated muscle, which reached fatigue sooner. Furthermore, these functional benefits were observed in ischemic soleus muscles, which are distal to the injury/treatment site (gastrocnemius muscle), highlighting the potential of the matrix to mediate vascular and muscle regeneration beyond the site of application.

In order to achieve maximal recovery of skeletal muscle from ischemic injury, the formation of new vessels is a requirement before the regeneration of myocytes will occur (Grounds, 2008a; Ko et al., 2007). Experimentally, it has been demonstrated that skeletal myogenesis is correlated with vascular regeneration after stem cell transplantation (Shi et al., 2009). Our study also shows that while two matrix treatments both induce relatively similar amounts of myogenesis, the treatment with superior vasculogenesis (sLe^X-matrix) is the only one to lead to functional recovery in ischemic hindlimbs. One study has used an injectable alginate scaffold to release multiple regenerative growth factors in an attempt to restore skeletal muscle after ischemic injury (Borselli et al., 2010). Although a combined result of muscle and vascular regeneration occurred, the outcome depended greatly on the ability of the materials/releasing systems to function properly and this function is difficult to assess *in vivo*. Growth factor delivery strategies face various biological, engineering and technical limitations (Chen et al., 2010), such as loss of bioactivity, insufficient gradients and rapid cytokine depletion. Our results present an efficacious method of restoring both muscular and vascular profiles of skeletal muscle, overcoming the potential limitations that have been associated with material functionality after implantation.

Conclusion

We have presented evidence for the reperfusion and both phenotypic and functional regeneration of muscle damaged from an ischemic event after the application of a sialyl Lewis^X-enhanced injectable collagen matrix. Based on its mechanical properties and its ability to guide pluripotent cells towards a myogenic lineage, we believe that this injectable matrix has an inherent ability to support muscle regeneration. Considering the limited success of regenerative stem cell transplantation, the need for cell-free methods of regeneration may be necessary, and the non-invasive application of biocompatible, naturally derived materials that can augment neovascularization and myogenesis holds great promise as a future therapy for prevalent myopathies.

Acknowledgments

The authors would like to thank Carmine Nicoletti, Elaine Wong and Suzanne Crowe for their technical assistance, and Dr. Wankei Wan for the use of his mechanical testing facilities at the Fordham Centre for Biomedical Engineering, University of Western Ontario, Canada. This work was supported by grant-in-aid #T-6793 from the Heart & Stroke Foundation of Ontario (to EJS), by grants from the 7FP-Myoage, Fondazione Roma, and AFM (to AM) and by operating grant #84458 from the Canadian Institutes of Health Research (to ISS). DK was supported by a Canadian Institutes of Health Research Canadian Graduate Scholarship, DE was supported by a National Sciences and Engineering Research Council Alexander Graham Bell Award, PZ was supported by the Lawrence Soloway Research Fellowship award, DTP was supported by a University of Ottawa Cardiology Research Endowment Fellowship, KM

was supported by an Ontario Graduate Scholarship, and DK and TS were supported by Heart and Stroke Foundation of Ontario Master's Awards.

CHAPTER 5. A necrotic stimulus is required to maximize matrix-mediated myogenesis in mice

This chapter has been published in *Disease Models & Mechanisms*, as per the following citation:

D. Kuraitis, M.G. Berardinelli, E.J. Suuronen and A. Musarò (2013) A necrotic stimulus is required to maximize matrix-mediated myogenesis. *Dis Model Mech*;6(3):793-801.

Notes on Chapter

The study in Chapter 4 successfully demonstrated the ability of a collagen matrix to augment myogenesis. The source of the regenerated muscle was not entirely clear; the gene expression of Pax7 over time did not overtly suggest the role of satellite cells in the regeneration process. It was obvious that in order to define the role of muscle progenitors in the observed matrix-mediated myogenesis, further studies would be necessary. Antonio Musarò graciously offered to host and oversee these studies at his laboratory at the University of Rome, which were designed to further characterize the potential of our materials to augment myogenesis.

Contributions of co-authors:

M.G. Berardinelli assisted with gene expression analysis [Fig. 5.3H,I,J,K].

A. Musarò and E.J. Suuronen were involved in experimental planning and manuscript editing.

Abstract

Biomaterials that are similar to skeletal muscle extracellular matrix have been shown to augment regeneration in ischemic muscle. In this study, treatment with a collagen-based matrix stimulated molecular myogenesis in an mdx murine model of necrosis. Matrix-treated animals ran ≥40% further, demonstrating functional regeneration, and expressed increased levels of myogenic transcripts. In contrast, matrix treatment was unable to induce transcriptional or functional changes in an MLC/SOD1^{G93A} atrophic mouse model. *In vitro*, satellite cells were cultured: 1) under standard conditions, 2) on matrix, 3) in the presence of myocyte debris (to simulate a necrotic-like environment), or 4) with both matrix and necrotic stimuli. Exposure to both stimuli induced the greatest increases in mef2c, myf5, myoD and myogenin transcripts. Furthermore, conditioned medium collected from satellite cells cultured with both stimuli contained elevated levels of factors that modulate satellite cell activation and proliferation, such as FGF-2, HGF and SDF-1. Application of the conditioned medium to C2C12 myoblasts accelerated maturation, demonstrated by increased mef2c, myf5 and myogenin transcripts and fusion indexes. In summary, the collagen matrix required a necrotic stimulus to enhance the maturation of satellite cell and their secretion of a myogenic cocktail. Considering that matrix treatment supports myogenesis only in *in vivo* models that exhibit necrosis, this study demonstrates that a necrotic environment is required to maximize matrix-mediated myogenesis.

Introduction

Skeletal muscle regeneration is a coordinated process in which several factors are sequentially activated to maintain and preserve muscle structure and function after injury. Muscle regeneration occurs in four interrelated and time-dependent phases: degeneration, inflammation, regeneration, and remodeling-repair (Carosio et al., 2011). Injury of myofibers results in rapid necrosis, which activates a defined inflammatory response characterized by the sequential invasion of muscle by specific inflammatory cell populations (Tidball, 2005). This response is followed by a regenerative phase, characterized by satellite cell (SC) activation and the presence of regenerating fibers. The final phase is a period during which the regenerated myofibers mature, the extracellular matrix (ECM) undergoes remodeling, and the injured muscles functionally recover. The major roles of growth, remodeling and regeneration are played by SCs, a quiescent population of myogenic progenitor cells that resides between the basal lamina and plasmalemma and are rapidly activated in response to appropriate stimuli.

The potential for endogenous or supplementary stem cells to restore the form and function of damaged tissues is particularly promising for overcoming the restricted regenerative capacity of skeletal muscle in different pathologic conditions, including Duchenne's muscular dystrophy (DMD) and amyotrophic lateral sclerosis (ALS). DMD is an X-linked degenerative disease in which the absence of dystrophin expression renders the muscle fibers more sensitive to mechanical damage. The main consequence of dystrophin absence is that the normal regenerative capacity of skeletal muscle cannot compensate for increased susceptibility to damage, resulting in the replacement of muscle fibers with fibrotic or fat tissue (Gillis, 1999; Grounds, 2008b). In DMD patients, the SC response is to replace

degenerating myofibres with new myofibres that still lack dystrophin, a cycle that proceeds and ultimately depletes SC pools. Furthermore, the rate of myocyte telomere loss is 14 times greater in DMD patients (Decary et al., 2000) and their SCs appear to have a reduced potential for proliferation (Renault et al., 2000). Ultimately, poor quality progenitors regenerate poor quality muscle, and this muscle is still weak and still experiences necrotic degeneration. ALS is a neuromuscular disease that manifests as progressive motor neuron degeneration, muscle atrophy and paralysis. This degeneration occurs without evident signs of necrosis. Atrophic muscle maintains fewer SCs and these SCs are dysfunctional with respect to their abilities to proliferate and differentiate into myotubes (Mitchell and Pavlath, 2004). ALS-derived SCs have also been observed to be abnormally senescent and fail to fully differentiate (Pradat et al., 2011) and ALS patients also display myopathic changes (Dupuis and Echaniz-Laguna, 2010). Thus, in such disease states characterized by insufficient myogenesis, SC contributions are not optimal and may be a key reason for poor recovery and regeneration of healthy muscle.

In skeletal muscle diseases, whether characterized by necrotic degeneration or atrophic wasting, there is a homeostatic imbalance towards muscle loss and away from muscle regeneration. Despite having genetic causes, strategies (such as gene transfer, protein delivery and stem cell transplantation) that can shift this equilibrium towards muscle regeneration may offer time and hope for patients suffering from these debilitating conditions. However, no strategy has yet emerged as ideal for enhancing muscle regeneration in the clinic. There is a great need for regenerative strategies that can enhance or initiate muscle regeneration (Turner and Badylak, 2012). Although biomaterials for the regeneration of bone, cardiovascular and nerve tissues have been extensively investigated, little research

has been performed to evaluate biomaterial treatment for muscle diseases. The use of naturally-derived materials that mimic healthy ECM is a promising therapeutic option, and also bypasses risks associated with other treatments, such as the need for immunosuppressant drugs, induction of endogenous inflammatory responses and the difficulties associated with cell culture (Kuraitis et al., 2012c). We have recently used collagen-based matrices to augment regeneration in ischemic skeletal muscle (Kuraitis et al., 2012b). The objectives of this study were to: (i) evaluate the potential of a myogenesis-augmenting collagen matrix in different muscle disease states; (ii) characterize the interaction of this collagen matrix with SCs; and (iii) explore the role of necrotic stimuli in matrix-mediated myogenesis.

Results

Matrix treatment confers functional improvements in mdx mice

Matrix or PBS was injected into the extensor digitorum longus (EDL) muscle of mice. The EDL was chosen to receive treatment, as it allows for basic animal motility. As a model for DMD, the *mdx* mouse was used. Matrix-treated *mdx* mice were able to run distances 47% greater than shams (p=0.02) and 40% greater than PBS-treated mice (p=0.01; Fig. 5-1A). Matrix-treated mice also resisted physical exhaustion until reaching speeds of 22 m/s, unlike sham and PBS-treated mice who reached exhaustion at 17 (p=0.02) and 18 m/s (p=0.02), respectively (Fig. 5-1B).

Myogenic transcripts increase with matrix treatment in mdx mice

Compared to PBS, matrix treatment induced transcription of myogenic genes in mdx muscle (Fig. 5-1C). Specifically, increases were observed for crucial factors regulating the entry of SCs into the myogenic program, proliferation and commitment, such as Pax3 (5.9×; p=0.02), myf5 (3.5×; p=0.05), desmin (2.3×; p=0.04) and myogenin (3.0×; p=0.02). A favorable trend for increased transcription of Pax7 was also observed with matrix treatment (1.7×; p=0.1). No difference in transcript levels of the late regeneration gene encoding muscle creatine kinase (MCK) was observed between treatments (p=0.5).

Figure 5-1 - Functional and molecular regeneration in mdx muscle with matrix treatment. Matrix-treated mdx mice were able to run at greater speeds (A) and greater distances (B) than PBS-treated littermates. Early- and mid-stage myogenic gene transcription was also increased with matrix treatment when compared to untreated contralateral muscle (C). *$p \leq 0.05$ vs. PBS; **$p \leq 0.02$ vs. all other treatments.

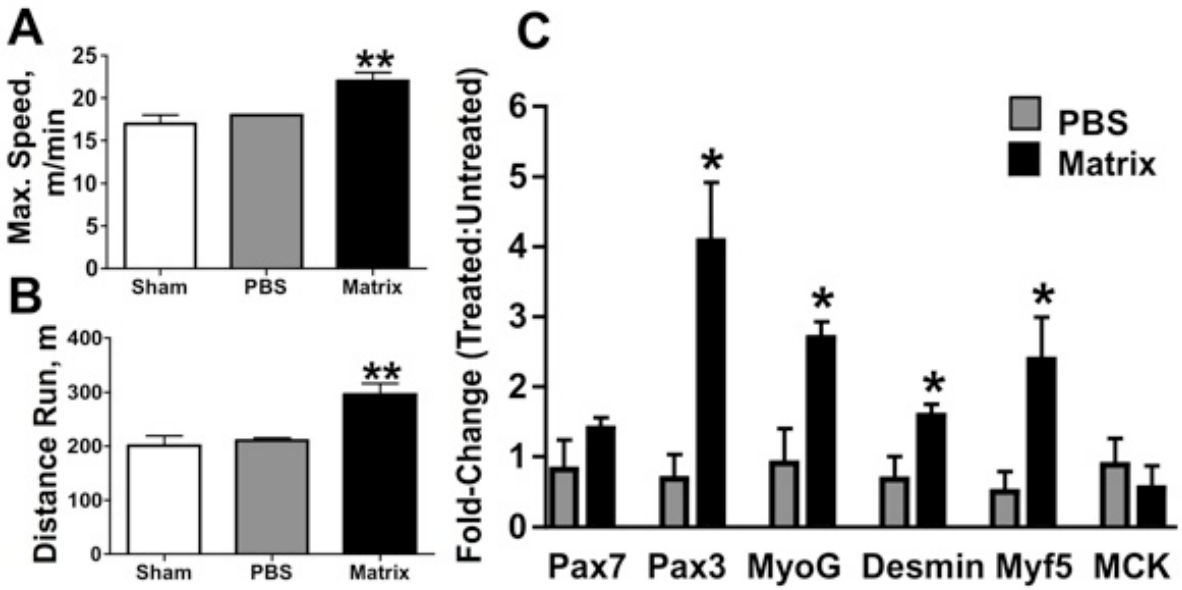
A
Max. Speed, m/min
25
20
15
10
5
0
**
Sham
PBS
Matrix
B
Distance Run, m
400
300
200
100
0
**
Sham
PBS
Matrix
C
Fold-Change (Treated:Untreated)
6
5
4
3
2
1
0
PBS
Matrix
*
*
*
*
Pax7
Pax3
MyoG
Desmin
Myf5
MCK

Matrix treatment does not support functional recovery or myogenic gene transcription in a mouse model of muscle atrophy

Similarly, matrix treatment was also evaluated in the MLC/SOD1^{G93A} mouse, a model for ALS. No differences were observed with respect to the maximal distances run by MLC/SOD1^{G93A} mice ($p \geq 0.3$; Fig. 5-2A), nor the speed at which exhaustion occurred ($p \geq 0.5$; Fig. 5-2B) among sham, PBS and matrix treatments. Differences in myogenic transcript levels were also not observed between treatments for Pax7 ($p=0.3$), Pax3 ($p=0.6$), myf5 ($p=0.5$), desmin ($p=0.3$), myogenin ($p=0.2$) and MCK ($p=0.6$; Fig. 5-2C).

Figure 5-2 - Lack of observable regeneration in matrix-treated atrophic mice. Matrix treatment did not improve the running speed (A) or maximum distance run (B) of MLC/SOD1^{G93A} mice, nor was there any observed difference in levels of myogenic transcripts with matrix treatment (C).

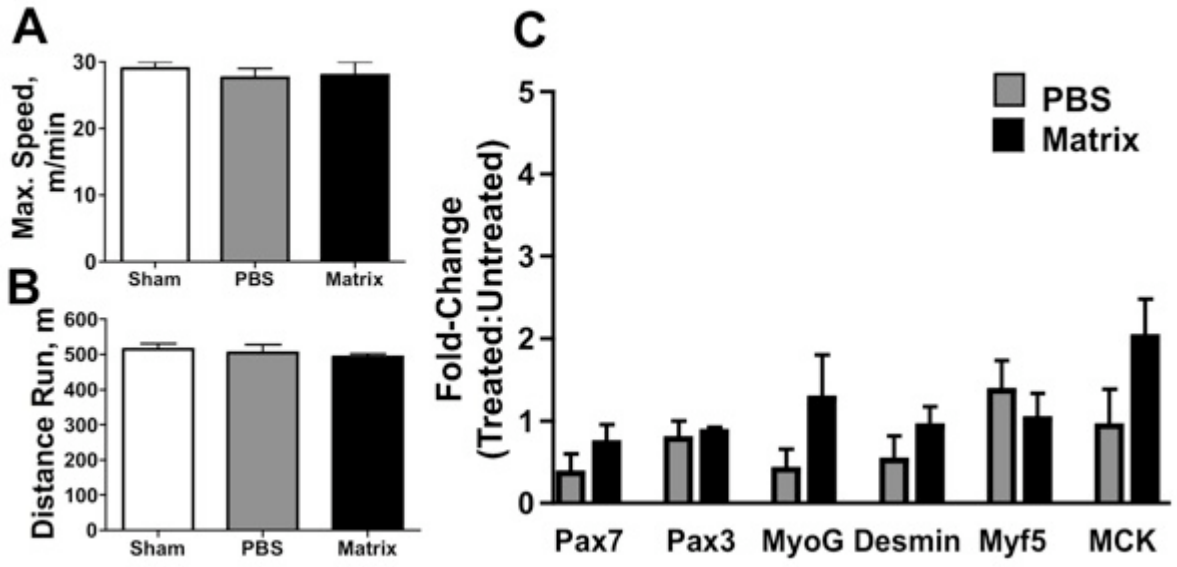
A
Max. Speed, m/min
30
20
10
0
Sham
PBS
Matrix
B
Distance Run, m
600
500
400
300
200
100
0
Sham
PBS
Matrix
C
Fold-Change (Treated:Untreated)
5
4
3
2
1
0
PBS
Matrix
Pax7
Pax3
MyoG
Desmin
Myf5
MCK

Matrix stimulus increases primary myoblast-derived myotube maturation and a necrotic co-stimulus increases myotube size

To investigate the matrix's effect on SCs, primary myoblasts were cultured on traditional collagen I-coated dishes or matrix substrate. SC populations were differentiated using low serum and after 24h, cells were collected and analyzed. Additionally, necrotic myocyte debris (NMD) was added to paired cultures to act as a necrotic stimulus. Four culture conditions were therefore created: i) control; ii) NMD; iii) matrix; and iv) NMD-matrix. Morphologically, the presence of NMD and/or matrix stimuli altered the shape of SC-derived myotubes (Fig. 5-3A-D). Matrix culture, regardless of NMD stimulus, increased the amount of generated myotubes to 13.9 ± 1.3, which was significant compared to control cultures and NMD stimuli (5.0 ± 0.9; $p<0.0001$; Fig. 5-3E). However, matrix exposure in the presence of the necrotic stimuli increased the robustness of these myotubes, generating myotubes that were at least 1.5× longer ($p\leq0.003$; Fig. 5-3F) and 1.2× thicker ($p\leq0.02$; Fig. 5-3G). In addition to increasing myotube frequency, matrix culture (either with or without NMD) also supported beating and self-alignment of myotubes (Table 5-1).

In a necrotic context, matrix stimulus greatly amplifies myogenic gene transcription in satellite cell cultures

Compared to control (no NMD or matrix stimuli) cultures, matrix exposure increased transcription of myoD by 2.2× ($p=0.03$; Fig. 6-3I), myogenin by 1.3× ($p=0.04$; Fig. 5-3J) and mef2c by 1.2× ($p=0.02$; Fig. 6-3K). When a necrotic stimulus was added to matrix cultures, transcriptional myogenesis was greatly enhanced. Compared to all other treatment conditions, simultaneous matrix and NMD stimulation increased transcript levels of myf5 by 4.9× ($p\leq0.02$; Fig. 5-3H), myoD by 13.1× ($p\leq0.03$; Fig. 5-3I), myogenin by 12.8× ($p\leq0.02$;

Fig. 5-3J) and mef2C by 4.5× ($p \leq 0.04$; Fig. 5-3J). NMD stimulus alone did not induce any changes.

Figure 5-3 - Matrix and necrotic stimuli co-activate satellite cells. Combinations of NMD and matrix culture conditions generated myotubes at different stages of maturation after 24 h (A-D). Culture on matrix increased the number of SC-derived myotubes (E), but addition of the NMD co-stimulus allowed for the generation of larger myotubes (F,G). Myogenic gene transcription was greatest in SC cultures on matrix with the addition of NMD (H-K). *$p \leq 0.04$ vs. control; **$p \leq 0.04$ vs. all other treatments; ***$p < 0.0001$.

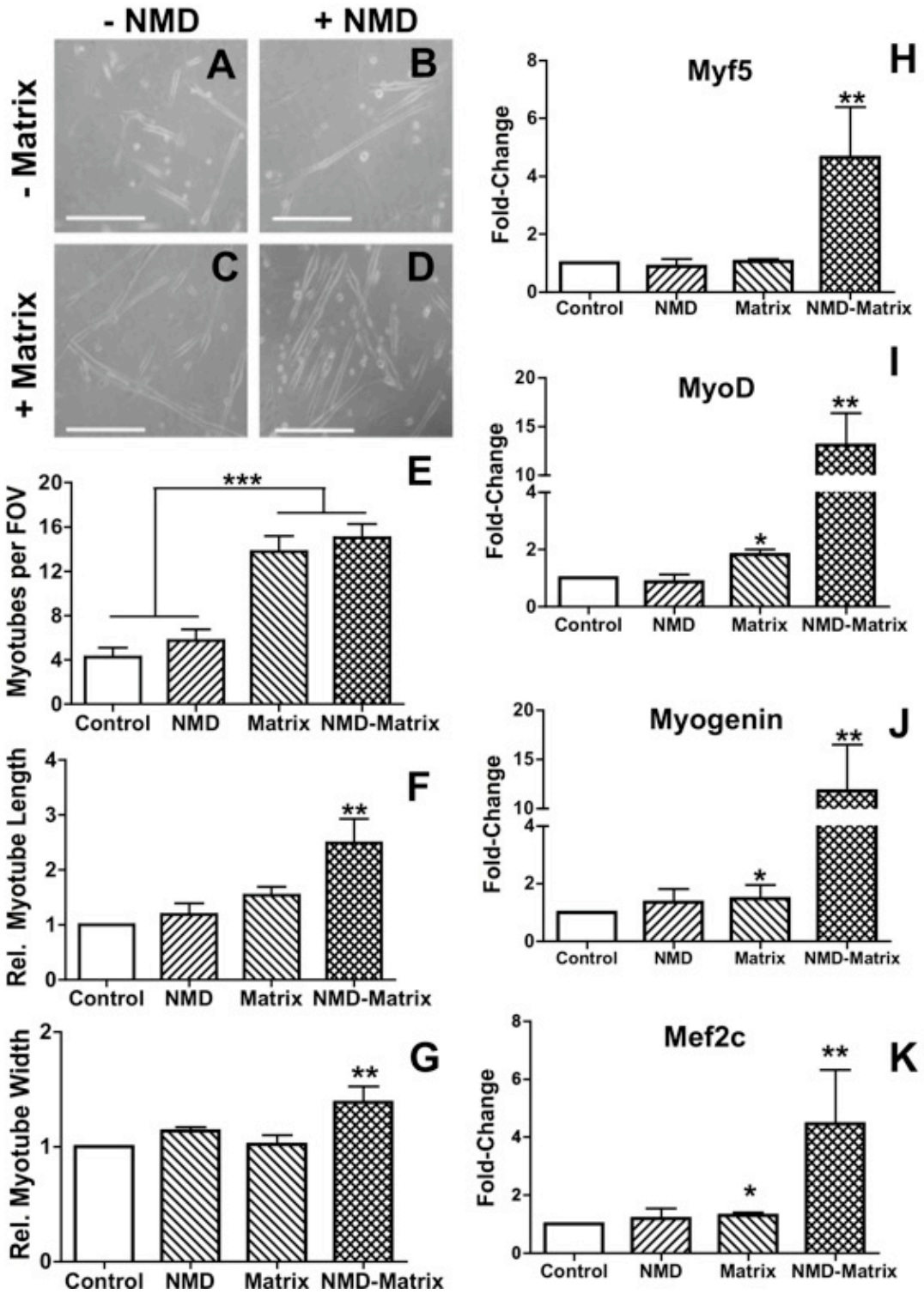
- NMD
+ NMD
- Matrix
+ Matrix
A
B
C
D
E
Myotubes per FOV
***
Control
NMD
Matrix
NMD-Matrix
F
Rel. Myotube Length
**
G
Rel. Myotube Width
H
Myf5
Fold-Change
I
MyoD
J
Myogenin
K
Mef2c
*

Table 5-1 – Observed behavior of myotubes for the four culture conditions after 24 hours.

	Control	NMD stimulus	Matrix stimulus	NMD + Matrix co-stimuli
Stimulus				
NMD	-	+	-	+
Matrix	-	-	+	+
Myotube behaviour				
Spontaneous beating (*n*=6)	0	0	4	5
Self-alignment of myotubes (*n*=6)	0	0	5	6

Satellite cell populations experiencing necrotic and matrix stimuli produce a paracrine cocktail with potent myogenic effects

To investigate the potential for the matrix to induce myogenesis via activation of paracrine signaling, supernatants collected from SC cultures (±NMD, ±matrix stimuli) were applied to proliferating C2C12 myoblast cultures. After 24h of exposure to conditioned medium from SC cultures (or control medium), C2C12 transcription of myogenic markers was increased only when supplemented with conditioned medium from matrix-NMD SC cultures. Specifically, myf5 increased by 4.5× ($p \leq 0.03$; Fig. 5-4A), myogenin increased by 213.4× ($p \leq 0.02$; Fig. 5-4B) and mef2C increased by 191.9× ($p \leq 0.0002$; Fig. 5-4C). These changes were abrogated for all markers at 48 h ($p \geq 0.3$).

At 24h, C2C12 cultures exposed to NMD-matrix conditioned medium corroborated the transcriptional profile; these myoblast cultures tended to demonstrate a greater fusion index (3.8% vs. 1.2–2.4%; $p \leq 0.09$; Fig. 5-4D); however, the increased fusion index became more pronounced at 48h (16.1% vs. 6.5–10.0%; $p \leq 0.05$; Fig. 5-4D). At 48h, all myoblast cultures were morphologically representative of proliferation/early differentiation (Fig. 5-4E-N).

Figure 5-4 - Paracrine effects of SCs after matrix and necrotic cell debris exposure. The addition of conditioned medium from SC cultures exposed to matrix and NMD accelerated the transcription of myf5 (A), myogenin (B) and mef2c (C) in SC at 24 h, compared to all other conditioned medium treatments and with standard myoblast differentiation conditions with DM. At 48 h, there was an increase in cell fusion of myoblasts cultured with conditioned medium from matrix-NMD SC cultures (D). Representative images of differentiating myoblasts at 24 h (E-I) and 48 h (J-N). Cells are visualized with anti-laminin (green) and nuclei with Hoescht (blue) stains. Scale bar = 100 µm. *$p \leq 0.09$ vs. all other treatments at 24 h; **$p \leq 0.05$ vs. all other treatments at each time point; ***$p \leq 0.0002$ vs. all other treatments at 24 h.

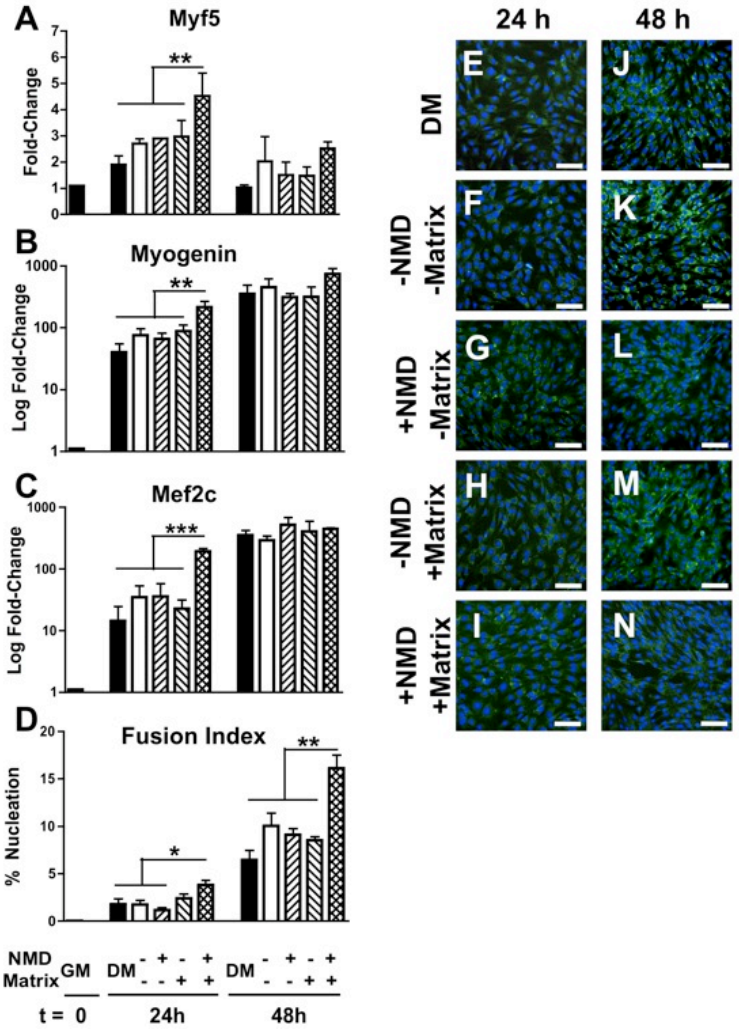
A
Myf5
Fold-Change
**
B
Myogenin
Log Fold-Change
**
C
Mef2c
Log Fold-Change
***
D
Fusion Index
% Nucleation
**
*
NMD
Matrix
GM
DM
DM
t = 0
24h
48h
24 h
48 h
DM
-NMD -Matrix
+NMD -Matrix
-NMD +Matrix
+NMD +Matrix
E
J
F
K
G
L
H
M
I
N

Matrix and necrotic co-stimuli cause satellite cells to produce both inflammatory and regenerative cytokines

To elucidate the paracrine factors responsible for accelerating C2C12 myoblast maturation, supernatant collected from SC cultures (control, NMD, matrix and NMD-matrix) was screened using a cytokine array. NMD and/or matrix stimuli did not induce changes in the amount of SC-produced myogenic regulatory factors insulin-like growth factor (IGF)-I (*p*=0.2; Fig. 5-5A), IGF-II (*p*=0.6; Fig. 5-5B), IGF binding protein (IGFBP)-2 (*p*=0.6; Fig. 5-5C), IGFBP-5 (*p*=0.3; Fig. 5-5D) or IGFBP-6 (*p*=0.2; Fig. 5-5E). NMD-matrix stimuli increased interleukin (IL)-1α production by 2.1× ($p \leq 0.05$; Fig. 5-5F), but did not alter IL-1β production (*p*=0.5; Fig. 5-5G). Both NMD and NMD-matrix conditions increased IL-4 by 2.7× and 2.0×, respectively ($p \leq 0.003$; Fig. 5-5H). IL-6 was increased by 4.7× only under NMD-matrix conditions ($p \leq 0.01$; Fig. 5-5I). No conditions induced changes in production of IL-10 (*p*=0.2; Fig. 5-5J) or tumor necrosis factor-α (TNF-α; *p*=0.2; Fig. 5-5K). Monocyte chemoattractant protein-1 (MCP-1) trended towards a 23% reduction in all treatments, compared to control (no NMD, no matrix stimuli) conditions ($p \leq 0.06$; Fig. 5-5L). Both NMD and NMD-matrix conditions increased fibroblast growth factor-2 (FGF-2) levels by 2.8× and 3.3×, respectively ($p \leq 0.02$; Fig. 5-5M). Only NMD-matrix conditions increased levels of hepatocyte growth factor (HGF; by 1.5×; $p \leq 0.02$; Fig. 5-5N) and stromal cell-derived factor-1 (SDF-1; by 1.5×; $p \leq 0.05$; Fig. 5-5O).

Figure 5-5 - Identification of paracrine factors produced by satellite cells after exposure to matrix and necrotic cell debris stimuli for 24 h. Matrix-NMD stimuli did not induce changes in the production of IGF-I (A), IGF-II (B), IGFBP-2 (C), IGFBP-5 (D) or IGFBP-6 (E). Changes in production of some inflammatory cytokines were observed with matrix and NMD exposure; IL-1α (F), IL-1β (G), IL-4 (H), IL-6 (I), IL-10 (J), TNFα (K) and MCP-1 (L). Matrix and NMD co-stimuli enhanced the production of regenerative cytokines FGF-2 (M), HGF (N) and SDF-1 (O). **$p \leq 0.02$ vs. treatments without NMD stimulus; ***$p \leq 0.05$ vs. all other treatments; ****$p \leq 0.06$ vs. all other treatments.

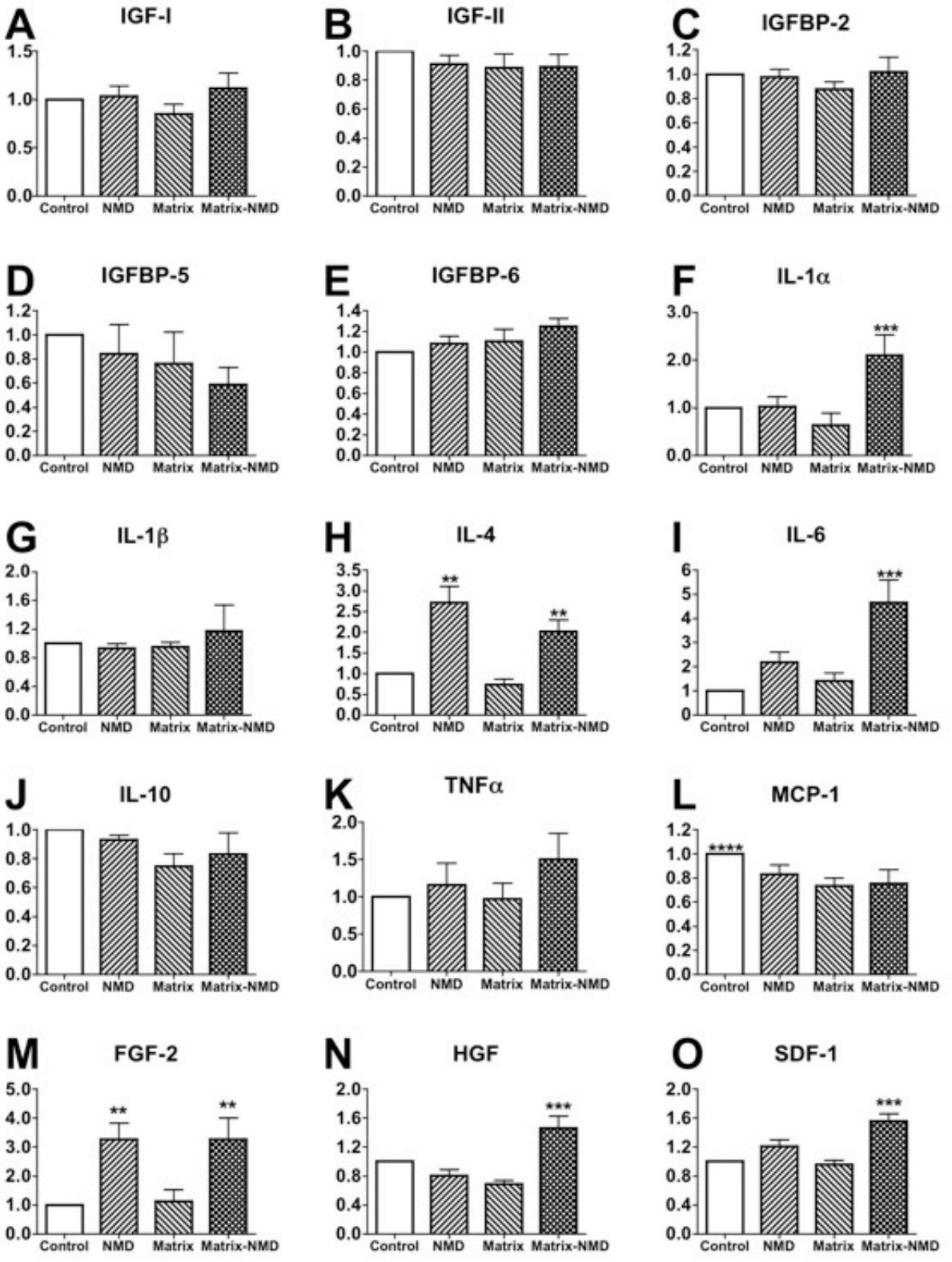
A
IGF-I
1.5
1.0
0.5
0.0
Control
NMD
Matrix
Matrix-NMD
B
IGF-II
1.0
0.8
0.6
0.4
0.2
0.0
C
IGFBP-2
1.2
1.0
0.8
0.6
0.4
0.2
0.0
D
IGFBP-5
E
IGFBP-6
1.4
F
IL-1α
3.0
2.0
***
G
IL-1β
2.0
1.6
H
IL-4
3.5
3.0
2.5
2.0
1.5
0.5
**
I
IL-6
6
5
4
3
2
1
J
IL-10
K
TNFα
L
MCP-1
****
M
FGF-2
5.0
4.0
N
HGF
O
SDF-1

Discussion

In dystrophic mice, collagen matrix treatment stimulated myogenesis, likely contributing to the observed functional improvements. It is important to note that the model was unilateral; therefore, the functional results probably underestimate the potential of this treatment should both legs receive treatment. Mid-stage myogenic gene encoding myogenin was increased, as were the early-stage genes encoding desmin and myf5. SC marker Pax3 was also increased, but interestingly the SC marker Pax7 was not. Pax3 and Pax7 have similar roles in specifying myogenic cell fate and both may be used to identify SCs (Horst et al., 2006; Relaix et al., 2006). It is possible that the increase in only Pax3 mRNA may be attributed to a sub-population of SCs. A new myogenic $Pax3^{+}Pax7^{-}$ population, found in the interstitium and not the basal lamina, has previously been identified (Kuang et al., 2006). It has also been reported that Pax3 is expressed in quiescent muscle satellite cells in a subset of muscles and it plays an important role in regulating the entry of satellite cells into the myogenic program (Buckingham, 2007; Relaix et al., 2006). Thus, Pax3 plays a distinct role in this context, as it is expressed in proliferating SCs before they exit the cell cycle (Conboy and Rando, 2002), thereby suggesting that $Pax3^{+}$ SC proliferation may be greater in matrix-treated muscles. MCK, a late marker of myogenesis, was not increased with matrix treatment, implying that the observed myogenesis had not yet reached a stage of late maturation. Treatment of ischemic muscle – another disease state characterized by necrotic degeneration – with the same collagen matrix also resulted in increased expression of myogenic genes, but not in Pax7 transcripts (Kuraitis et al., 2012b). It is curious that despite the striking functional improvements and molecular myogenesis in the mdx and ischemic

models, no indication of myogenesis was evident in atrophic animals. The obvious differences between the models are the muscle microenvironment and the modes by which muscle is lost: dystrophic muscles and ischemic muscles are characterized by degeneration of necrotic myofibres and inflammation, whereas atrophic muscles do not present significant amounts of necrotic or non-apoptotic dead myocytes. The difference between these microenvironments' abilities to modulate myogenesis was further explored with *in vitro* studies.

Exposure to a collagen matrix improved the number of SC-generated myotubes; however, the addition of a necrotic stimulus increased their size and induced functional beating, something that is not typically seen in SC cultures until 2–3 days after differentiation. Similarly, matrix exposure induced mild increases in myogenic genes, but in a necrotic context, the matrix markedly amplified transcription of a greater number of myogenic genes. We have recently demonstrated that this collagen matrix has an inherent potential for myogenesis: when it was used as a substrate for the culture of pluripotent embryonic stem cells, multinucleated $Pax3^{+}$ populations were generated that also expressed myogenin and myf5 (Kuraitis et al., 2012b). This matrix also mimics skeletal muscle elasticity. ECM elasticity is one of the key parameters that govern progenitor cell differentiation (Engler et al., 2006), as maximal myoblast-to-myotube differentiation has been shown to occur when the substrate's elasticity mimics that of native skeletal muscle (Engler et al., 2004; Gilbert et al., 2010). The novelty of our study is that matrix and necrotic co-stimuli aggrandize myogenesis from SCs. Dehne *et al* have shown that muscle cell debris exposure activates myoblasts and signals for the production of regenerative factors (Dehne et al., 2011). Thus, a necrotic mechanism – in particular, direct SC-necrotic myocyte contact – may be necessary

in order to achieve maximal myogenesis with collagen matrix treatment. Because the DMD phenotype is exacerbated from the lack of functional glycoprotein complexes to link the ECM and cytoskeleton (Straub and Campbell, 1997), the *in vitro* observations support the hypothesis that provision of a material that potentially mimics healthy ECM may at least partially compensate and support robust regeneration in mdx mice.

Muscle turnover and regeneration is a complex process and highly coordinated among myocytes, progenitor and inflammatory cells. Because of this cross talk, it is difficult to identify the sources of regenerative signals. Myotube incubation with muscle cell debris appears to produce autocrine and/or paracrine factors, because application of this supernatant alone was able to activate other myotubes that were not exposed to cell debris (Dehne et al., 2011). Application of conditioned medium from SC cultures (± NMD, matrix stimuli) to myoblasts revealed that exposure to both the matrix and necrotic stimuli generated a paracrine cocktail that could induce myogenesis in myoblasts 24 h after exposure. The acceleration of myf5, myogenin and mef2c transcription was no longer apparent at 48 h, but increased cell fusion was maintained at the later time point. It would have been interesting to observe these effects later into stages of myotube maturation, but after 48 h, cell media could not be replaced with fresh media of known contents and thus the experiment could not be continued beyond this time point.

Arrays were used to identify paracrine factors whose presence might explain why the conditioned medium from NMD-matrix SC cultures can accelerate myogenesis. Surprisingly, treatment conditions did not generate different amounts of IGF-I, -II, or their binding proteins. IGFs and their binding proteins have important and known roles in myogenesis (Duan et al., 2010). SCs exposed to both stimuli produced IL-1α, IL-4 and IL-6. Under

proinflammatory stimuli, SC-derived myocytes naturally produce inflammatory interleukin cytokines (Nagaraju et al., 1998). Considered one of the most degenerative cytokines, it may be favourable that TNFα levels were not elevated. The presence of IL-4 is required for myoblast fusion with myotubes and its absence leads to myotubes of reduced size (Horsley et al., 2003). IL-6 is produced by SCs and growing myofibres and its absence reduces myoblast proliferation and migration (Serrano et al., 2008). Thus, SCs exposed to a combination of matrix and necrotic stimuli increase their production of inflammatory cytokines that have defined roles in myoblast function and maturation. The chemokine MCP-1 is important for recruitment of mononuclear cells post-injury (Chazaud et al., 2003) and *MCP-1*$^{-/-}$ animals display impaired regeneration (Shireman et al., 2007). However, SCs appear to produce MCP-1 immediately after activation and emigration from quiescence, and this production tapers off over time (Chazaud et al., 2003). Given that SCs appeared to mature under NMD or matrix stimuli and that the control conditions were least supportive of SC maturation, it is plausible that the precursor cells in control conditions produced greater amounts of MCP-1 because they are in a more primitive stage of the myocytic lineage and have not yet matured to a phenotype with ablated MCP-1 production.

In addition to inflammatory cytokines, skeletal muscle regeneration requires coordinated growth factor signals (Turner and Badylak, 2012). Of the cytokines with known roles in myogenesis, the production of HGF, FGF-2 and SDF-1 was greatly increased by SCs in response to NMD-matrix co-stimuli. HGF is a potent growth factor produced in an autocrine fashion, and is capable of stimulating quiescent SC activation (Tatsumi et al., 1998) and proliferation (Sheehan et al., 2000). FGF-2 is also produced by muscle progenitor cells (Joseph-Silverstein et al., 1989) and has a strong ability to induce SC proliferation (Deasy et

al., 2002). Furthermore, HGF and FGF-2 synergistically increase SC proliferation (Sheehan and Allen, 1999). SDF-1 is a chemoattractant capable of recruiting a variety of progenitor cell populations, including SCs (Miller et al., 2008; Ratajczak et al., 2003). It has been suggested that based on its ability to attract SCs, SDF-1 may play a bimodal role and function to recruit cells both to a quiescent niche and also to sites of injury or regeneration (Miller et al., 2008). Together, the cytokines produced by SCs under NMD-matrix conditions are supportive of myoblast activation, proliferation and maturation, as we demonstrated by the accelerated myogenesis in C2C12 myoblast cultures in the presence of this cytokine cocktail.

This study employed a collagen-based matrix, containing chondroitin sulfate-C, which has physical properties similar to those of native, healthy skeletal muscle. It is noteworthy that provision of a matrix – containing only two ECM components – is able to support and accelerate myogenesis. Future studies will need to better understand how the ECM changes in disease states; and how we can best replicate "healthy" ECM in order to facilitate recovery and regeneration. When designing therapeutic biomaterials, such studies will likely exploit specific regenerative cues that already exist in the ECM in order to best harness and benefit from endogenous cues for regeneration (Kuraitis et al., 2012c).

The conclusions of this study are multiple: (i) treatment with a collagen-based matrix can augment myogenesis, but this regeneration is context-dependent and may require a necrotic environment as a mechanism for achieving maximum regeneration; (ii) under necrotic conditions, the matrix superactivates SC populations to mature and also to produce a potent myogenic cocktail of secreted proteins; and (iii) instead of attempting to modulate necrosis and inflammation, this study provides a novel therapy that may harness the constant necrosis

that occurs in DMD and use it as a “Trojan Horse” for regeneration that translates into improved function. Perhaps more globally, this study also highlights that the disease state must be carefully considered when applying therapeutic biomaterials, because the matrix presented in this study only induced myogenesis in states of active necrosis and failed to induce myogenesis in an atrophic model.

Materials & Methods

Unless otherwise specified, all materials and reagents were obtained from Sigma-Aldrich (Schnelldorf, Germany).

Matrix preparation

Collagen matrix was prepared on ice, as previously described (Kuraitis et al., 2011b). N-(3-dimethylaminopropyl)-N'-ethylcarbodiimide hydrochloride (EDC) and N-hydroxysuccinimide (NHS) were mixed in a 1:1 molar ratio (13 mM) in 2(-N-morpholino) ethanesulfonic acid (MES) buffer. This EDC/NHS cross-linker was added to a solution of 1 % (w/v) type I collagen (Nippon Ham, Tskuba, Japan) and 40 % (w/v) chondroitin sulfate-C (CSC; Wako Chemicals, Osaka, Japan). The solution was diluted with PBS before adjusting the pH to 7.2±0.2. The final concentrations of collagen and CSC were 0.59 and 2.4 % (w/v), respectively. For *in vivo* use, the matrix was kept on ice and transferred to a cold syringe immediately prior to use. For *in vitro* use, 150 µl was spread onto 6 cm tissue culture polystyrene plates before being thermogelled at 37°C and rinsed with PBS before cell application.

Animal model

The animals were housed in a temperature-controlled (22°C) room with a 12:12 hr light-dark cycle. All of the mice were maintained according to the institutional guidelines of the animal facilities of DIEM-National Institute of Health-Italy.

Two mouse lines were used to evaluate the matrix' potential for myogenesis. The well-characterized mdx mouse (Willmann et al., 2012) was used as a model for DMD. The MLC/SOD1^{G93A} mouse, recently characterized in (Dobrowolny et al., 2008), was used as a model for muscle atrophy and ALS. Given its ability to represent animal motility and muscle

function, the EDL muscle was chosen to evaluate matrix treatment. The left EDL of 1-month old male mdx and 4 month-old female MLC/SOD1^{G93A} mice was surgically exposed and received a 5 µl injection of either PBS or matrix. Treadmill tests were performed at 6 weeks for mdx mice and at 6 months for MLC/SOD1^{G93A} mice. After collection of treadmill data, animals were sacrificed and EDL muscles were harvested, flash frozen in liquid nitrogen and stored at -80°C.

Functional analysis with a forced treadmill test

To assess the function of treated muscles, mice were subjected to a forced treadmill protocol. They were conditioned to the treadmill process for 1 week prior to final testing at an incline of 0° for 5 min at 5 m/s and 5 min at 10 m/s. Animals that did not maintain the treadmill speed received a shock of 0.5 mA. The maximal test of exhaustion was modified from Ferreira *et al*. (Ferreira et al., 2008). In brief, the treadmill speeds increased every 3 minutes at a rate of 3 m/min. Animals were removed from the treadmill when they could no longer manage to return to the treadmill from the shock platform. Total distance and speed at which exhaustion occurred were recorded. The same parameters were also measured on untreated (sham) animals for both models.

C2C12 myoblast culture

All cells in culture were maintained at 37°C in a humidified incubator with 5% CO_2. C2C12 myoblasts were used between passages 6 and 9. Cells were maintained on 20 cm tissue culture dishes in growth medium (GM), consisting of DMEM supplemented with 20% fetal bovine serum (FBS), penicillin/streptomycin and 4 mM L-glutamine. Upon reaching ~85% confluence, cells were differentiated by replacing their GM with differentiation medium (DM), which is equivalent to the GM formulation but containing only 2% FBS. To

store amplified cells, 1×10^5 C2C12 myoblasts were suspended in GM and DMSO in a 9:1 ratio and frozen at -80°C.

Necrotic myocyte debris preparation

Confluent C2C12 myoblasts were differentiated into early-stage myotubes for 24 h. NMD was prepared by manually scraping myotubes, centrifuging and storing the collected debris at -80°C at a concentration of 2×10^6 cells/ 100 µl PBS. Application of NMD to other cell populations allows for the observation of interactions that stem from direct cell contact with dead myocytes (Dehne et al., 2011). Prior to application in culture, NMD was confirmed to contain non-viable cells by examination under a light microscope using trypan blue dye.

Satellite cell isolation

Wild-type C57 mice, 3–4 weeks of age, were sacrificed and the hindlimb muscle was harvested under sterile conditions. Muscles were minced and enzymatic digestion using collagenase and dispase was performed, as previously described (Musaro and Barberi, 2010). After digestion, the solutions were pre-plated on tissue culture dishes to remove contaminating fibroblasts, for 1× 45 min and then 1× 30 min. SCs were amplified on collagen I-coated plates in GM, consisting of DMEM supplemented with 20% horse serum, penicillin/streptomycin, L-glutamine (4 mM) and 3% chick embryo extract. One day after isolation, cells were lifted using 0.25% trypsin, pre-plated again for 30 min and re-plated on new collagen-coated dishes. Cells were washed with PBS and GM was changed every other day.

Satellite cell differentiation

After 4–5 days, $6–8\times10^5$ cells could be collected from the primary cultures derived from one mouse and 8×10^4 SCs were plated in 3 ml DM on 6 cm dishes coated with collagen

I (used as standard SC culture substrate (Musaro and Barberi, 2010)) or matrix. Cultures then received either 100 µl of NMD or 100 µl of PBS. Ultimately, four culture conditions were created: 1) standard culture conditions; 2) NMD stimulus; 3) matrix substrate stimulus; and 4) NMD-matrix stimuli. After 24 h in culture, cell observations were recorded and cells were imaged, then thoroughly rinsed with calcium- and magnesium-free PBS (CMF) to remove dead cells and NMD, and immediately frozen at -80°C. Cell images were analyzed using ImageJ 1.32s (National Institutes of Health, Bethesda, MD) for the number of myotubes per field-of-view (FOV), and their lengths and widths. Width was defined as the maximum width of a myotube. Based on myotube morphology, this measurement was taken at the centre, approximately equidistant from either end. The medium from these 24-hour cultures (for all 4 conditions) was flash frozen in liquid nitrogen and stored at -80°C to be used as conditioned medium in subsequent C2C12 studies.

C2C12 myoblast differentiation

As described, C2C12 myoblasts were differentiated into early-stage myotubes using low serum medium. Cultures were maintained on 3 cm dishes. Upon ~85% confluence, GM was replaced either with 3 ml DM or with 2 ml DM + 1 ml of conditioned medium from SC cultures (4 conditions tested: control, NMD, matrix, or NMD-matrix). Upon harvest at 0, 24 or 48 h, cells were rinsed with CMF and stored at -80°C for RNA extraction. A subset of differentiating myoblasts was prepared for fusion index analysis. Cells were fixed with 70% methanol for 20 min, blocked for 45 min with 10% goat serum in CMF, incubated for 2 h at room temperature with 1:200 goat anti-laminin in 1.5% goat serum and then incubated for 45 min at room temperature with 1:2000 mouse anti-goat Alexa488 (Invitrogen, Burlington, Canada) and 1:1000 Hoechst 33342 stain. Before and after each incubation step, cells were

washed 2× 10 min with 1% bovine serum albumin/ 0.2% triton-X in PBS. Cells were imaged using an inverted Axioskop 2 Plus microscope (Zeiss, Oberkochen, Germany) and images were processed using Axiovision 3.1 software (Zeiss). The fusion index was calculated as the percentage of nuclei present in multinucleated cells.

RNA preparation and quantitative PCR analysis

Total RNA was isolated from homogenized muscle and manually scraped cell cultures using TRIzol reagent (Invitrogen) as previously described (Rio et al., 2010). RNA was converted to cDNA using the QuantiTect Reverse Transcription kit according to the manufacturer's instructions (Qiagen, Milan, Italy). The reagent proportions as specified by the manufacturer were used for each 1 μg of RNA. cDNA concentrations were raised to 10 ng/ml with nuclease-free water and stored at -20°C. qPCR reactions were prepared with 5 μl cDNA, 6.25 μl nuclease-free water, 12.5 μl TaqMan PCR Master Mix (Applied Biosystems, Foster City, CA) and 1.25 μl TaqMan Probe (Applied Biosystems). TaqMan Probes were used for murine β-actin, desmin, GAPDH, muscle creatine kinase (MCK), mef2C, myoD, myoegnin, myf5, Pax3 and Pax7. The reaction was performed using an Applied Biosystems RealPlex 7500 Fast Real Time system and software. Relative gene expression was quantified using the $\Delta\Delta C_t$ method, as described (Livak and Schmittgen, 2001). Transcripts from treated muscles were expressed relative to those in untreated muscles (using housekeeping genes encoding GAPDH for mdx mice and β-actin for MLC/SOD^{G93A} mice; n=4). Transcripts from cultured cells were expressed relative to control treatments (using housekeeping genes encoding GAPDH for C2C12 myoblast cultures and β-actin for SC cultures; n=4 – 6).

Cytokine arrays

Conditioned medium collected from SC cultures was analyzed using a cytokine array, according to the manufacturer's instructions. Custom cytokine arrays (RayBioTech, Norcross, GA) were used to analyze protein levels of IGF-1, IGF-II, IGFBP-2, IGFBP-5, IGFBP-6, IL-1α, IL-1β, IL-4, IL-6, Il-10, TNFα, MCP-1, FGF-2, HGF and SDF-1.

Statistical analysis

All experiments were performed with n=4, except SC cultures and cytokine arrays, which were performed with n=6. Data between two experimental conditions were analyzed using a student's t-test and data between multiple groups was analyzed using a one-way analysis of variance with Tukey's post-hoc using Prism 4.0 (GraphPad, La Jolla, CA).

Acknowledgments

The authors would like to thank Carmine Nicoletti for assistance with animal care and Laura Barberi for assistance with cell culture. D.K. was supported by a Canadian Institutes of Health Research (CIHR) Canadian Graduate Scholarship and a Disease Models and Mechanism's Travelling Fellowship. This work was supported by Fondazione Roma, 7FP-Myoage and the French Muscular Dystrophy Associatino (AFM) (to A.M.) and by grant-in-aid T6793 from the Heart and Stroke Foundation of Ontario (to E.J.S.).

The authors declare that they do not have any competing or financial interests.

D.K., E.J.S. and A.M. conceived the study. D.K. performed all experiments, analyzed all data and wrote the manuscript. M.G.B. performed gene expression analysis. All authors contributed to manuscript editing.

Translational Impact

CLINICAL ISSUE

Diseases associated with muscle loss, including Duchenne's muscular dystrophy (DMD), represent a huge burden to society, and ideal therapies are not yet visible on the horizon. In such diseases, muscle loss can occur via active, necrotic degeneration, or muscle wasting via atrophic degeneration. Recent studies have shown that the application of biomaterials that mimic healthy extracellular matrix can provide stem cell niches and augment skeletal muscle regeneration.

RESULTS

In this study, the authors show that an injectable collagen matrix is able to successfully regenerate skeletal muscle in a mouse model of muscle necrosis, but not in an atrophic mouse model. This *in vivo* phenomenon was supported by *in vitro* observations: satellite cells (SCs) that were exposed to the matrix demonstrated an improvement in myogenesis that was maximized when SCs were cultured on the matrix in a necrotic environment. Furthermore, matrix and necrotic co-stimuli induced SCs to produce a cytokine cocktail containing myogenesis-regulating factors, and this mixture accelerated myogenesis in cultured myoblasts, and in dystrophic and ischemic muscle.

IMPLICATIONS & FUTURE DIRECTIONS

The clinical evaluation and application of biomaterials is becoming more prevalent every day. However, to date no gene, pharmacological or cell therapy has emerged as an ideal candidate to promote muscle regeneration. This study has broad implications: application of a "healthy" extracellular matrix-like material has the potential to activate muscle progenitor cells and functionally regenerate muscle. Regeneration conferred by this particular therapy

appears to be optimal under necrotic conditions, highlighting the importance of considering the disease environment when applying therapeutic biomaterials.

CHAPTER 6. General Discussion

The studies presented in this thesis have assessed feasibility and potential of various aspects of natural biomaterial therapy, from biomaterial modification of cell culture, to biomaterial systems for releasing growth factors, to injectable biomaterials for enhancing the regeneration of blood vessels and muscle. These studies were all novel to the field and will constitute platforms for future studies to assess safety and efficacy. Despite being early investigative studies *in vitro* and in small animals, they provide insight into biomaterial therapy as a whole.

Is Biomaterial Therapy Truly a Viable Option?

Perhaps the most important question is whether or not biomaterial therapy is truly a viable option. At this point in time, it may be too soon to predict the role that biomaterial therapy may play in the future of health care. In order to proceed, researchers need to present a strong case that supports pre-clinical and clinical trials. Given what we know so far, we can make some guarded conclusions regarding the potential that biomaterial therapy has for success.

Biomaterial therapy vs. cell therapy

Unarguably, clinical trials using CAC or CAC-like cell populations have produced underwhelming results given the expectations that preceded them; however, the results were at first very promising based on small and large animal studies (Martignoni et al., 2006; Mestas and Hughes, 2004; Nossner and Parham, 1995). Thus far, biomaterial studies in small animals have been exhaustive, but also hopeful. It remains to be seen whether or not

biomaterial translation to humans will follow the same pattern that CAC therapy did and similarly, yield modest results.

Various reasons have been proposed to explain the discrepancy between human and animal studies. In brief, human physiology is terribly difficult to replicate in an animal model and there are far more potentially confounding factors in human subjects than in animals, such as typical co-morbidities of cigarette smoking, obesity, exercise and diabetes. Few studies have attempted to address the impact biomaterial therapy may have in these contexts, and thus it is difficult to predict whether or not these factors will affect the use of biomaterials in humans.

Timing of biomaterial delivery

The timing of cell delivery appears to be an integral parameter governing the success of cell therapy. Early studies observed that cells delivered one week after myocardial infarction displayed improved engraftment and led to a greater angiogenic response compared to cells that were delivered 1 or 2 days post-infarction (Hu et al., 2007). However, other studies have shown that there is no significant difference in myocardial recovery using a similar delivery time frame (Swijnenburg et al., 2010). Research efforts still need to address when the optimal delivery times are for both cells and biomaterials.

Muscle disease or damage is accompanied by alterations in ECM composition and structure. Given the known roles of ECM interaction in regeneration, it is plausible that delivered ECM-like materials will also be subject to conditions similar to those experienced by native ECM. It is interesting that some sort of necrosis or active degeneration needs to be present in order to elicit potent myogenic responses when an injectable matrix is applied. These observations are supported by a study performed by laboratory colleague Tanja

Sofrenovic, where she used the same injectable material in infarcted mouse myocardium either 1 or 2 weeks post-MI. The closer to the MI event that the material is delivered, the more potent are its cardiomyogenic effects (Sofrenovic, unpublished data). The myocardium is highly necrotic immediately post-MI, but this drastic environment is tempered within days of the event (Boudoulas and Hatzopoulos, 2009). Thus, it is probable that temporal delivery of at least the injectable materials used in these studies is important and it appears that delivery will be optimized when the recipient tissue is experiencing a great degree of necrosis. Curiously, cell delivery is avoided when the relative level of necrosis is high, as it is expected that the environment would be too hostile for transplanted cells and negatively impact their viability and engraftment. Attempts to modulate the infarcted myocardium and suppress the degree of inflammation have had poor outcomes and failed to produce beneficial results (Hwang et al., 2001; Kloner et al., 1978).

While the studies presented in this thesis delivered cells or biomaterials, it is important to note that many studies currently assess the deployment of cells with biomaterial vehicles in order to capitalize on the benefits of both cell and biomaterial therapies. Although still in a phase of infancy, it will be interesting to observe whether or not biomaterials applied to hostile environments will be able to protect the health and function of delivered cells.

Timing of biomaterial delivery is also important in studies where growth factors are released. The ideal doses of growth factors that are released into the system are speculative. Is it advantageous to increase the amount of SDF-1 by releasing exogenous peptide when the endogenous SDF-1 is peaking? Or, is it better to maintain a longer duration of SDF-1 production and release? Our use of an SDF-1-releasing biomaterial at first focused on reducing the rate at which SDF-1 exits the system; this would prolong the presence of the

signal, and thus provide a greater temporal window of exposure. Both our group and others have performed growth factor release studies – designed to maximize the temporal exposure of the growth factor – in non-disease states and these results have all echoed the same conclusions: prolonged release of regenerative factors will ultimately enhance regeneration (Cai et al., 2005; Kuraitis et al., 2012a). Future studies should now assess how to tailor these systems to best coincide with endogenous regenerative signals so that we will be able to effectively induce regeneration in clinically-relevant disease states.

Ideal biomaterials: do they exist?

Some biomaterials will undoubtedly have limited potential for application in certain disease states. It would be illogical to use bone-mimicking materials as platforms for nervous tissue regeneration. However, it is not yet known how closely delivered biomaterials need to mimic healthy tissue. It is easy to imagine that the best biomaterial therapy would be one that can completely recapitulate a healthy ECM that also supports regeneration. Before we can build-up organs from scratch, we first need to better understand the role that the ECM plays and to what capacity we should be mimicking or modifying it for therapeutic benefit.

The ECM is a complex system and ECM from different tissues present an infinite amount of differences. In order to provide an ECM mimic or ECM-like environment for regeneration of a particular tissue, it is advantageous to take advantage of the endogenous cues present in a particular ECM. For example, Stern and colleagues investigated whether a simple collagen coating would have a similar effect on myoblasts as a natural, decellularized muscle ECM (Stern et al., 2009). As expected, there were cues in the skeletal muscle ECM that enhanced proliferation, maturation and fusion of myoblasts, compared the basic collagen

coating. Another study compared the interaction of myoblasts with muscle or small intestine ECM (Wolf et al., 2012). In a similar fashion, the muscle ECM better conferred cell survival and proliferation, and also helped maintain a myogenic response when cell-ECM constructs were applied in an abdominal wall injury model. However, by 35 days, there was no apparent benefit to using muscle-derived ECM over small intestine ECM. These studies provide evidence that tissue-specific ECMs are able to better guide regeneration of like tissues, perhaps to a limited extent. In this thesis (Chapters 3, 4 & 5), matrices were injected intramuscularly. The similarities that they had with native ECM were basic in nature: the main structural component was collagen type I and they shared a similar elastic modulus. It is notable that these similarities were sufficient to guide myogenesis and future research will attempt to better mimic natural ECM in order to have a more potent and direct control over regeneration.

When designing therapeutic biomaterials, one of the greatest concerns is safety and biocompatibility. All of the efforts put forth into creating biomaterials may be futile if the resulting product elicits harmful responses in the recipient. The materials used in this thesis were carefully designed to be safe for both small animal and future pre-clinical (and ideally, clinical) trials. Both collagen I and chondroitin sulfate, like most ECM components, are highly conserved among mammals, and neither is expected to trigger inflammatory responses (Hutter et al., 2000). Alginate, used to create microspheres, is considered relatively inert and in small amounts does not contribute to inflammatory responses (Augst et al., 2006). SDF-1 and sLe^X enhancements to matrices are both small molecules that are present in mammalian systems and are therefore recognized by cells. Furthermore, all studies using injectable

biomaterials assessed inflammation using cytokine arrays and demonstrated either no increase or a reduction in local inflammatory cytokines after matrix treatment.

Other than structural and signaling components of our injectable materials, we also employed an EDC/NHS cross-linking system for maintaining and preserving structure of the matrices. Both EDC and NHS are cytotoxic and were used in low concentrations to create the materials (increasing the concentration would reduce their degradation and also increase their stiffness). However, EDC/NHS coupling is now recognized as acceptable to use for *in vivo* implants and has even been used to cross-link collagen-based corneal substitutes in a human trial (Fagerholm et al., 2009; Fagerholm et al., 2010). Subsequent studies in our lab have also shown that the cytotoxicity of these compounds can be reduced by providing the material with excess glycine after the coupling reaction, allowing for inactivation of cytotoxic free aldehyde groups (McEwan et al., 2012). Thus, we have employed low levels of toxic components, but their cytotoxicity does not ultimately impede the successful regeneration that is mediated by the biomaterial constructs.

Limitations of Biomaterial Therapy

Although positive results were obtained that warrant the expansion of the studies presented in this thesis, there are limitations. However, the limitations are not unique to thi particular work; rather, they are applicable to the broad field of biomaterial therapy.

Biomaterial mechanisms

One of the biggest hurdles that the field of biomaterials faces is defining proper mechanisms by which particular biomaterials elicit regenerative responses. Studies are still

being proposed and executed; however, rationalization for pursuing this research tends to be phenomenon-based and not mechanism-based. Drug and antibody studies are simple in comparison; there are few targets/interactions of an introduced substance and physiological responses can be relatively well-anticipated. Applied biomaterials are different with regards to the fact that they are space-filling, respond to the host environment and are able to interact with a plethora of host cell types and factors. The materials used in this thesis were: space-filling (i.e., allowed for physical contact with cells) and interactive with host cell types (e.g., inflammatory cells, local and bone marrow-derived progenitor cells) and factors (e.g., necrosis-associated degradation products). It will be extremely difficult to tease out the specific and necessary roles that physical contact, degradation/turnover and cell interaction plays in order to identify a proper mechanism to explain "how biomaterial therapy works". In the face of these difficulties, the field is now established with many robust examples of the biomaterial successes and is now trending towards attempting to explain how these successes came about.

Physical interactions with substrates are known to greatly influence cell fate, such as differentiation pathways (Engler et al., 2006; Engler et al., 2007; Gilbert et al., 2010). Such studies have identified that the elastic modulus of the interacting substrate is a key regulator of cell fate, highlighting the important role of cell-substrate physical contact. Cells interact with their physical surroundings through various integrins and kinase receptors and particular ECM or ECM-like materials are able to use these cues to force cells down particular differentiation pathways. It has recently been shown that in remodeling skeletal muscle, myoblasts must maintain physical contact with their ECM in order for normal *in vivo* function (Modulevsky et al., 2012). Other studies have noted that mechanical stretching

(such as during ECM remodeling or muscle growth) is a potent activation factor of SCs to enter the maturation phase, but that this stretch also induces secondary effects of regenerative cytokine release (Tatsumi, 2010). In Chapter 2, it was shown that physical interaction with the matrix increased the phosphorylation of ERK1/2, which is associated with improvements in migratory and differentiation capacities. Together, these studies support the notion that physical interactions between biomaterials and progenitor cell populations are an important aspect in defining the mechanism of biomaterial therapy and help to guide future studies towards uncovering mechanisms to describe why biomaterial therapy works.

When discussing the inflammatory responses to biomaterials, the initial tone in biomaterial literature often considered inflammation to be something that was to be avoided. This will always hold true to one extreme; no ideal therapy will ever consist of overwhelming the body with inflammatory cells and cytokines to an extent that causes serious distress and rejection of the transplanted material. Over time, the perception of the role of the inflammatory system has changed. Studies have now shown that for functional recovery, at least some aspects of the inflammatory response are essential. Considering its central role in clearance of damaged tissue and secretome profile, the macrophage is the inflammatory cell whose role in regeneration is now best defined. The macrophage has long been observed to have "pro-inflammatory/M1" and "healing/M2" phenotypes. Macrophages are among the first cells to arrive to interact with transplanted materials and their presence has often been correlated with successful graft integration and tissue regeneration (Hibino et al., 2011). Furthermore, macrophages have been shown to assist transplanted SCs and encourage their persistence and proliferation (Segawa et al., 2008). In 2007, Arnold *et al*. were the first to elucidate the macrophage's role in muscle regeneration (Arnold et al., 2007).

In vitro, they noted that inflammatory macrophages readily switch to anti-inflammatory phenotypes after phagocytosis of muscle cell debris, and that different macrophage phenotypes would elicit either proliferation or differentiation of SCs. For mice in which circulating macrophages had been completely depleted, regeneration of the damaged muscle was wholly prevented. Mirza *et al*. performed a similar experiment to assess the macrophage's role in skin wound healing over time (Mirza et al., 2009). In this case, macrophage depletion did not prohibit regeneration, but it did delay re-epithelialization and impair the angiogenic response, and these defects are believed to result from impaired paracrine signaling. The presence of other inflammatory cell types, such as mast cells, lymphocytes and $CD8^+$ T-cells have been correlated with successful myogenesis (Kharraz et al., 2013). However, it remains to be seen whether or not these cell types are essential for coordinating the regenerative response in muscle, or if their roles in regeneration are minor in nature. The overlap between immunology and biomaterial therapy is rapidly growing. Many top research groups are now attempting to define the specific roles that inflammatory cells play in regeneration, with or without biomaterial delivery. Uncovering these mechanistic roles will be essential for future biomaterials studies so that researchers will be able to better create materials and therapies that harness and use the endogenous regenerative responses for therapeutic benefit.

Cytokine arrays were employed in each study presented in this thesis. These arrays are powerful tools that allow for the identification and relative quantification of soluble factors produced in response to a material. In addition to showing that all of the biomaterials tested supported the production of regenerative cytokines, they also served to highlight the complex signaling cascades that biomaterial therapy may have. This complexity further

muddies the ability of picking out one or two important mechanisms; it is plausible that every implicated cytokine has one role or another in regeneration. The final experimental chapter was able to narrow the field by demonstrating that cellular debris and/or inflammatory cytokines are essential for SC maturation and myogenesis. A recent clinical study utilized a similar pilot experiment: application of TNF-α to SCs induced the production of the myogenic cytokine IL-6 (Podbregar et al., 2013). Thus, in addition to inflammatory cells, inflammatory cytokines may also be responsible for regenerative cues in the body.

Although *a* mechanism by which the materials in this thesis induced regeneration was not identified, we can hypothesize that given (i) the matrices' ability to guide differentiation of ESCs, CACs and SCs, (ii) the matrices' ability to selectively enrich progenitor CAC populations, (iii) the heterogeneity of CAC and SC cultures, which often include contaminating inflammatory cells, and (iv) the secretome-modifying properties of the matrices both *in vitro* and *in vivo*, *it is plausible that the biomaterial matrices acted as a natural magnet for progenitor cells, facilitating their differentiation in vivo via physical cues and also through paracrine signaling, mediated by interactions with endogenous progenitor and inflammatory cell populations.*

Influence of age

Like many disease states, ageing also reduces the integrity and functional signaling of the ECM (Labat-Robert and Robert, 1988). Effects of the aging musculoskeletal and cardiovascular systems are not usually evident until around 40 to 50 years of age (Kurtz and Oh, 2012). Age-related changes in the ECM have known effects on progenitor cell differentiation, proliferation, recruitment and integration. Given the negative changes that occur to the ageing ECM, it is fair to propose this degeneration as a major reason why cell

therapy has yet to be demonstrate overwhelming success. In aged, hypertensive hearts, there is an increase in collagen I deposition (Querejeta et al., 2004; Varagic et al., 2001). Increased deposition of collagen increases the stiffness of cardiac tissue, and this increase in stiffness prevents future cell differentiation (Engler et al., 2008). In this context, ageing creates a degenerative cycle whereby ECM changes reduce regenerative cell responses and the lack of regeneration further allows for permanent changes in the ECM to occur.

In parallel to cell therapy studies, biomaterial studies have employed essentially only young or otherwise healthy animals. Kang *et al*. addressed this issue by attempting to restore therapeutic function to aged cells (Kang et al., 2012). MSCs from older donors failed to elicit regenerative responses in the same magnitude as those from younger donors; however, incorporation of older MSCs into a biomaterial scaffold containing VEGF and FGF-2 was able to rejuvenate these cells and restore their therapeutic potential, measured by functional outcomes after MI injury. This study is noteworthy as it is one of the first biomaterial studies to address the issue of ageing and proposes that biomaterials may be used in a way that overcomes the lack of regenerative potential in ageing patient populations.

Long-term studies

Biomaterials for soft tissue engineering must contain some degree of flexibility. Studies attempting to engineer bone or cartilage share a common goal of attempting to maintain long-term stability, or at least long enough for the endogenous system to remodel the implant with strong, natural tissue. These studies have already reached follow-up periods that extend beyond a decade post-implantation (Silvestri et al., 2011). Soft tissue experience physical forces that significantly different from hard tissue; both muscle and vasculature require degrees of elasticity and the ability to return to native forms after distortion. To this

effect, biomaterial strategies for soft tissue engineering currently aim to develop materials that will assist in mounting a regenerative response and then ultimately be remodeled into healthy tissue. As a consequence, these studies tend to utilize early end-points. Although early responses are important, it will also be critical to know whether or not improvements in perfusion, ejection fraction or muscle function will persist for the long-term. This is something that the studies in this thesis did not address. If the beneficial effects are indeed short-lived and transient, the non-invasive nature of applying injectable biomaterials will allow for semi-continual administration. Hopefully, this will be a topic of future studies now that proof-of-principles have been demonstrated.

Future Studies

In line with the previously discussed limitations of biomaterial studies, the proof-of-principle studies presented in this thesis now provide a platform for interesting future studies that can better elucidate mechanisms of biomaterial therapy and also help to better design therapeutic strategies.

Long-term assessment

As mentioned, our studies did not assess whether or not the beneficial changes mediated by biomaterial delivery would persist beyond the relatively short experimental window. Injectable matrix delivery is considered to be minimally invasive. With the advancements in minimally invasive surgical procedures and imaging technologies, the clinic is evolving such that repeat delivery of these materials should become a real possibility, if necessary. It would be interesting to perform similar experiments, but monitor animals over longer periods and include experimental groups that receive periodic re-injections.

Assessment of ageing

We now know that the integrity of the ECM is jeopardized with age and that the stem cell niche is compromised (Kurtz and Oh, 2012). Additionally, stem cells from aged patients have notably reduced functional capacities. These cells may experience a phenotypic rejuvenation with biomaterial therapy when they are co-transplanted, but it still remains to be observed whether or not transplantable biomaterials alters the aged cell response *in situ*. It would be simple and very informative to perform similar studies on young and old animal cohorts. Furthermore, it would be clinically relevant and important if biomaterials elicited the same regenerative responses in aged animals; if the results suggest that biomaterial therapy is less effective in aged hosts, then this would encourage researchers to focus on the rejuvenation effect that biomaterials may have, as a biomaterial + cell delivery may be best for the aged cohort.

Improvement of current biomaterial systems

CACs that express CD133 and CD34 are considered to be among the most potent CAC phenotypes. However, the frequency of these cells is often minimal. It is suggested that future studies employing a matrix pre-culture for improving the regenerative CAC phenotype also investigate the potential for increasing $CD133^{+}CD34^{+}$ cell frequency. This population is considered to be non-dividing *ex vivo*, but was shown to have the potential to proliferate on matrices in Chapter 2, and therefore expansion of this population would be of great relevance and novelty.

It was hypothesized that the SDF-1 releasing system would accelerate the restoration of perfusion in Chapter 3. This hypothesis did not hold true. It is highly suggested that such a growth factor-releasing system take into account current literature and the roles of multiple

growth factors in order to best recapitulate the natural response. This may mean incorporating other growth factors, such as FGF-2 and VEGF, as well as inflammatory cytokines, such as IL-4 and IL-6. Such a system of coordinated growth factors may be engineered to sequentially release the cytokines as they are produced in the body, thus mimicking what should occur in a healthy regenerative state.

The addition of sLe^X into a collagen matrix conferred better growth of new blood vessels and of muscle in Chapter 4. The additive sLe^X was chosen as it is the natural ligand for L-selectin, and it was hypothesized to mediate CAC recruitment and engraftment into the local environment. The evidence presented in this study suggests that sLe^X enhancement allows for rapid regeneration of vasculature, allowing for regeneration of muscle. It would be interesting to co-enhance the material with other small signaling factors to see if other aspects of regeneration could also be accelerated. Such options could include covalent binding of SCF to encourage c-kit^+ progenitor engraftment, or even incorporation of a SDF-1 releasing system to aggrandize the natural recruitment of CACs and SCs. As research continues to identify progenitor-specific surface ligands or receptors, we will be able to incorporate these discoveries into our materials in order to maximize the progenitor response to biomaterial therapy.

Generation of complex ECM mimics

Recent advances in manufacturing and processing technologies now allow researchers to create 3-dimensional (3-D) materials that mimic ECM in both structure and function. Structurally, polymers may be used to mimic a particular tissue's ECM with respect to physical properties. Functionally, novel cross-linking methods are now being employed to direct ligand and cell placement in 3-D (Culver et al., 2012; Hoffmann and West, 2010). It is

now possible to produce small biomimetic matrices that recapitulate natural ECM. Using cell-specific ligands and receptors, the framework for blood vessels can be created *ex vivo* and rapidly populated in culture for *in vivo* transplantation and ultimately, rapid integration into the host (Hoffmann and West, 2013). The field of using 3-D patterning is still in its infancy, but given what is now known about cell-ECM interactions, we are developing the ability to finely tune and adjust biomaterials tailored for regenerative therapies by exploiting these interactions. Long-term and large-scale, such techniques will allow for the generation of thick tissues or organs from scratch and may even emerge as a substitute option for organ transplants.

Allowing cells to do what they do best

The biomaterial studies in this thesis were passive in regards to how they elicited regenerative responses; materials were applied and the endogenous responses of cells and bodies took over. As cells interacted with the materials, the materials influenced the cells' function and fate. More aggressive modulation techniques such as gene therapy or surgical removal of diseased muscle were not employed. A recent study by Carosio *et al*. used another passive approach to regenerate tissue (Carosio et al., 2013). The study simply allowed for primary SCs to grow beyond the normal cell culture period. The researchers observed that eventually, the dense network of myotubes would fold-in on themselves and assemble into a large fibre-like structure. Transplantation of this structure into EDL muscles that were severed allowed for animals to regain grip strength. Furthermore, this construct was rapidly infiltrated by endogenous cells and vasculature, and also maintained characteristics similar to that of native muscle. This study is incredibly simplistic in nature, but also provides a novel approach to tissue engineering that is only just being accessed. Very little

intervention occurred and the hypothesis that the SC-derived myotubes would arrange themselves into functional muscle if left alone held true. Cells have innate abilities to recover and regenerate, and it may be that we need to provide avenues for cells to do this, rather than trying to force them to do so.

Clinically relevant studies

As discussed, there is a great need for both pre-clinical (i.e., large animal) and long-term studies. At this point, the field of biomaterial research is overloaded with examples of what biomaterials may do in small animals, but future large animal studies are absolutely essential in order to determine whether or not biomaterial studies should proceed to clinical trials for human benefit. Researchers will need to make a collective effort to select the most promising material systems for the more costly pre-clinical studies. The underlying theme in biomaterial research is that these studies are being performed in order to improve human well-being. Therefore, it is highly recommended that the field proceed in this direction so that afflicted patients will benefit from these therapies sooner rather than later.

List of References

Abdel-Latif, A., Bolli, R., Tleyjeh, I.M., Montori, V.M., Perin, E.C., Hornung, C.A., Zuba-Surma, E.K., Al-Mallah, M., and Dawn, B. (2007). Adult bone marrow-derived cells for cardiac repair: a systematic review and meta-analysis. Archives of internal medicine *167*, 989-997.

Aicher, A., Brenner, W., Zuhayra, M., Badorff, C., Massoudi, S., Assmus, B., Eckey, T., Henze, E., Zeiher, A.M., and Dimmeler, S. (2003). Assessment of the tissue distribution of transplanted human endothelial progenitor cells by radioactive labeling. Circulation *107*, 2134-2139.

Alavi, A., Hood, J.D., Frausto, R., Stupack, D.G., and Cheresh, D.A. (2003). Role of Raf in vascular protection from distinct apoptotic stimuli. Science (New York, NY *301*, 94-96.

Arnold, L., Henry, A., Poron, F., Baba-Amer, Y., van Rooijen, N., Plonquet, A., Gherardi, R.K., and Chazaud, B. (2007). Inflammatory monocytes recruited after skeletal muscle injury switch into antiinflammatory macrophages to support myogenesis. The Journal of experimental medicine *204*, 1057-1069.

Asahara, T., Masuda, H., Takahashi, T., Kalka, C., Pastore, C., Silver, M., Kearne, M., Magner, M., and Isner, J.M. (1999). Bone marrow origin of endothelial progenitor cells responsible for postnatal vasculogenesis in physiological and pathological neovascularization. Circulation research *85*, 221-228.

Askari, A.T., and Penn, M.S. (2003). Stromal cell-derived factor-1 mediates stem cell homing and tissue regeneration. Discov Med *3*, 46-47.

Askari, A.T., Unzek, S., Popovic, Z.B., Goldman, C.K., Forudi, F., Kiedrowski, M., Rovner, A., Ellis, S.G., Thomas, J.D., DiCorleto, P.E*., et al.* (2003). Effect of stromal-cell-derived factor 1 on stem-cell homing and tissue regeneration in ischaemic cardiomyopathy. Lancet *362*, 697-703.

Augst, A.D., Kong, H.J., and Mooney, D.J. (2006). Alginate hydrogels as biomaterials. Macromol Biosci *6*, 623-633.

Balciunas, M., Bagdonaite, L., Samalavicius, R., and Baublys, A. (2009). Markers of endothelial dysfunction after cardiac surgery: soluble forms of vascular-1 and intercellular-1 adhesion molecules. Medicina (Kaunas, Lithuania) *45*, 434-439.

Barallobre-Barreiro, J., Didangelos, A., Schoendube, F.A., Drozdov, I., Yin, X., Fernandez-Caggiano, M., Willeit, P., Puntmann, V.O., Aldama-Lopez, G., Shah, A.M*., et al.* (2012). Proteomics analysis of cardiac extracellular matrix remodeling in a porcine model of ischemia/reperfusion injury. Circulation *125*, 789-802.

Bayol, S., Loughna, P.T., and Brownson, C. (2000). Phenotypic expression of IGF binding protein transcripts in muscle, in vitro and in vivo. Biochemical and biophysical research communications *273*, 282-286.

Bayomy, A.F., Bauer, M., Qiu, Y., and Liao, R. (2012). Regeneration in heart disease-Is ECM the key? Life Sci *91*, 823-827.

Belch, J.J., Topol, E.J., Agnelli, G., Bertrand, M., Califf, R.M., Clement, D.L., Creager, M.A., Easton, J.D., Gavin, J.R., 3rd, Greenland, P.*, et al.* (2003). Critical issues in peripheral arterial disease detection and management: a call to action. Archives of internal medicine *163*, 884-892.

Bernal, A., San Martin, N., Fernandez, M., Covarello, D., Molla, F., Soldo, A., Latini, R., Cossu, G., and Galvez, B.G. (2011). L-selectin and SDF-1 enhance the migration of mouse and human cardiac mesoangioblasts. Cell Death Differ.

Biancone, L., Cantaluppi, V., Duo, D., Deregibus, M.C., Torre, C., and Camussi, G. (2004). Role of L-selectin in the vascular homing of peripheral blood-derived endothelial progenitor cells. J Immunol *173*, 5268-5274.

Blake, D.J., Weir, A., Newey, S.E., and Davies, K.E. (2002). Function and genetics of dystrophin and dystrophin-related proteins in muscle. Physiol Rev *82*, 291-329.

Bonaldo, P., and Sandri, M. (2013). Cellular and molecular mechanisms of muscle atrophy. Disease models & mechanisms *6*, 25-39.

Boodhwani, M., Voisine, P., Ruel, M., Sodha, N.R., Feng, J., Xu, S.H., Bianchi, C., and Sellke, F.W. (2008). Comparison of vascular endothelial growth factor and fibroblast growth factor-2 in a swine model of endothelial dysfunction. Eur J Cardiothorac Surg *33*, 645-650; discussion 251-642.

Borselli, C., Storrie, H., Benesch-Lee, F., Shvartsman, D., Cezar, C., Lichtman, J.W., Vandenburgh, H.H., and Mooney, D.J. (2010). Functional muscle regeneration with combined delivery of angiogenesis and myogenesis factors. Proceedings of the National Academy of Sciences of the United States of America *107*, 3287-3292.

Boudoulas, K.D., and Hatzopoulos, A.K. (2009). Cardiac repair and regeneration: the Rubik's cube of cell therapy for heart disease. Disease models & mechanisms *2*, 344-358.

Bourne, D. (2002). Pharmacokinetics. Banker GS, Rhodes CT, Modern Pharmaceuticals, 4th ed, Marcel Dekker Inc, New York, pp67-92.

Buckingham, M. (2007). Skeletal muscle progenitor cells and the role of Pax genes. C R Biol *330*, 530-533.

Cadee, J.A., de Groot, C.J., Jiskoot, W., den Otter, W., and Hennink, W.E. (2002). Release of recombinant human interleukin-2 from dextran-based hydrogels. J Control Release *78*, 1-13.

Cai, S., Liu, Y., Zheng Shu, X., and Prestwich, G.D. (2005). Injectable glycosaminoglycan hydrogels for controlled release of human basic fibroblast growth factor. Biomaterials *26*, 6054-6067.

Carosio, S., Barberi, L., Rizzuto, E., Nicoletti, C., Prete, Z.D., and Musaro, A. (2013). Generation of eX vivo-vascularized Muscle Engineered Tissue (X-MET). Sci Rep *3*, 1420.

Carosio, S., Berardinelli, M.G., Aucello, M., and Musaro, A. (2011). Impact of ageing on muscle cell regeneration. Ageing Res Rev *10*, 35-42.

Chazaud, B., Sonnet, C., Lafuste, P., Bassez, G., Rimaniol, A.C., Poron, F., Authier, F.J., Dreyfus, P.A., and Gherardi, R.K. (2003). Satellite cells attract monocytes and use macrophages as a support to escape apoptosis and enhance muscle growth. The Journal of cell biology *163*, 1133-1143.

Chen, F.M., Zhang, M., and Wu, Z.F. (2010). Toward delivery of multiple growth factors in tissue engineering. Biomaterials *31*, 6279-6308.

Cho, H.J., Lee, N., Lee, J.Y., Choi, Y.J., Ii, M., Wecker, A., Jeong, J.O., Curry, C., Qin, G., and Yoon, Y.S. (2007). Role of host tissues for sustained humoral effects after endothelial progenitor cell transplantation into the ischemic heart. The Journal of experimental medicine *204*, 3257-3269.

Cleland, J.G., Freemantle, N., Coletta, A.P., and Clark, A.L. (2006). Clinical trials update from the American Heart Association: REPAIR-AMI, ASTAMI, JELIS, MEGA, REVIVE-II, SURVIVE, and PROACTIVE. Eur J Heart Fail *8*, 105-110.

Conboy, I.M., and Rando, T.A. (2002). The regulation of Notch signaling controls satellite cell activation and cell fate determination in postnatal myogenesis. Dev Cell *3*, 397-409.

Corti, S., Nizzardo, M., Nardini, M., Donadoni, C., Salani, S., Ronchi, D., Simone, C., Falcone, M., Papadimitriou, D., Locatelli, F.*, et al.* (2010). Embryonic stem cell-derived neural stem cells improve spinal muscular atrophy phenotype in mice. Brain *133*, 465-481.

Culver, J.C., Hoffmann, J.C., Poche, R.A., Slater, J.H., West, J.L., and Dickinson, M.E. (2012). Three-dimensional biomimetic patterning in hydrogels to guide cellular organization. Adv Mater *24*, 2344-2348.

Dai, T., Zheng, H., and Fu, G. (2008). Hypoxia confers protection against apoptosis via the PI3K/Akt pathway in endothelial progenitor cells. Acta Pharmacologica Sinica *29*, 1425-1431.

Daley, W.P., Peters, S.B., and Larsen, M. (2008). Extracellular matrix dynamics in development and regenerative medicine. Journal of cell science *121*, 255-264.

De Falco, E., Porcelli, D., Torella, A.R., Straino, S., Iachininoto, M.G., Orlandi, A., Truffa, S., Biglioli, P., Napolitano, M., Capogrossi, M.C.*, et al.* (2004). SDF-1 involvement in

endothelial phenotype and ischemia-induced recruitment of bone marrow progenitor cells. Blood *104*, 3472-3482.

Deasy, B.M., Feduska, J.M., Payne, T.R., Li, Y., Ambrosio, F., and Huard, J. (2009). Effect of VEGF on the regenerative capacity of muscle stem cells in dystrophic skeletal muscle. Mol Ther *17*, 1788-1798.

Deasy, B.M., Qu-Peterson, Z., Greenberger, J.S., and Huard, J. (2002). Mechanisms of muscle stem cell expansion with cytokines. Stem cells (Dayton, Ohio) *20*, 50-60.

Decary, S., Hamida, C.B., Mouly, V., Barbet, J.P., Hentati, F., and Butler-Browne, G.S. (2000). Shorter telomeres in dystrophic muscle consistent with extensive regeneration in young children. Neuromuscul Disord *10*, 113-120.

Dehne, N., Kerkweg, U., Flohe, S.B., Brune, B., and Fandrey, J. (2011). Activation of hypoxia-inducible factor 1 in skeletal muscle cells after exposure to damaged muscle cell debris. Shock (Augusta, Ga *35*, 632-638.

Del Prete, Z., Musaro, A., and Rizzuto, E. (2008). Measuring mechanical properties, including isotonic fatigue, of fast and slow MLC/mIgf-1 transgenic skeletal muscle. Ann Biomed Eng *36*, 1281-1290.

Delewi, R., Andriessen, A., Tijssen, J.G., Zijlstra, F., Piek, J.J., and Hirsch, A. (2013). Impact of intracoronary cell therapy on left ventricular function in the setting of acute myocardial infarction: a meta-analysis of randomised controlled clinical trials. Heart *99*, 225-232.

Deng, C., Zhang, P., Vulesevic, B., Kuraitis, D., Li, F., Yang, A.F., Griffith, M., Ruel, M., and Suuronen, E.J. A collagen-chitosan hydrogel for endothelial differentiation and angiogenesis. Tissue engineering *16*, 3099-3109.

Deng, C., Zhang, P., Vulesevic, B., Kuraitis, D., Li, F., Yang, A.F., Griffith, M., Ruel, M., and Suuronen, E.J. (2010). A collagen-chitosan hydrogel for endothelial differentiation and angiogenesis. Tissue engineering *16*, 3099-3109.

Deng, M., Chen, W.L., Takatori, A., Peng, Z., Zhang, L., Mongan, M., Parthasarathy, R., Sartor, M., Miller, M., Yang, J.*, et al.* (2006). A role for the mitogen-activated protein kinase kinase kinase 1 in epithelial wound healing. Molecular biology of the cell *17*, 3446-3455.

Derkaoui, S.M., Labbe, A., Purnama, A., Gueguen, V., Barbaud, C., Avramoglou, T., and Letourneur, D. (2010). Films of dextran-graft-polybutylmethacrylate to enhance endothelialization of materials. Acta biomaterialia *6*, 3506-3513.

Devaraj, S., and Jialal, I. (2012). Dysfunctional endothelial progenitor cells in metabolic syndrome. Exp Diabetes Res *2012*, 585018.

Di Santo, S., Yang, Z., Wyler von Ballmoos, M., Voelzmann, J., Diehm, N., Baumgartner, I., and Kalka, C. (2009). Novel cell-free strategy for therapeutic angiogenesis: in vitro generated conditioned medium can replace progenitor cell transplantation. PloS one *4*, e5643.

Dimmeler, S., Burchfield, J., and Zeiher, A.M. (2008). Cell-based therapy of myocardial infarction. Arteriosclerosis, thrombosis, and vascular biology *28*, 208-216.

Dobrowolny, G., Aucello, M., Rizzuto, E., Beccafico, S., Mammucari, C., Boncompagni, S., Belia, S., Wannenes, F., Nicoletti, C., Del Prete, Z*., et al.* (2008). Skeletal muscle is a primary target of SOD1G93A-mediated toxicity. Cell Metab *8*, 425-436.

Donalies, M., Cramer, M., Ringwald, M., and Starzinski-Powitz, A. (1991). Expression of M-cadherin, a member of the cadherin multigene family, correlates with differentiation of skeletal muscle cells. Proceedings of the National Academy of Sciences of the United States of America *88*, 8024-8028.

Duan, C., Ren, H., and Gao, S. (2010). Insulin-like growth factors (IGFs), IGF receptors, and IGF-binding proteins: roles in skeletal muscle growth and differentiation. Gen Comp Endocrinol *167*, 344-351.

Dupuis, L., and Echaniz-Laguna, A. (2010). Skeletal muscle in motor neuron diseases: therapeutic target and delivery route for potential treatments. Curr Drug Targets *11*, 1250-1261.

Elliott, J.T., Woodward, J.T., Umarji, A., Mei, Y., and Tona, A. (2007). The effect of surface chemistry on the formation of thin films of native fibrillar collagen. Biomaterials *28*, 576-585.

Engler, A.J., Carag-Krieger, C., Johnson, C.P., Raab, M., Tang, H.Y., Speicher, D.W., Sanger, J.W., Sanger, J.M., and Discher, D.E. (2008). Embryonic cardiomyocytes beat best on a matrix with heart-like elasticity: scar-like rigidity inhibits beating. Journal of cell science *121*, 3794-3802.

Engler, A.J., Griffin, M.A., Sen, S., Bonnemann, C.G., Sweeney, H.L., and Discher, D.E. (2004). Myotubes differentiate optimally on substrates with tissue-like stiffness: pathological implications for soft or stiff microenvironments. The Journal of cell biology *166*, 877-887.

Engler, A.J., Sen, S., Sweeney, H.L., and Discher, D.E. (2006). Matrix elasticity directs stem cell lineage specification. Cell *126*, 677-689.

Engler, A.J., Sweeney, H.L., Discher, D.E., and Schwarzbauer, J.E. (2007). Extracellular matrix elasticity directs stem cell differentiation. J Musculoskelet Neuronal Interact *7*, 335.

Esposito, A., Germinario, E., Zanin, M., Palade, P.T., Betto, R., and Danieli-Betto, D. (2007). Isoform switching in myofibrillar and excitation-contraction coupling proteins contributes to diminished contractile function in regenerating rat soleus muscle. J Appl Physiol *102*, 1640-1648.

Ewton, D.Z., Coolican, S.A., Mohan, S., Chernausek, S.D., and Florini, J.R. (1998). Modulation of insulin-like growth factor actions in L6A1 myoblasts by insulin-like growth factor binding protein (IGFBP)-4 and IGFBP-5: a dual role for IGFBP-5. J Cell Physiol *177*, 47-57.

Fagerholm, P., Lagali, N.S., Carlsson, D.J., Merrett, K., and Griffith, M. (2009). Corneal regeneration following implantation of a biomimetic tissue-engineered substitute. Clin Transl Sci *2*, 162-164.

Fagerholm, P., Lagali, N.S., Merrett, K., Jackson, W.B., Munger, R., Liu, Y., Polarek, J.W., Soderqvist, M., and Griffith, M. (2010). A biosynthetic alternative to human donor tissue for inducing corneal regeneration: 24-month follow-up of a phase 1 clinical study. Sci Transl Med *2*, 46ra61.

Fan, Y., Maley, M., Beilharz, M., and Grounds, M. (1996). Rapid death of injected myoblasts in myoblast transfer therapy. Muscle Nerve *19*, 853-860.

Fazel, S., Cimini, M., Chen, L., Li, S., Angoulvant, D., Fedak, P., Verma, S., Weisel, R.D., Keating, A., and Li, R.K. (2006). Cardioprotective c-kit+ cells are from the bone marrow and regulate the myocardial balance of angiogenic cytokines. The Journal of clinical investigation *116*, 1865-1877.

Ferreira, J.C., Bacurau, A.V., Evangelista, F.S., Coelho, M.A., Oliveira, E.M., Casarini, D.E., Krieger, J.E., and Brum, P.C. (2008). The role of local and systemic renin angiotensin system activation in a genetic model of sympathetic hyperactivity-induced heart failure in mice. Am J Physiol Regul Integr Comp Physiol *294*, R26-32.

Formigli, L., Perna, A.M., Meacci, E., Cinci, L., Margheri, M., Nistri, S., Tani, A., Silvertown, J., Orlandini, G., Porciani, C.*, et al.* (2007). Paracrine effects of transplanted myoblasts and relaxin on post-infarction heart remodelling. Journal of cellular and molecular medicine *11*, 1087-1100.

Frangogiannis, N.G., Mendoza, L.H., Lindsey, M.L., Ballantyne, C.M., Michael, L.H., Smith, C.W., and Entman, M.L. (2000). IL-10 is induced in the reperfused myocardium and may modulate the reaction to injury. J Immunol *165*, 2798-2808.

Fujio, Y., and Walsh, K. (1999). Akt mediates cytoprotection of endothelial cells by vascular endothelial growth factor in an anchorage-dependent manner. The Journal of biological chemistry *274*, 16349-16354.

Fukushima, S., Varela-Carver, A., Coppen, S.R., Yamahara, K., Felkin, L.E., Lee, J., Barton, P.J., Terracciano, C.M., Yacoub, M.H., and Suzuki, K. (2007). Direct intramyocardial but not intracoronary injection of bone marrow cells induces ventricular arrhythmias in a rat chronic ischemic heart failure model. Circulation *115*, 2254-2261.

Gagnon, E., Cattaruzzi, P., Griffith, M., Muzakare, L., LeFlao, K., Faure, R., Beliveau, R., Hussain, S.N., Koutsilieris, M., and Doillon, C.J. (2002). Human vascular endothelial cells

with extended life spans: in vitro cell response, protein expression, and angiogenesis. Angiogenesis *5*, 21-33.

Gayraud-Morel, B., Chretien, F., Flamant, P., Gomes, D., Zammit, P.S., and Tajbakhsh, S. (2007). A role for the myogenic determination gene Myf5 in adult regenerative myogenesis. Dev Biol *312*, 13-28.

Gilbert, P.M., Havenstrite, K.L., Magnusson, K.E., Sacco, A., Leonardi, N.A., Kraft, P., Nguyen, N.K., Thrun, S., Lutolf, M.P., and Blau, H.M. (2010). Substrate elasticity regulates skeletal muscle stem cell self-renewal in culture. Science (New York, NY *329*, 1078-1081.

Gillis, J.M. (1999). Understanding dystrophinopathies: an inventory of the structural and functional consequences of the absence of dystrophin in muscles of the mdx mouse. J Muscle Res Cell Motil *20*, 605-625.

Gnecchi, M., He, H., Noiseux, N., Liang, O.D., Zhang, L., Morello, F., Mu, H., Melo, L.G., Pratt, R.E., Ingwall, J.S.*, et al.* (2006). Evidence supporting paracrine hypothesis for Akt-modified mesenchymal stem cell-mediated cardiac protection and functional improvement. Faseb J *20*, 661-669.

Gnecchi, M., Zhang, Z., Ni, A., and Dzau, V.J. (2008). Paracrine mechanisms in adult stem cell signaling and therapy. Circulation research *103*, 1204-1219.

Grounds, M.D. (2008a). Complexity of Extracellular Matrix and Skeletal Muscle Regeneration. In Skeletal Muscle Repair and Regeneration, S. Schiaffino, and T. Patridge, eds. (Springer), pp. 269-301.

Grounds, M.D. (2008b). Two-tiered hypotheses for Duchenne muscular dystrophy. Cell Mol Life Sci *65*, 1621-1625.

Guan, K., Rohwedel, J., and Wobus, A.M. (1999). Embryonic stem cell differentiation models: cardiogenesis, myogenesis, neurogenesis, epithelial and vascular smooth muscle cell differentiation in vitro. Cytotechnology *30*, 211-226.

Hadjiioannou, T.P., Christian, G.D., Koupparis, M.A., and Macheras, P.E. (1993). Quantitative Calculations in Pharmaceutical Practice and Research. VCH Publishers Inc, New York, pp345-348.

Hayward, R., Nossuli, T.O., Scalia, R., and Lefer, A.M. (1997). Cardioprotective effect of interleukin-10 in murine myocardial ischemia-reperfusion. Eur J Pharmacol *334*, 157-163.

Hibino, N., Yi, T., Duncan, D.R., Rathore, A., Dean, E., Naito, Y., Dardik, A., Kyriakides, T., Madri, J., Pober, J.S.*, et al.* (2011). A critical role for macrophages in neovessel formation and the development of stenosis in tissue-engineered vascular grafts. Faseb J *25*, 4253-4263.

Higuchi, T. (1963). Mechanism of Sustained-Action Medication. Theoretical Analysis of Rate of Release of Solid Drugs Dispersed in Solid Matrices. J Pharm Sci *52*, 1145-1149.

Hixson, A.W., and Crowell, J.H. (1931). Dependence of reaction velocity upon surface and agitation (I) theoretical consideration. Ind Eng Chem *23*, 923-931.

Hoffmann, J.C., and West, J.L. (2010). Three-dimensional photolithographic patterning of multiple bioactive ligands in poly(ethylene glycol) hydrogels
. Soft Matter.

Hoffmann, J.C., and West, J.L. (2013). Three-dimensional photolithographic micropatterning: a novel tool to probe the complexities of cell migration. Integr Biol (Camb).

Hofmann, M., Wollert, K.C., Meyer, G.P., Menke, A., Arseniev, L., Hertenstein, B., Ganser, A., Knapp, W.H., and Drexler, H. (2005). Monitoring of bone marrow cell homing into the infarcted human myocardium. Circulation *111*, 2198-2202.

Horsley, V., Jansen, K.M., Mills, S.T., and Pavlath, G.K. (2003). IL-4 acts as a myoblast recruitment factor during mammalian muscle growth. Cell *113*, 483-494.

Horst, D., Ustanina, S., Sergi, C., Mikuz, G., Juergens, H., Braun, T., and Vorobyov, E. (2006). Comparative expression analysis of Pax3 and Pax7 during mouse myogenesis. Int J Dev Biol *50*, 47-54.

Hosseinkhani, H., Hosseinkhani, M., Khademhosseini, A., Kobayashi, H., and Tabata, Y. (2006). Enhanced angiogenesis through controlled release of basic fibroblast growth factor from peptide amphiphile for tissue regeneration. Biomaterials *27*, 5836-5844.

Hristov, M., and Weber, C. (2004). Endothelial progenitor cells: characterization, pathophysiology, and possible clinical relevance. Journal of cellular and molecular medicine *8*, 498-508.

Hu, X., Wang, J., Chen, J., Luo, R., He, A., Xie, X., and Li, J. (2007). Optimal temporal delivery of bone marrow mesenchymal stem cells in rats with myocardial infarction. Eur J Cardiothorac Surg *31*, 438-443.

Huard, J., Roy, R., Bouchard, J.P., Malouin, F., Richards, C.L., and Tremblay, J.P. (1992). Human myoblast transplantation between immunohistocompatible donors and recipients produces immune reactions. Transplant Proc *24*, 3049-3051.

Huebsch, N., and Mooney, D.J. (2009). Inspiration and application in the evolution of biomaterials. Nature *462*, 426-432.

Hur, J., Yoon, C.H., Kim, H.S., Choi, J.H., Kang, H.J., Hwang, K.K., Oh, B.H., Lee, M.M., and Park, Y.B. (2004). Characterization of two types of endothelial progenitor cells and their different contributions to neovasculogenesis. Arteriosclerosis, thrombosis, and vascular biology *24*, 288-293.

Hur, J., Yoon, C.H., Lee, C.S., Kim, T.Y., Oh, I.Y., Park, K.W., Kim, J.H., Lee, H.S., Kang, H.J., Chae, I.H.*, et al.* (2007). Akt is a key modulator of endothelial progenitor cell trafficking in ischemic muscle. Stem cells (Dayton, Ohio) *25*, 1769-1778.

Hutter, H., Vogel, B.E., Plenefisch, J.D., Norris, C.R., Proenca, R.B., Spieth, J., Guo, C., Mastwal, S., Zhu, X., Scheel, J.*, et al.* (2000). Conservation and novelty in the evolution of cell adhesion and extracellular matrix genes. Science (New York, NY *287*, 989-994.

Hwang, M.W., Matsumori, A., Furukawa, Y., Ono, K., Okada, M., Iwasaki, A., Hara, M., Miyamoto, T., Touma, M., and Sasayama, S. (2001). Neutralization of interleukin-1beta in the acute phase of myocardial infarction promotes the progression of left ventricular remodeling. Journal of the American College of Cardiology *38*, 1546-1553.

Jaffe, R., and Strauss, B.H. (2007). Late and very late thrombosis of drug-eluting stents: evolving concepts and perspectives. Journal of the American College of Cardiology *50*, 119-127.

Jin, D.K., Shido, K., Kopp, H.G., Petit, I., Shmelkov, S.V., Young, L.M., Hooper, A.T., Amano, H., Avecilla, S.T., Heissig, B.*, et al.* (2006). Cytokine-mediated deployment of SDF-1 induces revascularization through recruitment of CXCR4+ hemangiocytes. Nature medicine *12*, 557-567.

Joseph-Silverstein, J., Consigli, S.A., Lyser, K.M., and Ver Pault, C. (1989). Basic fibroblast growth factor in the chick embryo: immunolocalization to striated muscle cells and their precursors. The Journal of cell biology *108*, 2459-2466.

Kalka, C., Masuda, H., Takahashi, T., Kalka-Moll, W.M., Silver, M., Kearney, M., Li, T., Isner, J.M., and Asahara, T. (2000). Transplantation of ex vivo expanded endothelial progenitor cells for therapeutic neovascularization. Proceedings of the National Academy of Sciences of the United States of America *97*, 3422-3427.

Kang, K., Sun, L., Xiao, Y., Li, S.H., Wu, J., Guo, J., Jiang, S.L., Yang, L., Yau, T.M., Weisel, R.D.*, et al.* (2012). Aged human cells rejuvenated by cytokine enhancement of biomaterials for surgical ventricular restoration. Journal of the American College of Cardiology *60*, 2237-2249.

Kaully, T., Kaufman-Francis, K., Lesman, A., and Levenberg, S. (2009). Vascularization--the conduit to viable engineered tissues. Tissue Eng Part B Rev *15*, 159-169.

Kawamoto, A., Gwon, H.C., Iwaguro, H., Yamaguchi, J.I., Uchida, S., Masuda, H., Silver, M., Ma, H., Kearney, M., Isner, J.M.*, et al.* (2001). Therapeutic potential of ex vivo expanded endothelial progenitor cells for myocardial ischemia. Circulation *103*, 634-637.

Kempen, D.H., Lu, L., Hefferan, T.E., Creemers, L.B., Maran, A., Classic, K.L., Dhert, W.J., and Yaszemski, M.J. (2008). Retention of in vitro and in vivo BMP-2 bioactivities in sustained delivery vehicles for bone tissue engineering. Biomaterials *29*, 3245-3252.

Kennedy, K.A., Porter, T., Mehta, V., Ryan, S.D., Price, F., Peshdary, V., Karamboulas, C., Savage, J., Drysdale, T.A., Li, S.C.*, et al.* (2009). Retinoic acid enhances skeletal muscle progenitor formation and bypasses inhibition by bone morphogenetic protein 4 but not dominant negative beta-catenin. BMC Biol *7*, 67.

Kharraz, Y., Guerra, J., Mann, C.J., Serrano, A.L., and Munoz-Canoves, P. (2013). Macrophage plasticity and the role of inflammation in skeletal muscle repair. Mediators Inflamm *2013*, 491497.

Kim, H.K., De La Luz Sierra, M., Williams, C.K., Gulino, A.V., and Tosato, G. (2006). G-CSF down-regulation of CXCR4 expression identified as a mechanism for mobilization of myeloid cells. Blood *108*, 812-820.

Kim, S.W., Kim, H., Cho, H.J., Lee, J.U., Levit, R., and Yoon, Y.S. Human peripheral blood-derived CD31+ cells have robust angiogenic and vasculogenic properties and are effective for treating ischemic vascular disease. Journal of the American College of Cardiology *56*, 593-607.

Kimura, Y., and Tabata, Y. Controlled release of stromal-cell-derived factor-1 from gelatin hydrogels enhances angiogenesis. Journal of biomaterials science *21*, 37-51.

Kimura, Y., and Tabata, Y. (2010). Controlled release of stromal-cell-derived factor-1 from gelatin hydrogels enhances angiogenesis. Journal of biomaterials science *21*, 37-51.

Klein, D., Hohn, H.P., Kleff, V., Tilki, D., and Ergun, S. (2010). Vascular wall-resident stem cells. Histol Histopathol *25*, 681-689.

Kloner, R.A., Fishbein, M.C., Lew, H., Maroko, P.R., and Braunwald, E. (1978). Mummification of the infarcted myocardium by high dose corticosteroids. Circulation *57*, 56-63.

Ko, H.C., Milthorpe, B.K., and McFarland, C.D. (2007). Engineering thick tissues--the vascularisation problem. European cells & materials *14*, 1-18; discussion 18-19.

Koffler, J., Kaufman-Francis, K., Yulia, S., Dana, E., Daria, A.P., Landesberg, A., and Levenberg, S. (2011). Improved vascular organization enhances functional integration of engineered skeletal muscle grafts. Proceedings of the National Academy of Sciences of the United States of America *108*, 14789-14794.

Koike, T., Vernon, R.B., Gooden, M.D., Sadoun, E., and Reed, M.J. (2003). Inhibited angiogenesis in aging: a role for TIMP-2. J Gerontol A Biol Sci Med Sci *58*, B798-805.

Korsmeyer, R.W., Gurny, R., Doelker, E., Buri, P., and Peppas, N.A. (1983). Mechanisms of solute release from porous hydrophilic polymers. Int J Pharm *15*, 25-35.

Kovanen, V. (2002). Intramuscular extracellular matrix: complex environment of muscle cells. Exerc Sport Sci Rev *30*, 20-25.

Kroehne, V., Heschel, I., Schugner, F., Lasrich, D., Bartsch, J.W., and Jockusch, H. (2008). Use of a novel collagen matrix with oriented pore structure for muscle cell differentiation in cell culture and in grafts. Journal of cellular and molecular medicine *12*, 1640-1648.

Kuang, S., Charge, S.B., Seale, P., Huh, M., and Rudnicki, M.A. (2006). Distinct roles for Pax7 and Pax3 in adult regenerative myogenesis. The Journal of cell biology *172*, 103-113.

Kuang, S., Kuroda, K., Le Grand, F., and Rudnicki, M.A. (2007). Asymmetric self-renewal and commitment of satellite stem cells in muscle. Cell *129*, 999-1010.

Kucia, M., Ratajczak, J., Reca, R., Janowska-Wieczorek, A., and Ratajczak, M.Z. (2004). Tissue-specific muscle, neural and liver stem/progenitor cells reside in the bone marrow, respond to an SDF-1 gradient and are mobilized into peripheral blood during stress and tissue injury. Blood Cells Mol Dis *32*, 52-57.

Kuraitis, D., Arzhangi, Z., Hyatt, A.J., Vulesevic, B., Merrett, K., Zhang, J., Suuronen, E., and Griffith, M. (2012a). Tertiary biomaterial encapsulation controls the release of FGF-2 witout impacting bioactivity. Open Tiss Eng Regen Med J *5*, 43-49.

Kuraitis, D., Ebadi, D., Zhang, P., Rizzuto, E., Vulesevic, B., Padavan, D.T., Al Madhoun, A., McEwan, K.A., Sofrenovic, T., Nicholson, K.*, et al.* (2012b). Injected matrix stimulates myogenesis and regeneration of mouse skeletal muscle after ischaemic injury. European cells & materials *24*, 175-196.

Kuraitis, D., Giordano, C., Ruel, M., Musaro, A., and Suuronen, E.J. (2012c). Exploiting extracellular matrix-stem cell interactions: a review of natural materials for therapeutic muscle regeneration. Biomaterials *33*, 428-443.

Kuraitis, D., Hou, C., Zhang, Y., Vulesevic, B., Sofrenovic, T., McKee, D., Sharif, Z., Ruel, M., and Suuronen, E.J. (2011a). Ex vivo generation of a highly potent population of circulating angiogenic cells using a collagen matrix. Journal of molecular and cellular cardiology.

Kuraitis, D., Zhang, P., Zhang, Y., Padavan, D.T., McEwan, K., Sofrenovic, T., McKee, D., Zhang, J., Griffith, M., Cao, X.*, et al.* (2011b). A stromal cell-derived factor-1 releasing matrix enhances the progenitor cell response and blood vessel growth in ischaemic skeletal muscle. European cells & materials *22*, 109-123.

Kurtz, A., and Oh, S.J. (2012). Age related changes of the extracellular matrix and stem cell maintenance. Prev Med *54 Suppl*, S50-56.

Kutschka, I., Chen, I.Y., Kofidis, T., Arai, T., von Degenfeld, G., Sheikh, A.Y., Hendry, S.L., Pearl, J., Hoyt, G., Sista, R.*, et al.* (2006). Collagen matrices enhance survival of transplanted cardiomyoblasts and contribute to functional improvement of ischemic rat hearts. Circulation *114*, I167-173.

Labat-Robert, J., and Robert, L. (1988). Aging of the extracellular matrix and its pathology. Exp Gerontol *23*, 5-18.

Lanasa, S.M., and Bryant, S.J. (2009). Influence of ECM proteins and their analogs on cells cultured on 2-D hydrogels for cardiac muscle tissue engineering. Acta biomaterialia.

Le Grand, F., and Rudnicki, M.A. (2007). Skeletal muscle satellite cells and adult myogenesis. Current opinion in cell biology *19*, 628-633.

Li, Q., Li, B., Wang, X., Leri, A., Jana, K.P., Liu, Y., Kajstura, J., Baserga, R., and Anversa, P. (1997). Overexpression of insulin-like growth factor-1 in mice protects from myocyte death after infarction, attenuating ventricular dilation, wall stress, and cardiac hypertrophy. The Journal of clinical investigation *100*, 1991-1999.

Li, S.H., Lai, T.Y., Sun, Z., Han, M., Moriyama, E., Wilson, B., Fazel, S., Weisel, R.D., Yau, T., Wu, J.C.*, et al.* (2009). Tracking cardiac engraftment and distribution of implanted bone marrow cells: Comparing intra-aortic, intravenous, and intramyocardial delivery. The Journal of thoracic and cardiovascular surgery *137*, 1225-1233 e1221.

Li, Z., Liu, H.Y., Lei, Q.F., Zhang, C., and Li, S.N. (2011). Improved motor function in dko mice by intravenous transplantation of bone marrow-derived mesenchymal stromal cells. Cytotherapy *13*, 69-77.

Limbourg, A., Korff, T., Napp, L.C., Schaper, W., Drexler, H., and Limbourg, F.P. (2009). Evaluation of postnatal arteriogenesis and angiogenesis in a mouse model of hind-limb ischemia. Nature protocols *4*, 1737-1746.

Liu, W., Griffith, M., and Li, F. (2008). Alginate microsphere-collagen composite hydrogel for ocular drug delivery and implantation. Journal of materials science *19*, 3365-3371.

Liu, Y., Chu, A., Chakroun, I., Islam, U., and Blais, A. (2010). Cooperation between myogenic regulatory factors and SIX family transcription factors is important for myoblast differentiation. Nucleic Acids Res *38*, 6857-6871.

Livak, K.J., and Schmittgen, T.D. (2001). Analysis of relative gene expression data using real-time quantitative PCR and the 2(-Delta Delta C(T)) Method. Methods *25*, 402-408.

Lu, S., Lu, C., Han, Q., Li, J., Du, Z., Liao, L., and Zhao, R.C. Adipose-derived mesenchymal stem cells protect PC12 cells from glutamate excitotoxicity-induced apoptosis by upregulation of XIAP through PI3-K/Akt activation. Toxicology *279*, 189-195.

Lutolf, M.P., Gilbert, P.M., and Blau, H.M. (2009). Designing materials to direct stem-cell fate. Nature *462*, 433-441.

Mangi, A.A., Noiseux, N., Kong, D., He, H., Rezvani, M., Ingwall, J.S., and Dzau, V.J. (2003). Mesenchymal stem cells modified with Akt prevent remodeling and restore performance of infarcted hearts. Nature medicine *9*, 1195-1201.

Martignoni, M., Groothuis, G.M., and de Kanter, R. (2006). Species differences between mouse, rat, dog, monkey and human CYP-mediated drug metabolism, inhibition and induction. Expert Opin Drug Metab Toxicol *2*, 875-894.

Martin, T.A., Watkins, G., Lane, J., and Jiang, W.G. (2005). Assessing microvessels and angiogenesis in human breast cancer, using VE-cadherin. Histopathology *46*, 422-430.

Martin-Rendon, E., Brunskill, S.J., Hyde, C.J., Stanworth, S.J., Mathur, A., and Watt, S.M. (2008). Autologous bone marrow stem cells to treat acute myocardial infarction: a systematic review. European heart journal *29*, 1807-1818.

McEwan, K., Padavan, D.T., Deng, C., Vulesevic, B., Kuraitis, D., Korbutt, G.S., and Suuronen, E.J. (2012). Tunable Collagen Hydrogels are Modified by the Therapeutic Agents They are Designed to Deliver. Journal of biomaterials science *23*, 1467-1843.

McGeachie, J.K., and Grounds, M.D. (1987). Initiation and duration of muscle precursor replication after mild and severe injury to skeletal muscle of mice. An autoradiographic study. Cell and tissue research *248*, 125-130.

Mestas, J., and Hughes, C.C. (2004). Of mice and not men: differences between mouse and human immunology. J Immunol *172*, 2731-2738.

Metallo, C.M., Mohr, J.C., Detzel, C.J., de Pablo, J.J., Van Wie, B.J., and Palecek, S.P. (2007). Engineering the stem cell microenvironment. Biotechnology progress *23*, 18-23.

Miller, R.J., Banisadr, G., and Bhattacharyya, B.J. (2008). CXCR4 signaling in the regulation of stem cell migration and development. J Neuroimmunol *198*, 31-38.

Millon, L.E., Oates, C.J., and Wan, W. (2009). Compression properties of polyvinyl alcohol--bacterial cellulose nanocomposite. J Biomed Mater Res B Appl Biomater *90*, 922-929.

Mirza, R., DiPietro, L.A., and Koh, T.J. (2009). Selective and specific macrophage ablation is detrimental to wound healing in mice. The American journal of pathology *175*, 2454-2462.

Misiak-Tloczek, A., and Brzezinska-Blaszczyk, E. (2009). IL-6, but not IL-4, stimulates chemokinesis and TNF stimulates chemotaxis of tissue mast cells: involvement of both mitogen-activated protein kinases and phosphatidylinositol 3-kinase signalling pathways. APMIS *117*, 558-567.

Mitchell, P.O., and Pavlath, G.K. (2004). Skeletal muscle atrophy leads to loss and dysfunction of muscle precursor cells. American journal of physiology *287*, C1753-1762.

Mitra, T., Sailakshmi, G., Gnanamani, A., Raja, S.T., Thiruselvi, T., Gowri, V.M., Selvaraj, N.V., Ramesh, G., and Mandal, A.B. Preparation and characterization of a thermostable and biodegradable biopolymers using natural cross-linker. International journal of biological macromolecules.

Modulevsky, D.J., Tremblay, D., Gullekson, C., Bukoresthliev, N.V., and Pelling, A.E. (2012). The physical interaction of myoblasts with the microenvironment during remodeling of the cytoarchitecture. PloS one *7*, e45329.

Mogi, M., Walsh, K., Iwai, M., and Horiuchi, M. (2008). Akt-FOXO3a signaling affects human endothelial progenitor cell differentiation. Hypertens Res *31*, 153-159.

Montarras, D., Morgan, J., Collins, C., Relaix, F., Zaffran, S., Cumano, A., Partridge, T., and Buckingham, M. (2005). Direct isolation of satellite cells for skeletal muscle regeneration. Science *309*, 2064-2067.

Morales-Ruiz, M., Fulton, D., Sowa, G., Languino, L.R., Fujio, Y., Walsh, K., and Sessa, W.C. (2000). Vascular endothelial growth factor-stimulated actin reorganization and migration of endothelial cells is regulated via the serine/threonine kinase Akt. Circulation research *86*, 892-896.

Muller, A.L., Hryshko, L.V., and Dhalla, N.S. (2013). Extracellular and intracellular proteases in cardiac dysfunction due to ischemia-reperfusion injury. Int J Cardiol *164*, 39-47.

Murohara, T., Ikeda, H., Duan, J., Shintani, S., Sasaki, K., Eguchi, H., Onitsuka, I., Matsui, K., and Imaizumi, T. (2000). Transplanted cord blood-derived endothelial precursor cells augment postnatal neovascularization. The Journal of clinical investigation *105*, 1527-1536.

Murry, C.E., Reinecke, H., and Pabon, L.M. (2006). Regeneration gaps: observations on stem cells and cardiac repair. Journal of the American College of Cardiology *47*, 1777-1785.

Musaro, A., and Barberi, L. (2010). Isolation and Culture of Mouse Satellite Cells. In Methods in Molecular Biology, A. Ward, and D. Tosh, eds. (Springer).

Musaro, A., and Rosenthal, N. (1999). Maturation of the myogenic program is induced by postmitotic expression of insulin-like growth factor I. Mol Cell Biol *19*, 3115-3124.

Nabeshima, Y., Hanaoka, K., Hayasaka, M., Esumi, E., Li, S., and Nonaka, I. (1993). Myogenin gene disruption results in perinatal lethality because of severe muscle defect. Nature *364*, 532-535.

Nagaraju, K., Raben, N., Merritt, G., Loeffler, L., Kirk, K., and Plotz, P. (1998). A variety of cytokines and immunologically relevant surface molecules are expressed by normal human skeletal muscle cells under proinflammatory stimuli. Clin Exp Immunol *113*, 407-414.

Ning, Y., Schuller, A.G., Bradshaw, S., Rotwein, P., Ludwig, T., Frystyk, J., and Pintar, J.E. (2006). Diminished growth and enhanced glucose metabolism in triple knockout mice containing mutations of insulin-like growth factor binding protein-3, -4, and -5. Mol Endocrinol *20*, 2173-2186.

Nossner, E., and Parham, P. (1995). Species-specific differences in chaperone interaction of human and mouse major histocompatibility complex class I molecules. The Journal of experimental medicine *181*, 327-337.

Parise, G., O'Reilly, C.E., and Rudnicki, M.A. (2006). Molecular regulation of myogenic progenitor populations. Appl Physiol Nutr Metab *31*, 773-781.

Park, S., Tepper, O.M., Galiano, R.D., Capla, J.M., Baharestani, S., Kleinman, M.E., Pelo, C.R., Levine, J.P., and Gurtner, G.C. (2004). Selective recruitment of endothelial progenitor

cells to ischemic tissues with increased neovascularization. Plastic and reconstructive surgery *113*, 284-293.

Pasinelli, P., and Brown, R.H. (2006). Molecular biology of amyotrophic lateral sclerosis: insights from genetics. Nat Rev Neurosci *7*, 710-723.

Pelosi, L., Giacinti, C., Nardis, C., Borsellino, G., Rizzuto, E., Nicoletti, C., Wannenes, F., Battistini, L., Rosenthal, N., Molinaro, M.*, et al.* (2007). Local expression of IGF-1 accelerates muscle regeneration by rapidly modulating inflammatory cytokines and chemokines. FASEB J *21*, 1393-1402.

Podbregar, M., Lainscak, M., Prelovsek, O., and Mars, T. (2013). Cytokine response of cultured skeletal muscle cells stimulated with proinflammatory factors depends on differentiation stage. ScientificWorldJournal *2013*, 617170.

Pradat, P.F., Barani, A., Wanschitz, J., Dubourg, O., Lombes, A., Bigot, A., Mouly, V., Bruneteau, G., Salachas, F., Lenglet, T.*, et al.* (2011). Abnormalities of satellite cells function in amyotrophic lateral sclerosis. Amyotroph Lateral Scler *12*, 264-271.

Prater, D.N., Case, J., Ingram, D.A., and Yoder, M.C. (2007). Working hypothesis to redefine endothelial progenitor cells. Leukemia *21*, 1141-1149.

Querejeta, R., Lopez, B., Gonzalez, A., Sanchez, E., Larman, M., Martinez Ubago, J.L., and Diez, J. (2004). Increased collagen type I synthesis in patients with heart failure of hypertensive origin: relation to myocardial fibrosis. Circulation *110*, 1263-1268.

Rabbany, S.Y., Pastore, J., Yamamoto, M., Miller, T., Rafii, S., Aras, R., and Penn, M. Continuous delivery of stromal cell-derived factor-1 from alginate scaffolds accelerates wound healing. Cell transplantation *19*, 399-408.

Radisavljevic, Z., Avraham, H., and Avraham, S. (2000). Vascular endothelial growth factor up-regulates ICAM-1 expression via the phosphatidylinositol 3 OH-kinase/AKT/Nitric oxide pathway and modulates migration of brain microvascular endothelial cells. The Journal of biological chemistry *275*, 20770-20774.

Ratajczak, M.Z., Majka, M., Kucia, M., Drukala, J., Pietrzkowski, Z., Peiper, S., and Janowska-Wieczorek, A. (2003). Expression of functional CXCR4 by muscle satellite cells and secretion of SDF-1 by muscle-derived fibroblasts is associated with the presence of both muscle progenitors in bone marrow and hematopoietic stem/progenitor cells in muscles. Stem cells (Dayton, Ohio) *21*, 363-371.

Relaix, F., Montarras, D., Zaffran, S., Gayraud-Morel, B., Rocancourt, D., Tajbakhsh, S., Mansouri, A., Cumano, A., and Buckingham, M. (2006). Pax3 and Pax7 have distinct and overlapping functions in adult muscle progenitor cells. The Journal of cell biology *172*, 91-102.

Renault, V., Piron-Hamelin, G., Forestier, C., DiDonna, S., Decary, S., Hentati, F., Saillant, G., Butler-Browne, G.S., and Mouly, V. (2000). Skeletal muscle regeneration and the mitotic clock. Exp Gerontol *35*, 711-719.

Ridgeway, A.G., and Skerjanc, I.S. (2001). Pax3 is essential for skeletal myogenesis and the expression of Six1 and Eya2. J Biol Chem *276*, 19033-19039.

Rio, D.C., Ares, M., Hannon, G.J., and W., N.T. (2010). Purification of RNA using TRIzol (TRI reagent). Cold Spring Harbor protocols, prot 5439.

Robinson, M.J., and Cobb, M.H. (1997). Mitogen-activated protein kinase pathways. Current opinion in cell biology *9*, 180-186.

Rossi, C.A., Pozzobon, M., and De Coppi, P. (2010). Advances in musculoskeletal tissue engineering: moving towards therapy. Organogenesis *6*, 167-172.

Roy, S., Khanna, S., Kuhn, D.E., Rink, C., Williams, W.T., Zweier, J.L., and Sen, C.K. (2006). Transcriptome analysis of the ischemia-reperfused remodeling myocardium: temporal changes in inflammation and extracellular matrix. Physiological genomics *25*, 364-374.

Rudnicki, M.A., Schnegelsberg, P.N., Stead, R.H., Braun, T., Arnold, H.H., and Jaenisch, R. (1993). MyoD or Myf-5 is required for the formation of skeletal muscle. Cell *75*, 1351-1359.

Ruel, M., Song, J., and Sellke, F.W. (2004). Protein-, gene-, and cell-based therapeutic angiogenesis for the treatment of myocardial ischemia. Molecular and cellular biochemistry *264*, 119-131.

Ruel, M., Suuronen, E.J., Song, J., Kapila, V., Gunning, D., Waghray, G., Rubens, F.D., and Mesana, T.G. (2005). Effects of off-pump versus on-pump coronary artery bypass grafting on function and viability of circulating endothelial progenitor cells. The Journal of thoracic and cardiovascular surgery *130*, 633-639.

Ruvinov, E., Leor, J., and Cohen, S. The effects of controlled HGF delivery from an affinity-binding alginate biomaterial on angiogenesis and blood perfusion in a hindlimb ischemia model. Biomaterials *31*, 4573-4582.

Ruvinov, E., Leor, J., and Cohen, S. The promotion of myocardial repair by the sequential delivery of IGF-1 and HGF from an injectable alginate biomaterial in a model of acute myocardial infarction. Biomaterials *32*, 565-578.

Ruvinov, E., Leor, J., and Cohen, S. (2011). The promotion of myocardial repair by the sequential delivery of IGF-1 and HGF from an injectable alginate biomaterial in a model of acute myocardial infarction. Biomaterials *32*, 565-578.

Sabourin, L.A., and Rudnicki, M.A. (2000). The molecular regulation of myogenesis. Clin Genet *57*, 16-25.

Saif, J., Schwarz, T.M., Chau, D.Y., Henstock, J., Sami, P., Leicht, S.F., Hermann, P.C., Alcala, S., Mulero, F., Shakesheff, K.M.*, et al.* (2010). Combination of injectable multiple growth factor-releasing scaffolds and cell therapy as an advanced modality to enhance tissue neovascularization. Arteriosclerosis, thrombosis, and vascular biology *30*, 1897-1904.

San Antonio, J.D., and Iozzo, R.V. (2006). The two-phase model for angiogenesis regulation by the extracellular matrix. In Encyclopedia of the Microvasculature, D. Shepro, ed. (Burlington, Elsevier Academic Press), pp. 127-136.

Sandstedt, J., Jonsson, M., Lindahl, A., Jeppsson, A., and Asp, J. C-kit+ CD45- cells found in the adult human heart represent a population of endothelial progenitor cells. Basic research in cardiology *105*, 545-556.

Sato, K., Wu, T., Laham, R.J., Johnson, R.B., Douglas, P., Li, J., Sellke, F.W., Bunting, S., Simons, M., and Post, M.J. (2001). Efficacy of intracoronary or intravenous VEGF165 in a pig model of chronic myocardial ischemia. Journal of the American College of Cardiology *37*, 616-623.

Savage, J., Conley, A.J., Blais, A., and Skerjanc, I.S. (2009). SOX15 and SOX7 differentially regulate the myogenic program in P19 cells. Stem cells (Dayton, Ohio) *27*, 1231-1243.

Schatteman, G.C., Hanlon, H.D., Jiao, C., Dodds, S.G., and Christy, B.A. (2000). Blood-derived angioblasts accelerate blood-flow restoration in diabetic mice. The Journal of clinical investigation *106*, 571-578.

Seale, P., Ishibashi, J., Scime, A., and Rudnicki, M.A. (2004). Pax7 is necessary and sufficient for the myogenic specification of CD45+:Sca1+ stem cells from injured muscle. PLoS Biol *2*, E130.

Seeger, F.H., Rasper, T., Koyanagi, M., Fox, H., Zeiher, A.M., and Dimmeler, S. (2009). CXCR4 expression determines functional activity of bone marrow-derived mononuclear cells for therapeutic neovascularization in acute ischemia. Arteriosclerosis, thrombosis, and vascular biology *29*, 1802-1809.

Segawa, M., Fukada, S., Yamamoto, Y., Yahagi, H., Kanematsu, M., Sato, M., Ito, T., Uezumi, A., Hayashi, S., Miyagoe-Suzuki, Y.*, et al.* (2008). Suppression of macrophage functions impairs skeletal muscle regeneration with severe fibrosis. Experimental cell research *314*, 3232-3244.

Segers, V.F., Tokunou, T., Higgins, L.J., MacGillivray, C., Gannon, J., and Lee, R.T. (2007). Local delivery of protease-resistant stromal cell derived factor-1 for stem cell recruitment after myocardial infarction. Circulation *116*, 1683-1692.

Selvin, E., and Erlinger, T.P. (2004). Prevalence of and risk factors for peripheral arterial disease in the United States: results from the National Health and Nutrition Examination Survey, 1999-2000. Circulation *110*, 738-743.

Senger, D.R., Perruzzi, C.A., Streit, M., Koteliansky, V.E., de Fougerolles, A.R., and Detmar, M. (2002). The alpha(1)beta(1) and alpha(2)beta(1) integrins provide critical support for vascular endothelial growth factor signaling, endothelial cell migration, and tumor angiogenesis. The American journal of pathology *160*, 195-204.

Serrano, A.L., Baeza-Raja, B., Perdiguero, E., Jardi, M., and Munoz-Canoves, P. (2008). Interleukin-6 is an essential regulator of satellite cell-mediated skeletal muscle hypertrophy. Cell Metab *7*, 33-44.

Shamoun, F., Sural, N., and Abela, G. (2008). Peripheral artery disease: therapeutic advances. Expert Rev Cardiovasc Ther *6*, 539-553.

Sharma, G.D., He, J., and Bazan, H.E. (2003). p38 and ERK1/2 coordinate cellular migration and proliferation in epithelial wound healing: evidence of cross-talk activation between MAP kinase cascades. The Journal of biological chemistry *278*, 21989-21997.

Sheehan, S.M., and Allen, R.E. (1999). Skeletal muscle satellite cell proliferation in response to members of the fibroblast growth factor family and hepatocyte growth factor. J Cell Physiol *181*, 499-506.

Sheehan, S.M., Tatsumi, R., Temm-Grove, C.J., and Allen, R.E. (2000). HGF is an autocrine growth factor for skeletal muscle satellite cells in vitro. Muscle Nerve *23*, 239-245.

Shi, M., Ishikawa, M., Kamei, N., Nakasa, T., Adachi, N., Deie, M., Asahara, T., and Ochi, M. (2009). Acceleration of skeletal muscle regeneration in a rat skeletal muscle injury model by local injection of human peripheral blood-derived CD133-positive cells. Stem cells (Dayton, Ohio) *27*, 949-960.

Shireman, P.K., Contreras-Shannon, V., Ochoa, O., Karia, B.P., Michalek, J.E., and McManus, L.M. (2007). MCP-1 deficiency causes altered inflammation with impaired skeletal muscle regeneration. Journal of leukocyte biology *81*, 775-785.

Silvestri, M., Rasperini, G., and Milani, S. (2011). 120 infrabony defects treated with regenerative therapy: long-term results. J Periodontol *82*, 668-675.

Skyschally, A., Schulz, R., and Heusch, G. (2008). Pathophysiology of myocardial infarction: protection by ischemic pre- and postconditioning. Herz *33*, 88-100.

Sofrenovic, T., McEwan, K., Crowe, S., Marier, J., Davies, R., Suuronen, E.J., and Kuraitis, D. (2012). Circulating angiogenic cells can be derived from cryopreserved peripheral blood mononuclear cells. PloS one *7*, e48067.

Srinivasan, R., Zabuawala, T., Huang, H., Zhang, J., Gulati, P., Fernandez, S., Karlo, J.C., Landreth, G.E., Leone, G., and Ostrowski, M.C. (2009). Erk1 and Erk2 regulate endothelial cell proliferation and migration during mouse embryonic angiogenesis. PloS one *4*, e8283.

Srivastava, S.P., Kumar, K.U., and Kaufman, R.J. (1998). Phosphorylation of eukaryotic translation initiation factor 2 mediates apoptosis in response to activation of the double-

stranded RNA-dependent protein kinase. The Journal of biological chemistry *273*, 2416-2423.

Stern, M.M., Myers, R.L., Hammam, N., Stern, K.A., Eberli, D., Kritchevsky, S.B., Soker, S., and Van Dyke, M. (2009). The influence of extracellular matrix derived from skeletal muscle tissue on the proliferation and differentiation of myogenic progenitor cells ex vivo. Biomaterials *30*, 2393-2399.

Straub, V., and Campbell, K.P. (1997). Muscular dystrophies and the dystrophin-glycoprotein complex. Curr Opin Neurol *10*, 168-175.

Su, E.J., Cioffi, C.L., Stefansson, S., Mittereder, N., Garay, M., Hreniuk, D., and Liau, G. (2003). Gene therapy vector-mediated expression of insulin-like growth factors protects cardiomyocytes from apoptosis and enhances neovascularization. American journal of physiology *284*, H1429-1440.

Sun, D., Martinez, C.O., Ochoa, O., Ruiz-Willhite, L., Bonilla, J.R., Centonze, V.E., Waite, L.L., Michalek, J.E., McManus, L.M., and Shireman, P.K. (2009). Bone marrow-derived cell regulation of skeletal muscle regeneration. Faseb J *23*, 382-395.

Sun, Q., Silva, E.A., Wang, A., Fritton, J.C., Mooney, D.J., Schaffler, M.B., Grossman, P.M., and Rajagopalan, S. Sustained release of multiple growth factors from injectable polymeric system as a novel therapeutic approach towards angiogenesis. Pharmaceutical research *27*, 264-271.

Sutton, M.G., and Sharpe, N. (2000). Left ventricular remodeling after myocardial infarction: pathophysiology and therapy. Circulation *101*, 2981-2988.

Suuronen, E.J., Hazra, S., Zhang, P., Vincent, R., Kumarathasan, P., Zhang, Y., Price, J., Chan, V., Sellke, F.W., Mesana, T.G.*, et al.* Impairment of human cell-based vasculogenesis in rats by hypercholesterolemia-induced endothelial dysfunction and rescue with L-arginine supplementation. The Journal of thoracic and cardiovascular surgery *139*, 209-216 e202.

Suuronen, E.J., Kuraitis, D., and Ruel, M. (2008). Improving cell engraftment with tissue engineering. Seminars in thoracic and cardiovascular surgery *20*, 110-114.

Suuronen, E.J., Nakamura, M., Watsky, M.A., Stys, P.K., Muller, L.J., Munger, R., Shinozaki, N., and Griffith, M. (2004). Innervated human corneal equivalents as in vitro models for nerve-target cell interactions. Faseb J *18*, 170-172.

Suuronen, E.J., Price, J., Veinot, J.P., Ascah, K., Kapila, V., Guo, X.W., Wong, S., Mesana, T.G., and Ruel, M. (2007). Comparative effects of mesenchymal progenitor cells, endothelial progenitor cells, or their combination on myocardial infarct regeneration and cardiac function. The Journal of thoracic and cardiovascular surgery *134*, 1249-1258.

Suuronen, E.J., Veinot, J.P., Wong, S., Kapila, V., Price, J., Griffith, M., Mesana, T.G., and Ruel, M. (2006). Tissue-engineered injectable collagen-based matrices for improved cell

delivery and vascularization of ischemic tissue using CD133+ progenitors expanded from the peripheral blood. Circulation *114*, I138-144.

Suuronen, E.J., Zhang, P., Kuraitis, D., Cao, X., Melhuish, A., McKee, D., Li, F., Mesana, T.G., Veinot, J.P., and Ruel, M. (2009). An acellular matrix-bound ligand enhances the mobilization, recruitment and therapeutic effects of circulating progenitor cells in a hindlimb ischemia model. Faseb J *23*, 1447-1458.

Swijnenburg, R.J., Govaert, J.A., van der Bogt, K.E., Pearl, J.I., Huang, M., Stein, W., Hoyt, G., Vogel, H., Contag, C.H., Robbins, R.C.*, et al.* (2010). Timing of bone marrow cell delivery has minimal effects on cell viability and cardiac recovery after myocardial infarction. Circ Cardiovasc Imaging *3*, 77-85.

Takagi, Y., Hashimoto, N., Phan, S.H., Imaizumi, K., Matsuo, M., Nakashima, H., Hashimoto, I., Hayashi, Y., Kawabe, T., Shimokata, K.*, et al.* (2009). Erythromycin-induced CXCR4 expression on microvascular endothelial cells. Am J Physiol Lung Cell Mol Physiol *297*, L420-431.

Tang, J., Wang, J., Zheng, F., Kong, X., Guo, L., Yang, J., Zhang, L., and Huang, Y. Combination of chemokine and angiogenic factor genes and mesenchymal stem cells could enhance angiogenesis and improve cardiac function after acute myocardial infarction in rats. Molecular and cellular biochemistry *339*, 107-118.

Tatsumi, R. (2010). Mechano-biology of skeletal muscle hypertrophy and regeneration: possible mechanism of stretch-induced activation of resident myogenic stem cells. Anim Sci J *81*, 11-20.

Tatsumi, R., Anderson, J.E., Nevoret, C.J., Halevy, O., and Allen, R.E. (1998). HGF/SF is present in normal adult skeletal muscle and is capable of activating satellite cells. Dev Biol *194*, 114-128.

Tedesco, F.S., Dellavalle, A., Diaz-Manera, J., Messina, G., and Cossu, G. (2010). Repairing skeletal muscle: regenerative potential of skeletal muscle stem cells. The Journal of clinical investigation *120*, 11-19.

Thevenot, P.T., Nair, A.M., Shen, J., Lotfi, P., Ko, C.Y., and Tang, L. The effect of incorporation of SDF-1alpha into PLGA scaffolds on stem cell recruitment and the inflammatory response. Biomaterials *31*, 3997-4008.

Tidball, J.G. (2005). Inflammatory processes in muscle injury and repair. Am J Physiol Regul Integr Comp Physiol *288*, R345-353.

Tobler, K., Freudenthaler, A., Baumgartner-Parzer, S.M., Wolzt, M., Ludvik, B., Nansalmaa, E., Nowotny, P.J., Seidinger, D., Steiner, S., Luger, A.*, et al.* (2010). Reduction of both number and proliferative activity of human endothelial progenitor cells in obesity. Int J Obes (Lond) *34*, 687-700.

Tonnesen, M.G., Feng, X., and Clark, R.A. (2000). Angiogenesis in wound healing. J Investig Dermatol Symp Proc *5*, 40-46.

Turan, R.G., Bozdag-Turan, I., Ortak, J., Akin, I., Kische, S., Schneider, H., Turan, C.H., Rehders, T.C., Rauchhaus, M., Kleinfeldt, T.*, et al.* Improved Mobilization of the CD34(+) and CD133(+) Bone Marrow-Derived Circulating Progenitor Cells by Freshly Isolated Intracoronary Bone Marrow Cell Transplantation in Patients with Ischemic Heart Disease. Stem cells and development.

Turner, N.J., and Badylak, S.F. (2012). Regeneration of skeletal muscle. Cell and tissue research *347*, 759-774.

Uraoka, M., Ikeda, K., Nakagawa, Y., Koide, M., Akakabe, Y., Nakano-Kurimoto, R., Takahashi, T., Matoba, S., Yamada, H., Okigaki, M.*, et al.* (2009). Prorenin induces ERK activation in endothelial cells to enhance neovascularization independently of the renin-angiotensin system. Biochemical and biophysical research communications *390*, 1202-1207.

Urbich, C., Aicher, A., Heeschen, C., Dernbach, E., Hofmann, W.K., Zeiher, A.M., and Dimmeler, S. (2005). Soluble factors released by endothelial progenitor cells promote migration of endothelial cells and cardiac resident progenitor cells. Journal of molecular and cellular cardiology *39*, 733-742.

Varagic, J., Susic, D., and Frohlich, E. (2001). Heart, aging, and hypertension. Current opinion in cardiology *16*, 336-341.

Vignaud, A., Hourde, C., Medja, F., Agbulut, O., Butler-Browne, G., and Ferry, A. (2010). Impaired skeletal muscle repair after ischemia-reperfusion injury in mice. J Biomed Biotechnol *2010*, 724914.

Villalta, S.A., Rinaldi, C., Deng, B., Liu, G., Fedor, B., and Tidball, J.G. (2011). Interleukin-10 reduces the pathology of mdx muscular dystrophy by deactivating M1 macrophages and modulating macrophage phenotype. Hum Mol Genet *20*, 790-805.

Wang, J.S., Liu, X., Xue, Z.Y., Alderman, L., Tilan, J.U., Adenika, R., Epstein, S.E., and Burnett, M.S. (2011). Effects of aging on time course of neovascularization-related gene expression following acute hindlimb ischemia in mice. Chin Med J (Engl) *124*, 1075-1081.

Wang, Z.F., Wang, N.P., Harmouche, S., Philip, T., Pang, X.F., Bai, F., and Zhao, Z.Q. (2013). Postconditioning promotes the cardiac repair through balancing collagen degradation and synthesis after myocardial infarction in rats. Basic research in cardiology *108*, 318.

Whitman, S.C., Rateri, D.L., Szilvassy, S.J., Yokoyama, W., and Daugherty, A. (2004). Depletion of natural killer cell function decreases atherosclerosis in low-density lipoprotein receptor null mice. Arteriosclerosis, thrombosis, and vascular biology *24*, 1049-1054.

Williams, D.F. (1999). The Williams dictionary of biomaterials. (Liverpool, LIverpool University Press).

Willmann, R., Luca, A.D., Benatar, M., Grounds, M., Dubach, J., Raymackers, J.M., and Nagaraju, K. (2012). Enhancing translation: guidelines for standard pre-clinical experiments in mdx mice. Neuromuscul Disord *22*, 43-49.

Wojakowski, W., Tendera, M., Michalowska, A., Majka, M., Kucia, M., Maslankiewicz, K., Wyderka, R., Ochala, A., and Ratajczak, M.Z. (2004). Mobilization of CD34/CXCR4+, CD34/CD117+, c-met+ stem cells, and mononuclear cells expressing early cardiac, muscle, and endothelial markers into peripheral blood in patients with acute myocardial infarction. Circulation *110*, 3213-3220.

Wolf, M.T., Daly, K.A., Reing, J.E., and Badylak, S.F. (2012). Biologic scaffold composed of skeletal muscle extracellular matrix. Biomaterials *33*, 2916-2925.

Yang, J., Wang, F., and Tianwei, T. (2010). Degradation Behavior of Hydrogel Based on Crosslinked Poly(aspartic acid). Journal of Applied Polymer Science *117*, 178-185.

Yin, H., Price, F., and Rudnicki, M.A. (2013). Satellite cells and the muscle stem cell niche. Physiol Rev *93*, 23-67.

Yoder, M.C., and Ingram, D.A. (2009). Endothelial progenitor cell: ongoing controversy for defining these cells and their role in neoangiogenesis in the murine system. Curr Opin Hematol *16*, 269-273.

Yoon, C.H., Hur, J., Park, K.W., Kim, J.H., Lee, C.S., Oh, I.Y., Kim, T.Y., Cho, H.J., Kang, H.J., Chae, I.H.*, et al.* (2005). Synergistic neovascularization by mixed transplantation of early endothelial progenitor cells and late outgrowth endothelial cells: the role of angiogenic cytokines and matrix metalloproteinases. Circulation *112*, 1618-1627.

Zanotti, S., Saredi, S., Ruggieri, A., Fabbri, M., Blasevich, F., Romaggi, S., Morandi, L., and Mora, M. (2007). Altered extracellular matrix transcript expression and protein modulation in primary Duchenne muscular dystrophy myotubes. Matrix Biol *26*, 615-624.

Zhang, G., Nakamura, Y., Wang, X., Hu, Q., Suggs, L.J., and Zhang, J. (2007). Controlled release of stromal cell-derived factor-1 alpha in situ increases c-kit+ cell homing to the infarcted heart. Tissue engineering *13*, 2063-2071.

Zhang, Y., Thorn, S., DaSilva, J., Lamoreux, M., deKemp, R., Beanlands, R., Ruel, M., and Suuronen, E. (2008). Collagen-Based Matrices Improve the Delivery of Transplanted Circulating Progenitor Cells. Circulation: Cardiovascular Imaging *1*, 197-204.

Zimmermann, W.H., Schneiderbanger, K., Schubert, P., Didie, M., Munzel, F., Heubach, J.F., Kostin, S., Neuhuber, W.L., and Eschenhagen, T. (2002). Tissue engineering of a differentiated cardiac muscle construct. Circulation research *90*, 223-230.

APPENDICES

Appendix A – Authorizations

Authorization for Chapter #2 manuscript

Supplier: Elsevier Limited

The Boulevard, Langford Lane

Kidlington, Oxford, OX5 1GB, UK

Registered Company Number: 1982084

Customer Name: Drew Kuraitis

License Number: 3067971059529

Licensed Content Publisher: Elsevier

Licensed Content Publication: Journal of Molecular and Cellular Cardiology

Licensed Content Title: Ex vivo generation of a highly potent population of circulating angiogenic cells using a collagen matrix

Licensed Content Author: Drew Kuraitis, Chenchen Hou, Yan Zhang, Branka Vulesevic, Tanja Sofrenovic, Daniel McKee, Zahra Sharif, Marc Ruel, Erik J. Suuronen

Licensed Content Date: August 2011

Licensed Content Volume Number: 51

Licensed Content Issue Number: 2

Number of Pages: 11

Start Page: 187

End Page: 197

Type of Use: Reuse in a thesis/dissertation

Portion: Full article

Format: Both print and electronic

Authorizations for Chapters #3, 4 and 5

The manuscripts presented in Chapters #4, 5 and 6 were published in the journals *European Cells & Materials* and *Disease Models & Mechanisms*, both of which have open access policies and do not require authorizations to be granted in order for manuscripts to be reproduced.

Appendix B – Summary of genes and gene products analyzed in this thesis

Table A- 1 – Summary of gene products analyzed and/or discussed in this thesis, including other synonyms common in literature, form and location of each molecule, and general function, as it relates to the work presented in this thesis.

Molecule	Molecule form	General molecule function, relative to this thesis
Akt	Intracellular enzyme	Regulation of cell survival; anti-apoptotic
bFGF (FGF-2)	Secreted cytokine	Regeneration of many tissues; especially pro-angiogenic/vasculogenic
C-kit	Cell surface receptor	Binds SCF; ubiquitous hallmark of many different progenitor populations
Caspase-3	Intracellular protein	Once activated, plays central role in apoptosis
CD31 (PECAM-1)	Cell surface protein	Forms endothelial-endothelial intercellular junctions
CD34	Cell surface glycoprotein	Mediates binding of bone marrow-derived stem cells to bone marrow ECM
CD45 (leukocyte common antigen)	Cell surface glycoprotein	Direction of immune system & responses; exclusive to leukocyte linage
CD133	Cell surface glycoprotein	General marker of bone marrow-derived stem cells; function unknown
CD144 (VECAM)	Cadherin	Forms endothelial-endothelial adherens junctions
CXCR4	Cell surface receptor	Permits cell homing towards the source of its exclusive ligand, SDF-1
Desmin	Muscle cytoskeletal protein	Maintains integrity of structure and mechanics during muscle cell contraction
ERK1/2	Intracellular enzyme	Receives and transmits signals from physical, extrinsic influences, such as ECM

Flk-1 (VEGFR-2)	Cell surface receptor	Binds VEGF; found on progenitor cells with potential for vascular lineage differentiation
GCSF	Secreted cytokine	Stimulates bone marrow to produce and release both stem cells and granulocytes
HGF	Secreted cytokine	Many aspects of tissue regeneration
IGF-I	Secreted cytokine	Controls muscle growth and regeneration in adults
IGF-II	Secreted cytokine	Similar role to IGF-I, but primarily in fetal or developing muscle
IGFBP-2	Secreted cytokine	Binds IGF molecules to control their bioactivity and distribution
IGFBP-5	Secreted cytokine	Binds IGF molecules to control their bioactivity and distribution
IGFBP-6	Secreted cytokine	Binds IGF molecules to control their bioactivity and distribution
IL-1α	Secreted cytokine	Pro-inflammatory; broadly activates immune responses
IL-1β	Secreted cytokine	Pro-inflammatory; broadly activates immune responses
IL-4	Secreted cytokine	Pro-inflammatory, also involved in myoblast fusion
IL-6	Secreted cytokine	Pro-inflammatory, also involved in myoblast migration and proliferation
IL-10	Secreted cytokine	Anti-inflammatory; inhibits pro-inflammatory cytokine secretion
L-Selectin	Cell surface receptor	Adhesion and homing of bone marrow and endothelial lineages
M-cadherin	Cadherin	Cell-cell muscle precursor adhesion and terminal differentiation
MCK	Intramitochondrial enzyme	ATP provision in functional myocytes

MCP-1	Secreted cytokine	Recruitment of mononuclear cells in disease or injury
Mef2c	Transcription factor	Myocyte maturation and regeneration
MHC3	Myocyte thick filament	Skeletal muscle contraction
MHC7	Myocyte thick filament	Skeletal muscle contraction
MIP-3α	Secreted cytokine	Pro-inflammatory; lymphocyte chemoattractant
Myf5	Transcription factor	Muscle lineage specification and precursor differentiation
MyoD	Transcription factor	Represents commitment to myogenic differentiation
Myogenin	Transcription factor	Muscle cell maturation in both the embryo and adult
P-Selectin	Cell surface receptor	Mediates leukocyte recruitment to endothelium
Pax3	Transcription factor	Expressed by proliferating satellite cells
Pax7	Transcription factor	Expressed by quiescent satellite cells
SCF	Secreted cytokine	Self-renewal and localization of bone marrow-derived progenitor cells
SDF-1α	Secreted cytokine	Initiates mobilization and guides homing of CXCR4-exprssing cells
TIMP-1	Secreted cytokine	Inhibits ECM/tissue remodeling peptidases
TIMP-2	Secreted cytokine	Inhibits ECM/tissue remodeling peptidases
VCAM-1	Cell adhesion molecule	Mediates adhesion of inflammatory cells to endothelium
VEGF	Secreted cytokine	Regeneration of many tissues; especially pro-angiogenic/vasculogenic

Appendix C – Response to examiner

In response to one examiner of this thesis, this section is meant to address specific questions regarding Chapters 2 – 5.

Point #1: *Sample size and analysis of studies in Chapter 2*. In this chapter, all *p* values are reported. In many figures, significant differences were reported with *n*=4. It is agreed that this sample size is small; however, this sample size was also sufficient to demonstrate statistically significant differences. The pattern of the results was also consistent: matrix exposure improved viability and enrichment of CACs. Furthermore, cells were isolated from one donor and used for each experiment. This allows the use of paired t-tests, which reduces the effect of donor variability and improves power. It is expected that a greater sample size would only increase the significance of the reported results.

Point #2: *Co-localization in Figure 2-4*. It is agreed that 3-dimensional, confocal microscopy would be ideal to confirm true co-localization of $DAPI^+$ CACs within the capillary structures formed by $CMTMR^+$ HUVECS.

Point #3: *Western blot in Figure 2-5*. It is agreed that a representative Western blot that is less exposed would have been a better choice to include with this figure. These results have since been reproduced in the lab and with better Western blots; there is still significantly more phosphorylated ERK when compared to pan-ERK. This figure was also analyzed again using a paired t-test, allowing us to describe the impact that matrix has on ERK phosphorylation by comparing cells from the same individual donor on both substrates. The

reported *p* values are derived from comparing the differences between fibronectin & matrix treatments for each individual donor.

Point #4: *Age of mdx mice*. It is agreed that at one month, when *mdx* mice were treated, the degree of impairment is minimal and that their performance on the treadmill should not be significantly different than non-*mdx*, matched animals. Mice at one month of age were chosen, as this age roughly corresponds to the age of DMD "onset" in humans. The onset of myocyte necrosis in the *mdx* mouse begins at around 3 weeks and evidence of regeneration is apparent shortly after (Grounds et al., 2008). The use of older mice (6 weeks – 6 months of age) may have yielded different results, as these animals experience significant fibrosis, accumulation of fatty connective tissue and atrophic loss of muscle mass. It would have been interesting to perform the same studies using an older cohort of animals, but this study was conceived with the hope of being able to circumvent some aspects of disease manifestation. It is more likely that patients will be available from a young age, rather than presenting themselves in the clinic at an older age after the disease has set-in. The effect of matrix treatment on older subjects has yet to be evaluated.

Point #5: *Use of cytokine arrays*. Chapters 2, 3, 4 and 5 used cytokine arrays to assess the relative levels of cytokines produced in response to matrix treatment. Sometimes cytokines of potential interest were not included in this analysis because they could not be included in the custom cytokine array. According to the manufacturer, some pairs of cytokine antibodies cannot be included together on the arrays.

Point #6: *Use of hindlimb ischemia model*. Chapters 2, 3 and 4 use a model of hindlimb ischemia to evaluate their respective therapies. In this model, the femoral artery is tied off. For each study, a large thread was chosen so that after forming a knot, the artery is not

completely occluded and approximately 40-50% of the baseline perfusion still remains. Many other studies that use this model reduce perfusion by 90% or more. In comparison, the injury caused in the studies in this thesis is far less severe; there is minimal apoptosis, minimal cell death, less inflammatory cell infiltration and fibrosis, and the loss of digits, feet or legs are not used as end-points. If a more severe model of ischemia was used, the effect of the matrix may have been different: treatment may have improved, or perhaps treatment may have been insufficient to overcome such severe contexts. Regardless, the rapid onset that the animals experience does not mimic the gradual progression that humans experience with PAD, and one must be cautious when comparing human diseases to their corresponding animal models.

Additional Reference

Grounds M.D., Radley H.G., Lynch G.S., Nagaraju K., and De Luca A. (2008). Towards developing standard operating procedures for pre-clinical testing in the mdx mouse model of Duchenne muscular dystrophy. Neurobiology of Disease 31:1-19.